

Influence of T cell activation, proliferation, and the use of Pifithrin- α on the size of large deletions upon CRISPR editing

Laurenz Thomas Ursch

Vollständiger Abdruck der von der TUM School of Medicine and Health der Technischen Universität München zur Erlangung eines
Doktors der Medizinischen Wissenschaften (Dr. med. sci.)
genehmigten Dissertation.

Vorsitz: Prof. Dr. Dirk H. Busch

Prüfende der Dissertation:

1. Prof. Kathrin Schumann, Ph. D.
2. Prof. Dr. Jürgen Ruland

Die Dissertation wurde am 02.07.2024 bei der Technischen Universität München eingereicht und durch die TUM School of Medicine and Health am 06.11.2024 angenommen.

Contents

Abbreviations	xi
1 Zusammenfassung/Summary	1
1.1 Summary/Zusammenfassung	1
1.1.1 Summary	1
1.1.2 Zusammenfassung	2
2 Introduction	5
2.1 The human immune system	5
2.1.1 T cell activation – CD4 and CD8 T cells	6
2.1.2 The mechanism of T cell activation	8
2.1.3 The impact of T cell activation and proliferation on the genomic stability	12
2.2 Bacterial adaptive immunity	12
2.3 Strategies to CRISPR-engineer human T cells	15
2.4 Harnessing immune mechanisms for therapy	16
2.5 Benefits of CRISPR-engineered T cells	17
2.6 Mechanisms and hurdles in gene-engineering	18
2.6.1 The role of p53 during CRISPR-editing	21
2.6.2 Specificity of CRISPR-engineering	23
3 Aim of the thesis	25
4 Material and Methods	27
4.1 Materials	27
4.1.1 guideRNA	27
4.1.2 Nucleofection Supply	27
4.1.3 Buffer and media	28
4.1.4 Chemicals and molecules	29
4.1.5 Antibodies	30
4.1.6 Cell culture	31

4.1.7	Amplicon Next Generation Sequencing (NGS)	32
4.1.8	Primer	32
4.1.9	Software	34
4.1.10	Equipment	35
4.2	Isolation and culture of primary human T cells	36
4.3	Cas9 RNP assembly and nucleofection	36
4.4	CFSE T cell proliferation assay	37
4.5	Flow cytometry staining	37
4.6	Flow cytometry cell sorting and DNA extraction	38
4.7	CAST-Seq analysis	38
4.8	Single cell copy number analysis and clustering (scKaryo-seq)	38
4.9	Polymerase chain reaction (PCR)	39
4.10	Amplicon NGS	39
5	Results	45
5.1	The frequency of large deletions is tied to the T cell activation status	45
5.2	The impact of T cell proliferation speed on deletion patterns	49
5.3	Modulation of deletion patterns via small molecules	52
5.4	Modulation of deletion patterns via PFT- α is independent of p53	56
5.5	Impact of the activation status and PFT- α treatment on deletions larger than 200 bps and chromosomal translocations	59
6	Discussion	67
6.1	Technical limitations	67
6.1.1	Experimental variables	67
6.1.2	Potential impact on different T cell subsets or other cell types	68
6.1.3	Dependency on gene locus	68
6.1.4	Size limitations of amplicon MiSeq NGS data	69
6.1.5	Effects of PFT- μ	70
6.1.6	Unclear mode of action of PFT- α	70
6.2	Biological and gene engineering implications	72
6.2.1	Involvement of p53 in CRISPR-editing	72
6.2.2	Large deletions in CRISPR-engineered cell lines	73
6.2.3	Large deletions and aneuploidy in CRISPR-engineered T cells	74
6.2.4	The use of PFT- α in genetic engineering	75

6.3	Evaluating potential targets for PFT- α	77
6.4	Addressing safety	79
6.4.1	Phenotypic characterization and killing capacity	79
6.4.2	Assessing the rate of aneuploidy	79
6.5	Possible applications	80
6.5.1	Increasing safety in gene edited T cell products	80
	Bibliography	81
	Danksagung	99

Abbreviations

A	Adenine
AAVS1	Adeno-Associated Virus Integration Site 1
Ab	Antibody
AhR	Aryl Hydrocarbon Receptor
Alt-NHEJ	Alternative NHEJ
AP1	Activator Protein 1
Apaf-1	Apoptotic Protease Activating Factor 1
APC	Antigen-Presenting-Cell Or Adenophycocyanin
ATM	Ataxia-Telangiectasia Mutated
ATR	Ataxia Telangiectasia And Rad3-Related Protein
B2M	Beta-2-Microglobulin
BAFFR	B-Cell Activating Factor Receptor
Bak	BCL2 Antagonist/killer
Bax	Bcl-2 Associated X-Protein
BCL-XL	B-Cell Lymphoma-Extra Large
BCL11A	B-Cell Lymphoma/leukemia 11A
Bcl2	B-Cell Lymphoma 2
BID	BH3 Interacting-Domain Death Agonist
bp	Base Pair
BRCA	Breast Cancer Type 1 Susceptibility Protein
BSA	Bovine Serum Albumine
BV	Brilliant Violet
C	Cytosin
C-NHEJ	Conventional NHEJ
Ca ²⁺	Calcium-Ion
CAR	Chimeric Antigen Receptor

Ca ²⁺	Calcium-Ion
CAR	Chimeric Antigen Receptor
Cas9	CRISPR-Associated Protein 9
CAST-Seq	Chromosomal Aberrations Analysis By Single Targeted Linker-Mediated PCR Sequencing
CD	Cluster Of Differentiation
CDE	CRISPR-Specific Differentially Essential Positive
CDK	Cyclin-Dependent-Kinase
CFSE	5-(and 6)-Carboxyfluorescein Diacetate Succinimidyl Ester
CHK	Checkpoint Kinase
CI	Confidence Intervall
CIITA	Class II, Major Histocompatibility Complex, Transactivator
COX2	Cyclooxygenase 2
CPM	Counts Per Million
CRISPR	Clustered Regularly Interspaced Short Palindromic Repeats
CRPMI	Complete Roswell Park Memorial Institute
crRNA	CRISPR RNA
CRS	Cytokine-Release-Syndrom
CTLA4	Cytotoxic T Lymphocyte Antigen 4
CXCR4	C-X-C Chemokine Receptor Type 4
DAG	Di-Acetyl-Glycerin
DC	Dendritic Cells
ddH ₂ O	Double Distilled Water
DDR	DNA-Damage-Response
DMSO	Dimethylsulfoxide
DNA	Desoxyribonucleic Acid
DNA-PKc	DNA-Dependent Protein Kinase, Catalytic Subunit
DSB	Double-Strand-Break
dsDNA	Double-Stranded DNA
E. Coli	Escherichia Coli
EDTA	Ethylenediaminetetraacetic Acid
ER	Endoplasmatic Reticulum
Exo1	Exonuclease 1
FACS	Fluorescence Activated Cell Sorting
FBS	Fetal Bovine Serum

FCS	Fetal Calf Serum
FITC	Fluorescein Isothiocyanate
FSC	Forward Scatter
fwd	Forward
G	Guanine
gRNA	Guide RNA
HBB	Hemoglobin Subunit Beta
HDR	Homology Directed Repair
HEPES	4-(2-Hydroxyethyl)-1-Piperazineethanesulfonic Acid
HTT	Huntingtin
i53BP1	Inhibitor Of 53BP1
ICOS	Inducible T Cell Costimulator
IFN	Interferone
Ig	Immunglobuline
IKK	I κ B Kinase
IL	Interleukine
IL2RA	Interleukin-2 Receptor Alpha Chain
Indel	Insertion-Deletion
iT _{reg}	Induced Regulatory T Cell
ITAM	Immunoreceptor Tyrosine-Based Activation Motif
I κ Ba	Inhibitory κ B
KI	Knock-In
KO	Knock-Out
KRAS	Kirsten Rat Sarcoma Virus
L-Glut	L-Glutamine
LAG3	Lymphocyte-Activation Gene 3
LAT	Linker For Activation Of T Cells
Lck	Lymphocyte-Specific Protein Tyrosine Kinase
LICOS	Ligand Of ICOS
LOH	Loss Of Heterozygosity
LT β R	Lymphotoxin- β Receptor
MAPK	Mitogen-Activated Protein Kinase
Mcl-1	Myeloid Cell Leukemia-1
MDC1	Mediator Of DNA Damage Checkpoint 1
MDM2	Mouse Double Minute 2

MHC	Major Histocompatibility Complex
MMEJ	Microhomology-Mediated End Joining
MRN	MRE11/RAD50/NBS1 Complex
mRNA	MessengerRNA
Na-Pyruvat	Sodium Pyruvate
NBS1	Nibrin
NEAA	Non Essential Amino Acids
NEMO	NF- κ B Essential Modulator
NF- κ B	Nuclear Factor ' κ -Light-Chain-Enhancer' Of Activated B-Cells
NFAT	Nuclear Factor Of Activated T-Cells
NGS	Next-Generation-Sequencing
NHEJ	Non-Homologous End Joining
NIR	Near Infrared
NLS	Nuclear Localization Signal
ns	Not Significant
nT _{reg}	Natural Regulatory T Cell
OMT	Off Target-Mediated Translocations
P/S	Penicillin / Streptomycin
PALP	Partner And Localizer Of BRCA2
PAM	Protospacer-Adjacent-Motif
PBMC	Peripheral Blood Mononuclear Cell
PBS	Phosphate-Buffered Saline
PCR	Polymerase Chain Reaction
PD-1	Programmed Cell Death 1
PDCD1	Programmed Cell Death Protein 1
PDL	PD-1 Ligand
PE	Phycoerythrin
PerCP	Peridinin-Chlorophyll-Protein
PFT- α	Pifithrin- α
PFT- μ	Pifithrin- μ
PI	Prpidium Iodide
PIP3	Inositoltriphosphat
PLC-gamma 1	Phospholipase C, Gamma 1,
PUMA	P53 Upregulated Modulator Of Apoptosis
RABL6	Rab-Like Protein 6

RANK	Receptor Activator Of Nuclear Factor K B
Ras	Rat Sarcoma Virus
RB	Retinoblastoma Protein
rev	Reverse
RNA	Ribonucleic Acid
RNP	Ribonucleoprotein
ROS	Reactive Oxygen Species
RPA	Replication Protein A
RT	Room Temperature
Sae2	SUMO-Activating Enzyme Subunit 2
ScKaryoSeq	Single Cell Molecular Karyotype Sequencing
SERPINA1	Serpin Family A Member 1
sgRNA	Single Guide RNA
shRNA	Short Hairpin RNA
siRNA	Small Interfering RNA
SSC	Sideward Scatter
ssDNA	Single-Stranded DNA
STAT	Signal Transducer And Activator Of Transcription
T	Thymin
T _{FH}	T Follicular Helper Cell
T _{H1}	Type 1 T helper cell
T _{H2}	Type 2 T helper cell
T _{H17}	T helper 17 cell
T _{reg}	Regulatory T Cell
TALEN	Transcription Activator-Like Effector Nucleases
TCR	T Cell Receptor
TGF	Transforming Growth Factor
TIGIT	T Cell Immunoreceptor With Immunoglobulin And Immunoreceptor Tyrosine-Based Inhibition Motif Domain
TIM3	T Cell Immunoglobulin And Mucin-Domain Containing-3
TNF	Tumor Necrosis Factor
TP53	Tumor Protein P53
TP53BP1	TP53 Binding Protein 1
TRAC	T Cell Receptor Alpha Constant
tracrRNA	Trans-Activating CrRNA

TRBC	T-Cell Receptor Constant B Chain
TRIS	Tris(hydroxymethyl)aminomethane
TTR	Transthyretin
VDJ	Variable–diversity–joining
WT	Wild Type
XLF	XRCC4-Like Factor
XRCC4	X-Ray Repair Cross-Complementing Protein 4
Zap70	Zeta-Chain-Associated Protein Kinase 70

List of Figures

2.1	Time course immune response	6
2.2	The interaction between T cell receptors and their MHC counterparts	7
2.3	The NFAT-pathway	11
2.4	The CRISPR/Cas system in bacteria	14
2.5	HDR and NHEJ DNA repair pathways	20
2.6	Schematic depiction of potential p53-mediated signalling pathways after CRISPR-induced DSB	22
5.1	General workflow	46
5.2	Flow cytometry gating Strategy for activated and non-activated T cells	47
5.3	Characterization of KO efficiencies in activated and non-activated T cells	48
5.4	Deletion patterns in activated and non-activated T cells	49
5.5	Insertion patterns in activated and non-activated T cells	49
5.6	KO efficiencies in pre- and post-activation stimulation protocols	50
5.7	Deletion patterns in pre- and post-activated T cells	50
5.8	Depiction of the general workflow of T cell proliferation experiments	51
5.9	Gating strategy for T cell proliferation experiments	52
5.10	Deciphering the impact of T cell proliferation on the deletion pattern	53
5.11	Analyzing the effect of p53 inhibitors on KO efficiencies and proliferation	54
5.12	Analyzing the effect of p53 inhibitors on deletion sizes	55
5.13	The impact of PFT- α on the deletion sizes in pre- and post-activated T cells	55
5.14	Gating strategy for <i>TIGIT</i> and <i>HAVCR2</i>	56
5.15	Distribution of deletions for <i>TIGIT</i> and <i>HAVCR2</i>	56
5.16	Distribution of deletions for <i>CXCR4</i> KO T cells	57
5.17	Workflow to generate <i>TP53</i> or <i>AAVS1</i> KO T cells and challenge with secondary KO and inhibitor treatment	58
5.18	Testing the p53-dependence of PFT- α and PFT- μ	59
5.19	Schematic depiction of Cast-Seq	61

5.20 CAST-Seq analysis of DMSO- or PFT- α -treated double KO cells	62
5.21 Circos-plots for double edited T cells with added DMSO or PFT- α	62
5.22 On-target results of CAST-Seq for T cells treated with DMSO or PFT- α	63
5.23 MiSeq analysis of DMSO- or PFT- α -treated double KO T cells	64
5.24 CAST-Seq results of chromosomal translocations to <i>PDCD1</i> target locus	65

1 Zusammenfassung/Summary

1.1 Summary/Zusammenfassung

1.1.1 Summary

The importance that CRISPR/Cas9 has gained in recent years for genetic engineering can hardly be overestimated. This new technology makes it possible to precisely modify the genome of cell lines, primary cells and entire organisms more easily and cost-effectively than before. In addition to other areas of application, this has proven to be particularly useful for T cell research. In addition to findings in basic experimental research, this also contributes to the improvement of clinical applications such as CAR-T cell therapies. However, it is becoming increasingly clear that the use of CRISPR/Cas9 is not as specific as initially assumed. There is increasing evidence that CRISPR editing can cause deletions spanning multiple kilobases or the loss of entire chromosomes. These CRISPR induced chromosomal abnormalities could possibly lead to malignant transformation of the edited T cells if for example tumor suppressor genes are affected. Efforts have been made to improve the specificity of CRISPR/Cas9 to reduce the risks of undesired off-target effects such as improved algorithms for guideRNA design or by generating high-fidelity Cas9 variants. The aim of this work was to dissect T cell-specific characteristics to reduce the rate of large deletions and chromosomal events during CRISPR editing in this therapy-relevant cell type. In my thesis, I established an experimental workflow that allows T cells to be genetically modified and to be flow-cytometry sorted based on the resulting knock-out (KO) and their proliferation rate. The DNA of these cells was then isolated, the target site PCR-amplified, and the deletion pattern analyzed within a 200 bp window using amplicon next generation sequencing. For several target genes, I could prove that the deletion sizes depend on both the activation status and the proliferation rate of the T cells. Strongly activated and rapidly proliferating cells have more large deletions than non-activated or slowly proliferating cells. These results were also confirmed for deletions larger than 200 bp and chromosomal translocations using CAST-Seq. Furthermore, an already known inhibitor called pifithrin- α (PFT- α) was used to analyze the link between large deletions and the p53-pathway. Surprisingly, the inhibitor reduces the average deletion size when added during the generation of a CRISPR KO in contrast to the known function of p53 as an initiator of DNA repair. However, PFT- α also reduces large deletion in p53-KO T cells, indicating a p53-independent

mechanism of action. Taken together, in my thesis I could identify two strategies to reduce the risk of unwanted large deletions in CRISPR-edited T cells. Both pathways can be easily integrated into existing T cell CRISPR editing protocols. This could make a contribution to making the future use of edited T cell therapeutics safer and more precise.

1.1.2 Zusammenfassung

Die Bedeutung, die CRISPR/Cas9 in den letzten Jahren für die Gentechnik gewonnen hat, kann kaum überschätzt werden. Diese neue Technologie ermöglicht es, präzise das Genom von Zelllinien, Primärzellen und ganzen Organismen einfacher und kostengünstiger als bisher zu verändern. Dies hat sich neben anderen Anwendungsgebieten insbesondere für die T Zell-Forschung als nützlich erwiesen. Neben Erkenntnissen in der experimentellen Grundlagenforschung trägt dies auch zur Verbesserung von klinischen Anwendungen wie CAR-T Zelltherapien bei. Es wird jedoch immer deutlicher, dass der Einsatz von CRISPR/Cas9 nicht so spezifisch ist, wie zunächst angenommen. Es gibt immer mehr Hinweise darauf, dass CRISPR-Editierung Deletionen über mehrere Kilobasen oder den Verlust ganzer Chromosomen verursachen kann. Diese CRISPR-induzierten Chromosomenabberationen könnten möglicherweise zu einer malignen Transformation der editierten T-Zellen führen, wenn zum Beispiel Tumorsuppressorgene betroffen sind. Es existieren zahlreiche Ansätze, um die Spezifität von CRISPR/Cas9 zu verbessern, um so das Risiko unerwünschter Off-Target-Effekte zu verringern, z. B. durch verbesserte Algorithmen für das Design von guideRNAs oder durch die Erzeugung von High-Fidelity-Cas9-Varianten.

Ziel dieser Arbeit war es, T Zell-spezifische Eigenschaften zu entschlüsseln, um die Rate großer Deletionen und chromosomaler Ereignisse beim CRISPR-Editing in diesem therapierelevanten Zelltyp zu reduzieren. In meiner Dissertation habe ich einen experimentellen Arbeitsablauf etabliert, der es ermöglicht, T-Zellen genetisch zu verändern und mittels Durchflusszytometrie anhand der resultierenden Knock-outs (KO) und ihrer Proliferationsrate zu sortieren. Die DNA dieser Zellen wurde dann isoliert, die Zielsequenz mittels PCR amplifiziert und das Deletionsmuster innerhalb eines 200 bp-Fensters mittels Amplicon Next Generation Sequencing analysiert. Für mehrere Zielgene konnte ich nachweisen, dass die Größe der Deletionen sowohl vom Aktivierungsstatus als auch von der Proliferationsrate der T-Zellen abhängt. Stark aktivierte und schnell proliferierende Zellen haben mehr große Deletionen als nicht aktivierte oder langsam proliferierende Zellen. Diese Ergebnisse wurden auch für Deletionen größer als 200 bp und chromosomale Translokationen mit CAST-Seq bestätigt.

Außerdem wurde ein bereits bekannter Inhibitor namens Pifithrin- α (PFT- α) verwendet, um die Verbindung zwischen großen Deletionen und der p53 Signalkaskade zu analysieren. Unerwarteterweise reduziert PFT- α die durchschnittliche Deletionsgröße, wenn es während der DNA-Editierung mittels CRISPR/Cas9 hinzugefügt wird. Dies steht im Widerspruch zur bekannten Funktion von p53 als Initiator der DNA-

Reparatur. Des Weiteren reduziert PFT- α auch die große Deletion in p53-KO T-Zellen, was auf einen p53-unabhängigen Wirkmechanismus hindeutet. Insgesamt konnte ich in meiner Arbeit zwei Strategien identifizieren, um das Risiko unerwünschter großer Deletionen in CRISPR-editierten T Zellen zu verringern. Beide Wege lassen sich leicht in bestehende CRISPR-Editierungsprotokolle für T Zellen integrieren. Dies könnte dazu beitragen, den zukünftigen Einsatz von editierten T Zell-Therapeutika sicherer und präziser zu machen.

2 Introduction

2.1 The human immune system

The human immune system is divided into two parts the innate immune system and the adaptive immune system. Both systems work closely together to orchestrate the immune response. After the initial response is executed by the innate immune system, the adaptive immune system strengthens the hosts reaction to the pathogen [169]. The adaptive immune system consists of antibodies, which are produced by B cells, and T cells.

	innate immune system	adaptive immune system
soluble	complement system, lysozym, defensine,	antibodies
cellular	macrophages, basophils, eosinophils, neutrophiles, mast cells, dendritic cells	B cells, T cells

Table 2.1 components of the immune system

The adaptive immune system has certain key features compared to the innate immune system. Key differences are:

- **Reaction speed:** The innate immune system can respond instantly via the use of its barrier functions and for example the presence of lysozyme in tear fluid [148], if it encounters a pathogen. The response of the adaptive immune system takes up to 7 days to fully unfold [24].
- **Specificity:** Through a complex order of genetic rearrangements, the adaptive immune system generates a large diversity of antibodies and TCRs [1]. Thus, the adaptive immune system is highly diverse in its capability to detect foreign antigens, but also very specific once it recognizes one certain antigen, since T cell activation requires the formation of the “immunological synapse”, which is tightly regulated.

- Immune Memory: The most important aspect of the adaptive immune system is its ability to "memorize" certain antigens and orchestrate a quick and measured response if the same antigen reappears at some point later in life. After a successful clonal expansion of the T and B cells, a certain amount of both cell populations differentiates into the respective memory cells [20]. These memory T and B cells remain in the body and can quickly and efficiently respond to future infections with the same antigen within a few hours [94]. This aspect of the adaptive immune system is the basis for vaccination. Shown in Figure 2.1 is a simplified time-course with the various ways the immune system responds to pathogens.

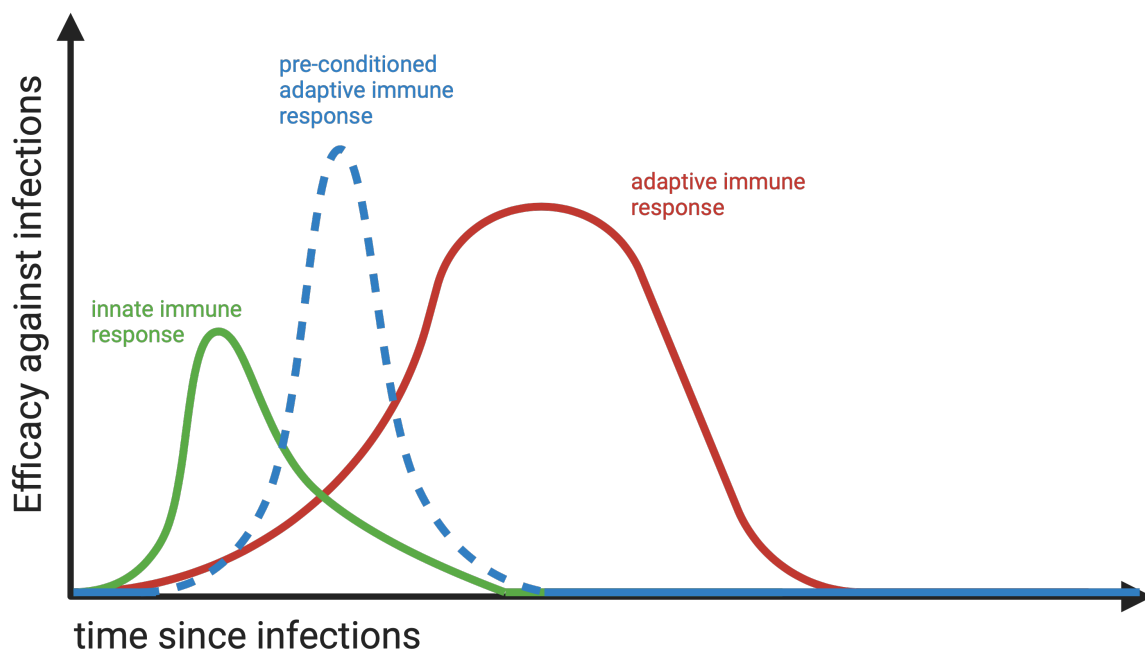


Figure 2.1 Time course immune response. While the first line of defense against pathogens is always the innate immunity (green), the adaptive immune system (red) is more efficient at clearing pathogens. If the adaptive immune system has encountered one specific antigen before, a subset of memory cells remains in the tissue of the host. This memory population (blue) can expand much quicker than the unconditioned adaptive immune system to execute the clearance of the pathogen

2.1.1 T cell activation – CD4 and CD8 T cells

T cells are one major cellular component of the adaptive immune system. T cells are activated through antigens presented on a major histocompatibility complex (MHC). There are two classes of MHCs, MHC class I (MHC I) and MHC class II (MHC II), that differ in their function and their expression profiles. Cells with MHC I present their antigens to CD8+ T cells and cells with MHC II to CD4+ T cells (Figure 2.2) [26].

MHC class I is expressed on each cell with a cell nucleus and is able to present "self" peptides of the respective cell. If a cell is infected with an intracellular pathogen like a virus or shows signs of malignancy,

the MHC class I will present these foreign peptides to CD8+ T cells. The activated cytotoxic T cells are then specifically killing the infected or malignant cells [7] [6]. Killing of the target cells can either happen via secretion of lytic proteins like granzymes in combination with perforin or via activation of the fas/fas ligand pathway on the target cells [32] [35].

MHC class II is only expressed on the surface of "professional" antigen-presenting cells (APCs). APCs phagocytose pathogens, break them down in endolysosomes and present the processed peptides on MHC class II [52]. MHC class II bind to CD4+ T cells, that are able to activate and regulate the other cells of the immune system, including B cells, CD8+ T cells, macrophages and thereby ensure a well-coordinated immune response.

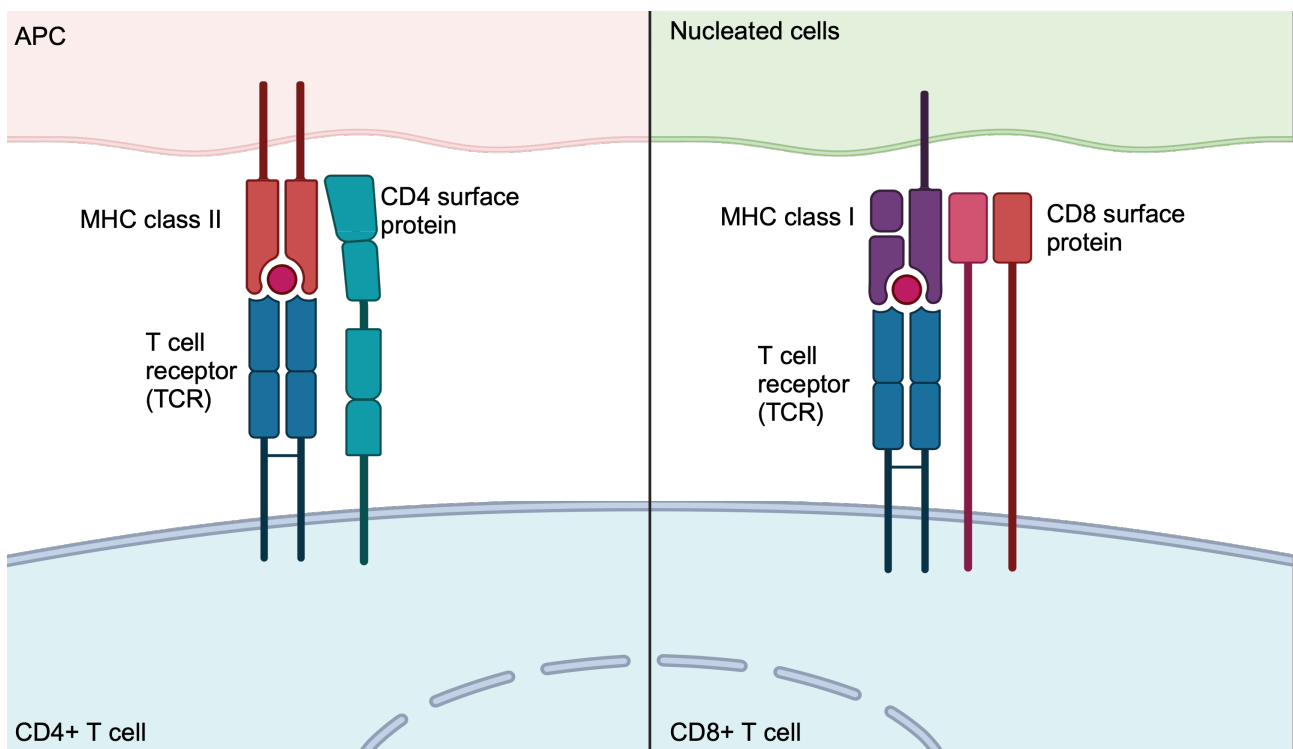


Figure 2.2 The interaction between T cell receptors and their MHC counterparts. On the left side, MHC class II is shown, which is expressed on antigen-presenting-cells (APCs) and can interact with CD4+ T cells. On the right MHC class I is depicted, which is expressed by all nucleated cells and can interact with CD8+ T cells.

The interaction between naïve CD4 T cell and APC induces the differentiation of the CD4 T cells into different T-helper cell subpopulations. The most important ones are:

- T_{H1} cells: T_{H1} cells produce the effector cytokines interferon- γ , TNF- α and IL-2. T_{H1} cells play an important role in providing help to APCs to ensure the eradication of intracellular pathogens. Some pathogens, especially mycobacteriae causing tuberculosis or lepra, can persist inside of macrophages after phagocytosis despite the usual neutralization mechanisms employed by the

macrophage. T_H1 cells can provide additional stimulations that enable the macrophage to destroy the intracellular pathogens. T_H1 cells also support the isotype class switch in B cells to IgG [65].

- T_{H2} cells: Upon activation T_{H2} cells secrete IL-4, IL-5 and IL-13. These cytokines support the defense against extracellular pathogens, especially parasites such as helminths. Effector molecules produced by T_{H2} cells recruit and activate eosinophils and mast cells, which can in turn attack the parasites. T_{H2} cells also enable isotype class switching to IgE antibodies in plasma cells [171].
- T_{H17} cells: These cells produce IL-17A, IL-17F and IL-22, which stimulate neutrophils and thereby support the defense against fungi and other extracellular pathogens. These effector cytokines also support the isotype class switch to IgG. Another function of T_{H17} cells is the stimulation of epithelial cells to produce antimicrobial peptides [98].
- T_{FH} cells: The main effector cytokine is IL-21. IL-21 supports germinal centre formation, independent of the type of pathogen [210].
- T_{reg} cells: T_{reg} cells represent the only subpopulation of CD4+ T cells, which does not increase, but dampen the immune response by several mechanisms including the secretion of TGF- β and IL-10. T_{reg} cells protect us from autoimmunity and allow a balanced immune response [88].

2.1.2 The mechanism of T cell activation

One of the crucial steps of adaptive immunity is the activation of T cells. Every time a T cell encounters a foreign antigen that matches its T cell receptor (TCR), the cell becomes activated. While initial antigen stimulation leads to T cell expansion and generation of memory T cells, restimulation is necessary to strengthen and maintain the T cell response, since transient antigen stimulation leads to T cell unresponsiveness [134]. Most T cells express an α/β -TCR and only a minority γ/δ -TCRs. Upon antigen binding with the TCR, the T cell activation complex is assembled, which consists of the TCR α and β chains as well as CD3 $\gamma\epsilon$, CD3 $\delta\epsilon$ and CD3 $\zeta\zeta$ [56] [197]. The TCR is necessary for the highly specific antigen recognition, whereas CD3 initializes the intracellular signalling cascade upon antigen presentation. Besides enabling the T cell to execute their effector functions, this also allows for the proliferation of the specific T cell, which is crucial for a sufficient immune response.

As already mentioned above, antigen presentation for T cells relies on the presentation of the processed antigens from APCs. These APCs present their antigen either on MHC class I or MHC class II. The former targets the TCR on CD8+ T cells, whereas the latter presents antigens to CD4+ T cells.

Both MHCs present their antigens to the TCR, additionally the antigen presentation is complemented by co-receptor surface proteins expressed by the T cells, either CD8 or CD4, which gave the respective

population their names. The engagement of the co-receptors increases the sensitivity of the T cell receptor and amplifies downstream signalling. Both co-receptors directly bind the respective MHC (Figure 2.2).

Following extracellular antigen presentation, the close proximity of the intracellular regions of either CD4 or CD8 with the so-called immunoreceptor tyrosine-based activation motifs (ITAMs) of the CD3 γ chain, CD3 δ chain, CD3 ϵ chains and the ζ -chains of the CD3 protein allows for the phosphorylation of the ITAMs via lymphocyte-specific protein tyrosine kinase (Lck) which is associated with CD4 or CD8 [9]. The phosphorylation of the ITAMs allows the recruitment of the tyrosine kinase ζ -chain associated protein kinase of 70 kDa (Zap70). Zap70 is activated via conformational changes by phosphorylation [81]. Activated Zap70 can phosphorylate the linker for activation of T cells (LAT), which allows LAT to recruit multiple proteins to form the LAT-signalosome [131]. The proteins recruited by LAT activate several signalling pathways, which are involved in cell adhesion, activation of genes for T cell growth and differentiation and actin-reorganization, necessary for T cell activation and proliferation [41] [74] [178].

The signalling intensity can be further modified by costimulatory receptors (strengthen the signalling) or co-inhibitory receptors (weaken the signalling). Examples for costimulatory receptors are:

- CD28: CD28 is the classical costimulatory receptor, which through downstream effects via Lck, enhances the T cell activation and adhesion of the MHC-TCR complex [48]. It is activated upon binding of either CD80 (B7-1) or CD86(B7-2), which are located on the surface of APCs.
- Inducible T cell costimulator (ICOS, CD278) is upregulated following T cell activation and binds LICOS (ligand of ICOS, CD275), which is expressed on dendritic cells (DCs) and B cells. It upregulates cytokine production and enhances proliferation in T cells [68] [53].
- Members of the TNF family like: OX40, 4-1BB, CD27, CD30 and HVEM (herpes-virus entry mediator) [62]

Co-inhibitory receptors reduce the TCR signalling strength and thereby induce a resting phase of the T cells or protect the cells from overstimulation. Often co-inhibitory receptors are induced upon TCR activation as a negative feedback loop. The best characterized co-inhibitory receptors are PD-1 and CTLA-4. However, up to 10 co-inhibitory receptors have been described to fine-tune the TCR signalling strength [213].

- Programmed cell death protein 1 (PD-1, CD279) is a co-inhibitory receptor protein, which is located on the surface membrane of T cells during activation. PD-1 executes its function to limit excessive T cell response upon binding of PD-1-Ligand 1 or 2 (PD-L1 or PD-L2) on cells which present the MHC-antigen complex [15] [51]. If PD-1 is activated it targets tyrosine phospho sites that mediate T cell receptor signaling, organization of the cytoskeleton, and immune synapse formation. It can also

lead to changes in the phosphorylation of threonine and serine in certain proteins, which regulate T cell activation [224]. PD-1 is also able to lock activated T cells in the G1 phase of the cell cycle via the inhibition of Akt and Ras signaling to prevent proliferation [129].

- Cytotoxic T lymphocyte antigen-4 (CTLA-4, CD152) is upregulated following T cell activation. CTLA-4 inhibits excessive T cells response through its structural homology to CD28, which allows it to bind to CD80 and CD86, but with a much higher affinity than CD28, without producing a stimulatory signal. This competitive nature prevents T cell stimulation via CD28 and therefore limits excessive cytokine production in T cells and accumulation of self-reactive T cells [103][29] [57]. If expressed in regulatory T cells, it can also inhibit inappropriate activation of naïve T cells [103].

One of the key steps downstream of T cell activation is the activation of transcription factors and their relocation to the nucleus, where they can promote the expression of genes for cytokines, cell surface receptors and clonal expansion. “Classical” transcription factors involved in these downstream events are NFAT and NF- κ B.

Examples for transcriptions factors are:

- NFAT: The group of nuclear factor of activated T cells (NFAT) transcription factors can be divided into 5 members, four of which are predominantly expressed in the immune system. NFAT1, NFAT2, and NFAT4 are controlled by the intracellular Ca^{2+} level. Antigen-recognition of the TCR leads to activation of the Phospholipase C- γ , which produces inositol triphosphate (PIP3). PIP3 opens intracellular calcium storages, which in turn activates calcium-dependent calcium channels on the cell membrane to further increase the intracellular Ca^{2+} . This increase in intracellular Ca^{2+} triggers the activation of calcineurin, which dephosphorylates NFAT, which induces its translocation to the nucleus (Figure 2.3). NFAT induces the transcription of genes involved in the immune response, including IL-2 which is crucial for the proliferation of activated T cells, via the STAT3 signaling pathway [73]. The transcriptional signatures induced by NFAT differ depending on its binding partners. The best characterized NFAT interaction partner is activator protein 1 (AP1), which is induced by the RAS-MAPK pathway, after TCR stimulation. NFAT1 has also been shown to regulate cell cycle control via the downregulation of cyclin-dependent kinase 4 (CDK4). This downregulation leads to an entry in the G0-phase [55].

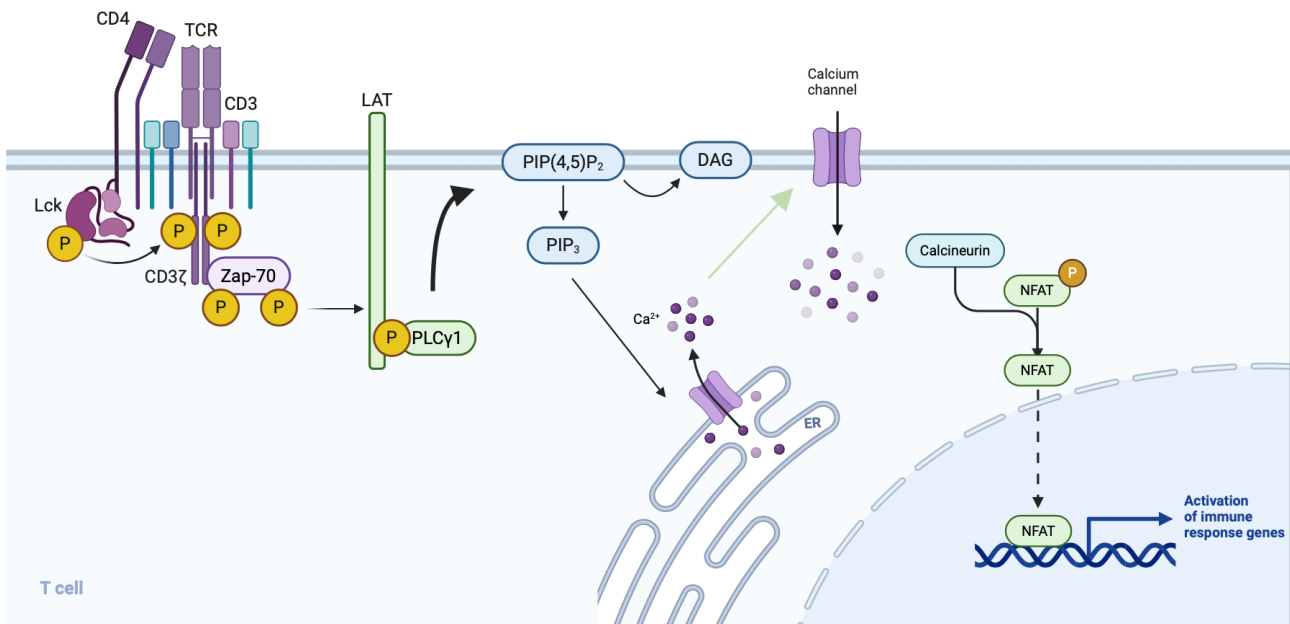


Figure 2.3 The NFAT-pathway. Upon TCR-activation, phosphorylation of Phospholipase C (PLC) is executed by Zap70. This leads to the generation of PIP₃. PIP₃ opens intracellular Ca²⁺ storages, which then trigger calcium-dependent calcium channels on the cell membrane. The resulting increase in calcium activated Calcineurin, which dephosphorylates NFAT. This leads to the translocation of NFAT to the nucleus of the cell. (Adapted from [73]) and generated with BioRender

- **NF-κB:** The Nuclear factor κB (NF-κB) family consists of p65 (Rel A), Rel B, c-Rel, NF-κB1/p50 and NF-κB2/ p52. NF-κB signalling can be mediated via two pathways, the canonical pathway and the non-canonical pathway. The canonical pathway is mediated via the degradation of IκBα by phosphorylation through the IKK complex, which is activated for example by TCR-stimulation. If IκBα is degraded, NF-κB is translocated to the nucleus [167]. The non-canonical pathway, which activates the RelB/p53 NF-κB complex, can be triggered by among others LTβR, BAFFR, CD40 and RANK, and does not rely on the degradation of IκBα but on the processing of a p52 precursor protein p100 [112]. p100 acts as a IκB-like molecule, which inhibits the nuclear translocation of RelB [61]. NF-κB-inducing kinase (NIK) induces p100 processing by ubiquitination [54]. This generates p52 and allows the nuclear translocation of the RelB/p52 NF-κB complex. NF-κB is involved in the control of activation, differentiation and effector function of activated T cells [97]. NF-κB signalling regulates apoptotic and proliferative responses in IL-2-responsive T cells [27]. Moreover NF-κB is involved in p53 mediated apoptosis [45], DNA-damage-response, autophagy, senescence and expression of pro-inflammatory genes [216]. The NF-κB signalling pathway is also intertwined with other major signalling pathways like the p53-pathway, which is required for TNF-induced NF-κB-

directed gene expression [110]. Furthermore, NF- κ B is known for having a direct influence on the cell cycle via the repression of Cyclin E [104] and the regulation of cyclin D1 [38].

The shared goal of all these intracellular changes is to generate a massive clonal expansion, followed by T cell differentiation and gain of effector functions for T cells.

To achieve the T cell expansion different interleukins are crucial. Undeniably, the most important of these is IL-2, which is secreted by the T cells itself upon activation and is mandatory for the proliferation of activated T cells acting in a positive feedback loop [2]. IL-2 is also necessary to sustain the T cell population, but can also induce IL-2-mediated activation-induced cell death upon high concentrations [14] [44]. Another important cytokine is IL-7, which can be secreted by a lot of different cells, for example thymic stromal and mesenchymal cells, lymphatic endothelial cells, and intestinal epithelial cells. Binding to the IL-7 receptor (CD127) upregulates the anti-apoptotic factors Bcl-2, Bcl-xL, and Mcl-1, while suppressing the pro-apoptotic genes Bax and Bak [229]. Dendritic cells, monocytes, and epithelial cells produce IL-15, which is recognized by the heterotrimeric IL-15 receptor [130]. It is important for T cell proliferation and inhibits IL-2 induced cell death [43].

2.1.3 The impact of T cell activation and proliferation on the genomic stability

The activation status of T cells also has an impacts the cellular DNA-damage response. CD3/CD28-dependent activation of T cells changes gene expression and chromatin structure in activated cells massively compared to resting T cells. T cell activation results among others in a strong upregulation of proteins of the DNA-repair [174]. This is in line with findings that resting CD4⁺ T cells are not able to sufficiently repair DNA damage since they fail to recruit gH2AX or 53BP1 to the damaged DNA- site, although DNA damage is recognized via ATM, ATR, and DNA-PKcs. This insufficient DNA-repair leads to apoptosis in a p53-independent but JNK/p73-dependent manner [183].

2.2 Bacterial adaptive immunity

Bacteriophages are viruses that infect bacteria and archaea [42]. A phage is composed of nucleic acid, either DNA or RNA, double- or single-stranded, and a protein capsid [144]. Unlike the complex immune systems found in eukaryotes, bacterial immunity is a streamlined yet highly effective network that employs various strategies to recognize and neutralize foreign DNA and RNA. The innate bacterial immune system includes physical barriers, such as cell walls, and nonspecific defense mechanisms, such as restriction-modification systems and RNA interference. On the other hand, the adaptive bacterial immune system is characterized by the ability to memorize past encounters with specific invaders, conferring a targeted and robust defense upon re-exposure [215].

A pivotal player in bacterial adaptive immunity is the Clustered Regularly Interspaced Short Palindromic Repeats (CRISPR) system, consisting of the CRISPR array in combination with the CRISPR-associated (Cas) proteins bound to a so-called guideRNA (gRNA). The CRISPR array was initially discovered as a repetitive sequence in the genomes of bacteria [8]. CRISPR arrays were later revealed to be storage places for viral genetic material within the bacterium's own DNA [102][80].

This mechanism allows CRISPR/Cas9 to recognize and to destroy the intruding virus through these previously "stored" DNA-sequences. The stored viral sequences are then included as protospacer sequence into a gRNA. The Cas9-gRNA complex is then able to destroy the DNA of the invading virus. This mechanism is depicted in Figure 2.4 in more detail.

- Adaption: DNA from intruding viruses is sampled and integrated into the CRISPR loci as so-called "spacers" by the Cas proteins, Cas1 and Cas2.
- Expression: Arrays of these spacers are transcribed and processed to generate small interfering CRISPR (cr)RNAs [89]. The 19-22 bp sequence of interest is thereby included into the protospacer sequence of the crRNA. The crRNA binds to the constant trans-activating RNA (tracrRNA), thereby forming the functional gRNA. Cas9 is functional after binding a crRNA-tracrRNA complex. The Cas9 enzyme has two active domains, the RuvC-like and the HNH nuclease domains.
- Interference: Cas9 endonucleases complexed with the gRNA binds and cleaves the respective DNA-sequence of the invading bacteriophage, guided by the crRNA [102]. A prerequisite of DNA-binding is a so-called protospacer adjacent motif (PAM), a DNA recognition signal, in the DNA of the bacteriophage [137]. The Cas9 enzyme has two active domains, the RuvC-like and the HNH nuclease domains. Each of the domains can cut one single DNA strand resulting together in a DNA-double strand break (DSB) [162].

Thereby, the CRISPR system enables a form of immunological "memory" in bacteria and archaea, through the integration of previously encountered viruses in the DNA. Newer studies have shown, that CRISPR also has implications for the pathogenicity of bacteria, as it enables regulation of specific genes encoding certain virulence factors [136].

In 2012, Emanuelle Charpentier and Jennifer Doudna described the mechanism of the CRISPR/Cas9 system as an RNA-guided DNA-endonuclease in their landmark paper Jinek et al. [126]. Furthermore, they recognized the potential of the CRISPR/Cas9 system as a cell engineering tool and were the first to fuse tracrRNA and crRNA into a single guide RNA (sgRNA), thereby reducing a three-component system to a two-component for future approaches [126]. The mechanism of CRISPR/Cas9 was independently confirmed by the work of Virginijus Šikšnys, who showed the cleavage activity of Cas9 *in vitro* for plasmids [123]. Only one year later, the potential of CRISPR/Cas9 in cell engineering was experimentally confirmed

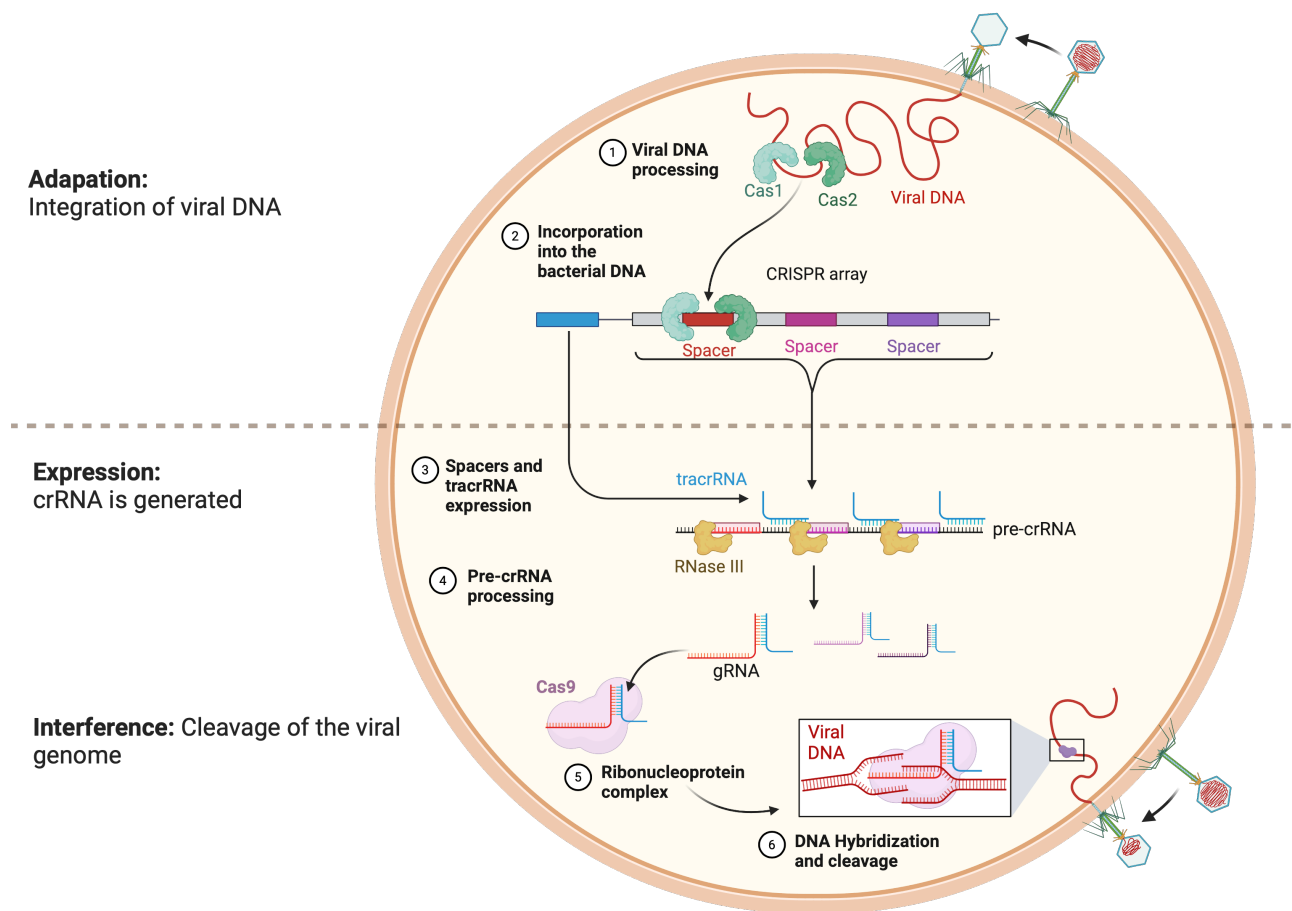


Figure 2.4 The CRISPR/Cas system in bacteria. The defense mechanism of bacteria with CRISPR/Cas consists of three phases, in the first phase the the viral DNA is integrated into the genome, to "remember" the virus. In the second phase functional crRNAs are generated. In the last phase the viral DNA is cleaved. (modified, created by Sebastián Felipe González Moraga, Nima Vaezzadeh citing: [202][170])

by expressing the CRISPR component in mammalian cells, including human cell lines, which resulted in successful targeted DSBs [132] [135].

Other gene engineering tools such as zinc finger nucleases and transcription activator-like effector nucleases (TALENs), were complex and time-consuming to produce, as the proteins need to be newly engineered for each DNA target site [139]. However, to adapt the CRISPR/Cas9 system to a new target sites only the protospacer sequence in the crRNA needs to be replaced [132].

This enables the CRISPR/Cas9 system to be highly specific, while also being highly flexible and relatively easy and cost-effective to apply to any desired DNA sequence as long as it is adjacent to a PAM sequence [132]. The PAM sequence of the widely used *Streptococcus pyogenes* Cas9, is NGG, whereas N can stand for any nucleotide. This short PAM motif can be frequently found in for example murine or human genomic

sequences [126]. Furthermore, compared to zinc finger nucleases and TALENs, CRISPR/Cas9 has a lower risk for off-target mutations [230].

2.3 Strategies to CRISPR-engineer human T cells

Several advances in CRISPR/Cas9 delivery for various applications and cell types have been developed over the years:

- Cas9 ribonucleoproteins (RNPs): Delivery of Cas9 via plasmids is not feasible for certain cell types, which are highly sensitive to cytosolic DNA, like T cells. To avoid DNA dependent toxicity, the Cas9 can be expressed as a protein, then complexed with the crRNA:tracrRNA duplexes and then nucleofected into the target cell [160]. The delivery as Cas9-RNP has enabled *in vitro* gene editing in T cells, with the added advantage, that Cas9 is only transiently active in the target cell and thereby reduces the risk of off-target effects [214]. Cas9 RNP nucleofection is also the method applies in this thesis.
- Peptide mediated: Cas9 RNPs can also be delivered into the target cell via amphiphilic peptides, which enable the RNPs to cross the cell membrane of the target cell [247]. This allows the omission of electroporation for RNP delivery, which is toxic for some cell types.
- Cas9 mRNA: Delivery of Cas9 as mRNA also limits the risk of off-target effects. Cas9 mRNA can be delivered via nucleofection or stacked into lentivirus-like particles (LVLP) [157] [204]. These particles are then pseudo-transduced into the target cell. This methodology can potentially enable CRISPR editing of cells *in-vitro* and *in vivo* including human T cells [204].
- Viral transduction: Lentiviral vectors are one of the most commonly applied ways to introduce Cas9 into target cells [149] [159] [154]. However, this leads to long-term expression of Cas9, which might lead to unwanted off-target effects or due to random integration into the genome can lead to interference with tumor suppressor genes [125]. Due to the large size of Cas9 the lentiviral transduction into human T cells is not very efficient [179].
- Lipid nano-particles: Another promising approach for *in-vitro* and *in vivo* CRISPR editing are lipid nano-particles. The addition of a lipid component encapsulates the Cas9-RNPs and allows targeting of organ tissue, for example liver or lung tissue, via intravenous injection in mice [226]. Lipid nano-particles can also be applied *in vitro* to human T cells and induces less cell death compared to nucleofection [248]

All of the the above mentioned options, which rely on nucleofection (Cas9 RNPs, Cas9 mRNA), enable the generation of a knock-in (KI) for the targeted locus by simply adding a dsDNA HDR-template during

the nucleofection. The addition of a dsDNA HDR-template is also possible for peptide-mediated delivery, although at a low KI-efficiency [247]. This HDR-template contains the desired sequence in addition to homology-arms for the respective target region. The addition of HDR-template allows the harnessing of the homology-directed DNA repair-pathway and a controlled incorporation of new DNA sequences into the genome. Additionally, it is also possible to provide a HDR-template for Cas9 delivery methods independent of nucleofection via adeno-associated-virus-mediated delivery [247].

Engineered Cas9 variants have been developed that do not rely on DSB or separate HDR templates:

- Base editing: Base editors consist of a Cas9 nickase, Cas9 with only one active nuclease domain, fused to enzymes such as cytidine deaminase which converts for example cytidine to thymidine. Base editing is able to modify individual bases of the DNA without cleavage of the DNA-backbone. This allows for highly specific editing of single nucleotide variants with minimal risk for off-target effects [222]
- Prime editing: Prime editing allows modification of the target gene locus without a DSB by introducing a DNA sequence containing the desired sequence via the use of a reverse transcriptase fused to Cas9 nickases. Genetic information is thereby directly copied from a prime editing gRNA (pegRNA) into the target locus whereas the pegRNA serves not only as a guide to the target locus but also serves as the RT template [193].

2.4 Harnessing immune mechanisms for therapy

In the last decade a new class of therapeutics came into fruition, called immune therapeutics. The key principle of immune therapeutics is the modification of the already existing immune response in patients to clear infections or cancer more effectively or dampen the immune response in autoimmune diseases.

Several strategies have been developed to modulate the immune system:

- Monoclonal antibodies target a specific surface proteins expressed on immune cells. For example the CD20 antibody rituximab is used in the therapy of B cell lymphomas, to ablate the malignant B cells [67] [111] [34].
- Checkpoint inhibitors are a sub-class of monoclonal antibodies: Certain types of cancer can escape the immune response by activating co-inhibitory signalling pathways thereby dampening the effector functions of cytotoxic CD8 T cells. This process can be prevented if the corresponding receptors on the T cells are blocked by checkpoint inhibitors. Currently, there are two main categories of checkpoint inhibitors available: PD-1 and CTLA-4 antibodies. CTLA-4 antibodies like Ipilimumab

block CTLA-4 from binding to CD80/CD86, which in turn decreases costimulation [119]. PD-1 targeting antibodies like Nivolumab bind to the PD-1 receptor on immune cells and block them from the anti-inflammatory signals of PD-L1, which can be expressed on tumor cells [164]. However, these strategies also have severe side-effects for the patients including the development of severe autoimmune diseases by reactivating autoreactive T cells or T_{reg} depletion [203] [219] [249].

- Cancer vaccination: Cancer vaccination strategies include preventive vaccination for viruses, which can cause certain cancers, like HPV or HBV or a therapeutic vaccination, which targets proteins expressed by the tumor in abundant levels or neoantigens only expressed by the tumor cells [63] [46]. Therapeutic vaccination primes the immune response to exert a more forceful immune response against these tumor antigens [116].
- Another immune therapy is based on T cells, either from the patient (autogenic) or a donor (allogeneic), which are extracted and conditioned to recognize certain antigens before being re-infused into the patient. Since CD8+ T cells are designed to neutralize infected or malignant cells, they are a perfect tool against cancer. First attempts of T cell-based therapies used *ex vivo* expanded tumor-infiltrating lymphocytes (TILs) derived from tumor biopsies [12] [5]. However, biopsies or sufficient numbers of TILs are not always available. As an alternative strategy, T cells can be isolated out of the peripheral blood and equipped with tumor-targeting receptors such as chimeric antigen receptors (CARs) or TCRs of certain specificities. CARs are synthetic receptors consisting of a single-chain antibody fab-fragment targeted against a tumor antigen and an intracellular signaling domain, classically consisting of domains derived from CD28 or CTLA-4 and CD3- ζ [11] [17]. The first CAR T cells successfully used in clinical trials targeted cells expressing CD19 on the cell surface in patients with B-cell acute lymphoblastic leukemia or non-hodgkin-lymphoma and now also systemic lupus erythematosus [106] [121] [243] [246]. TCRs and CARs can be introduced into the patients T cells via a lentiviral or retroviral vectors or alternatively introduced into the TCR locus via CRISPR-mediated knock-ins [208]

2.5 Benefits of CRISPR-engineered T cells

Although T cell therapies proved to be quite successful for certain applications, for example cancers of the haematopoietic systems, there are still some hurdles to overcome. Especially in solid tumors, one of the major challenges for CAR T cells is the microenvironment around the tumor. This microenvironment exerts immunosuppressive functions through myeloid-derived suppressor cells [47] and at least in some cases through T_{reg}-cells [70]. Other factors like inhibitory signals and low immunogenicity in the tumor also impair the immune response of CAR- or TCR-transgenic T cells and lead to decreased cell expansion,

short half-life and reduced efficacy [225] [172]. This phenomenon is also called "T cell exhaustion" and is characterized by a decrease in effector function like cytokine production, proliferation and an increase in inhibitory receptors, like PD-1 or CTLA-4. This limits the efficacy of T cell therapies, which could potentially be restored via gene editing of for example some of the inhibitory receptors like PD-1 [223] [99]. One possible solution for this problem is to genetically engineer the CAR T cells to no longer express these receptors, which was done by Stadtmauer et al. They removed the PD-1-receptor via CRISPR/Cas9 and ablated the TCR- α and β chains for better CAR expression. Engineered T cells could be monitored for up to nine months in the blood of patients with hematological malignancies in this clinical phase I study [223]. This study could prove the feasibility of this approach. Building on this, CRISPR-engineered T cells were also used in this study to express a synthetic TCR, which binds the individual neoantigens of tumor cells from 16 patients with different solid refractory cancers [238].

The possible side-effects of CAR T cells pose another challenge to their broader implementation into the clinic. The most common one is cytokine release syndrome (CRS). It is caused by the release of pro-inflammatory cytokines like interferon- γ and IL-6 [142]. CRS can be caused by treatments, which boost the immune response in a supra-physiological way, like monoclonal antibodies (for example rituximab) or CAR T cells. [166]. This abundance of pro-inflammatory signals can cause various symptoms, like fever, headache and fatigue, but can also result in organ-failure and even death [109]. Possible strategies to reduce the risk of CRS are a more physiological integration of the synthetic TCR into the genome, so that it underlies the physiological regulation of the T cell [208]. Another improvement of T cell therapeutics, which is enabled through CRISPR/Cas9 is a so-called "suicide switch" to destroy the infused cells in case of severe CRS through the induction of CRISPR/Cas9, which then causes severe DNA damage leading to apoptosis [244]. The possible cell engineering strategies with the CRISPR/Cas9 system are not limited to the above-mentioned examples, but also highlight the need to make modifications to the DNA in as highly controlled manner to avoid adverse effects. .

2.6 Mechanisms and hurdles in gene-engineering

To understand the unique challenges of gene-engineering via CRISPR/Cas9 a detailed understanding of the intracellular mechanisms during and after CRISPR editing is necessary. After successful introduction of a DSB, the cell can activate different DNA-repair mechanisms (Figure 2.5). The most prominent ones are the non-homologous end-joining pathway (NHEJ), the homology-directed repair pathway (HDR) and the microhomology-mediated end joining pathway (MMEJ).

NHEJ is one of the most common pathways for the repair of DSB [96] (Figure 2.5). If a DSB is sensed, a whole machinery is assembled at the cleavage site. Key components of this complex are:

- The Ku protein is a heterodimer consisting of Ku70 and Ku80. This heterodimer binds onto the two loose ends of the DNA and recruits the other proteins involved in NHEJ-mediated-repair. Ku directly interacts with DNA-dependent protein kinase catalytic subunit (DNA-PKc) and XRCC4-like factor (XLF) [87].
- DNA-dependent protein kinase catalytic subunit (DNA-PKc) binds to the Ku-complex and together with it converges the loose ends of the DNA.
- Artemis is involved in DNA-end processing. During this process the DNA ends get processed and shortened, so that either blunt end DNA or a 3' overhang is generated [107] [108] [60]
- XLF-XRCC4-DNA ligase IV complex facilitates the ligation of the DSB [82] [83].

NHEJ is a fast and efficient DNA repair mechanism, which is active throughout the cell-cycle [92]. However, NHEJ is also an error-prone process leading to point-mutations which can lead to pre-mature stop codons or dysfunctional proteins. Missing or additional nucleotides can lead to frame-shift mutations or premature stop codons thereby resulting in a protein KO [195] [132].

Homology-directed repair can mediate the controlled replacement or insertion of DNA sequences resulting in knockins (KIs), if DNA templates are provided (Figure 2.5). Classically the allele on the respective chromosome is used as a template [50]. This repair mechanism only takes place during the S and the G2 phases of the cell cycle [176] [69] [127]. During HDR-mediated DNA repair, DNA ends are bound by a complex consisting of: Mre11, Rad50 and NBS1. This results in an mostly error-free DNA repair. The individual steps of HDR-mediated-repair are:

- MRE11–RAD50–NBS1 (MRN) complex is formed on the damaged DNA-ends. This allows for the aggregation of further proteins necessary for DNA-repair [190].
- ATM then phosphorylates H2A histone family member X (H2AX) and form together a complex, which stabilizes the DNA-ends [133].
- In a next step 3' DNA overhangs are generated via the 5' exonucleases C-terminal-binding protein-interacting protein (CtIP) or exonuclease 1-Bloom helicase (Exo1-BLM) [147].
- Human replication protein A (RPA) binds to these overhangs and is then replaced by Rad51, PALB2, BRCA1 and BRCA2, which search for a homologous DNA-template [140].
- Finally, DNA ends are ligated by Resolvase A [91].

Microhomology-mediated end joining (MMEJ) is an alternative pathway to NHEJ acting independently of KU70 or DNA-PKCs [22]. MMEJ uses 5 – 25 bp long microhomologous sequences of the DNA target

region with the DSB. Similarly to other DNA-repair mechanisms, one of the first steps is the processing of DNA ends via 5'–3' resection by the MRX complex, Sae2 and Exo1. This continues until a homology region is reached, which leads to annealing of both strands. After that the DNA-flaps are trimmed and the DNA is ligated [93].

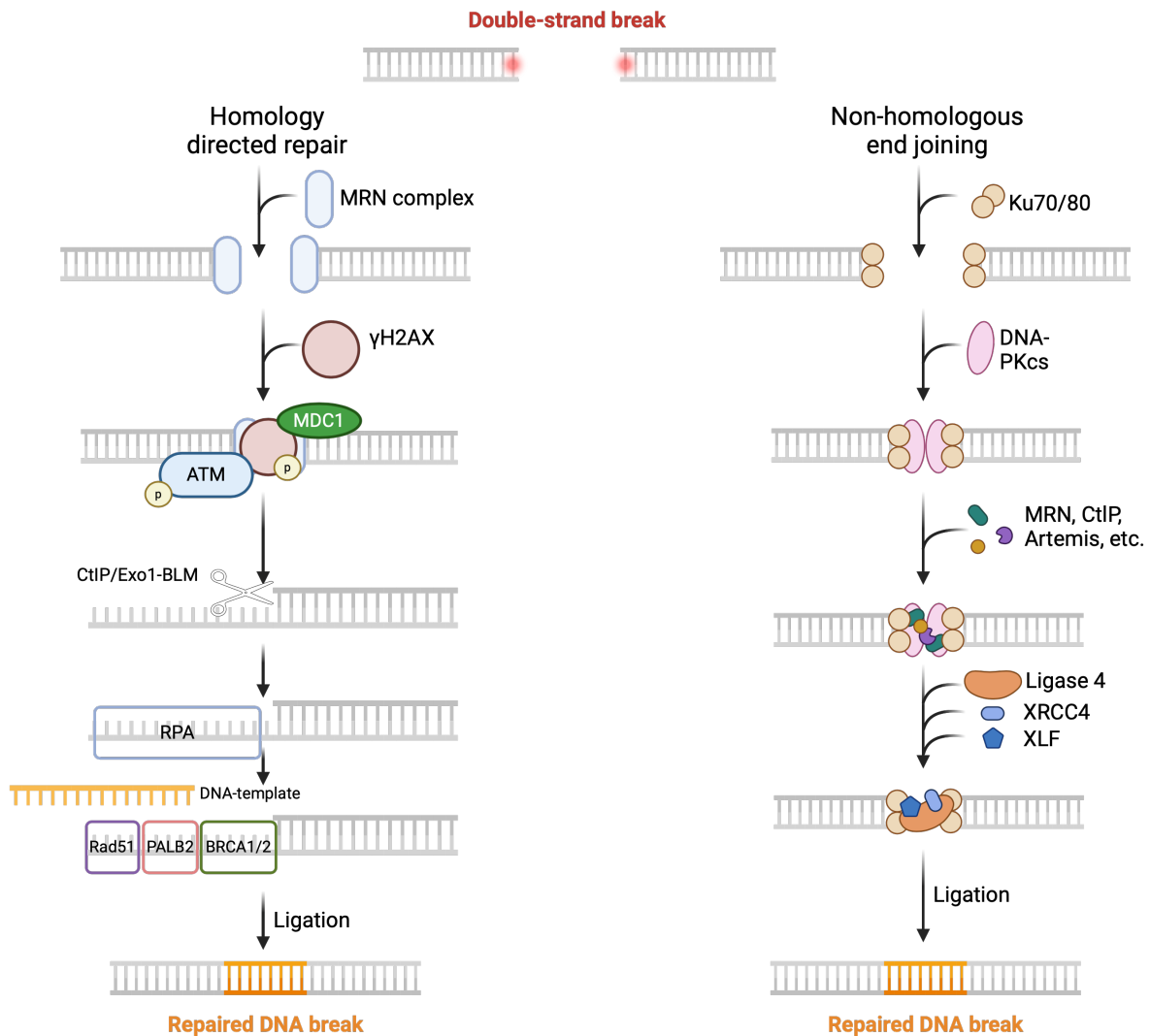


Figure 2.5 HDR and NHEJ DNA repair pathways. Shown here, are two possible DNA-repair pathways activated after a DNA DSB. On the left side, homology directed repair (HDR) is depicted, which included the accumulation of the MRN complex, phosphorylation of γ H2AX histones and ATM and MDC1 recruitment, to generate a 3' single-stranded overhang on the site of the DSB. Optionally an artificial HDR-template can be introduced into the cell, which can lead to the controlled replacement of DNA sequences. On the right side non-homologous end joining is shown, which connects DNA ends with via the KU70/KU80/DNA-PKcs complex, DNA end processing and DNA ligation (adapted from [212])

2.6.1 The role of p53 during CRISPR-editing

One of the main pathways for the detection of DNA-damage is mediated by the tumor suppressor gene p53, which is also known as the "guardian of the genome", as it is crucial for maintaining genomic stability. p53 also plays a role in the cellular response to oncogene activation, hypoxia or metabolic dysfunctions [115] [120] [23]. Several studies could show that CRISPR-induced DSBs lead to an recruitment and activation of p53 [182] [184] [181] [180].

p53 is encoded by the *TP53* locus and is translated at a steady rate [114] [95]. The intracellular level of p53 are normally not impacted by changes in *TP53* translation, but rather by modulation of p53-protein degradation. However, there are exceptions to this rule, for example after TCR-signalling, the rate of p53 translation is down-modulated [150]. p53 degradation is mediated by ubiquitin and executed by the E3 ubiquitin ligase mouse double minute 2 (MDM2) at a steady rate. To increase the stability of p53 and transfer into its active state, posttranslational modifications are added, which reduce the degradation rate and therefore increase the intracellular level of p53, which then in turn triggers p53's downstream functions [85] [31] [165].

Various stressors can induce DNA damage, like ionizing radiation, ultraviolet radiation or genotoxic agents like chemotherapeutics [4] [3] [138]. The DNA damage response (DDR) of p53 is mediated by ataxia telangiectasia mutated kinase (ATM) and ataxia telangiectasia and Rad3-related protein (ATR), both of which phosphorylate checkpoint kinase (CHK) 1 and 2 upon sensing of DNA-damage, which then phosphorylate p53 [75]. One of the functions of p53 is to initiate DNA-repair or, if this is not possible, to trigger apoptosis [64]. Thereby, p53 prevents cells with alterations in their genome from multiplying and therefore, prevents the spread of potential cancer cells [19].

p53 can reach this goal via various signalling pathways (Figure 2.6):

- cell cycle regulation: The first step in DNA repair is to stop the cell-cycle from progressing. The cell cycle arrest elongates the time for the respective DDR-pathways to execute their functions [64]. To achieve this p53 can induce the expression of the cyclin-dependent kinase inhibitor p21, which inhibits the activity of cyclin-dependent kinases (CDKs), responsible for cell cycle progression. This results in a cell cycle arrest at the G1/S or M/G1 checkpoints [21] [37].
- DNA-damage-repair: p53 can bind to p53-binding protein 1 (53BP1), which plays a crucial role in the choice of DNA repair pathways, since it promotes NHEJ and inhibits HDR upon DNA-binding [153].

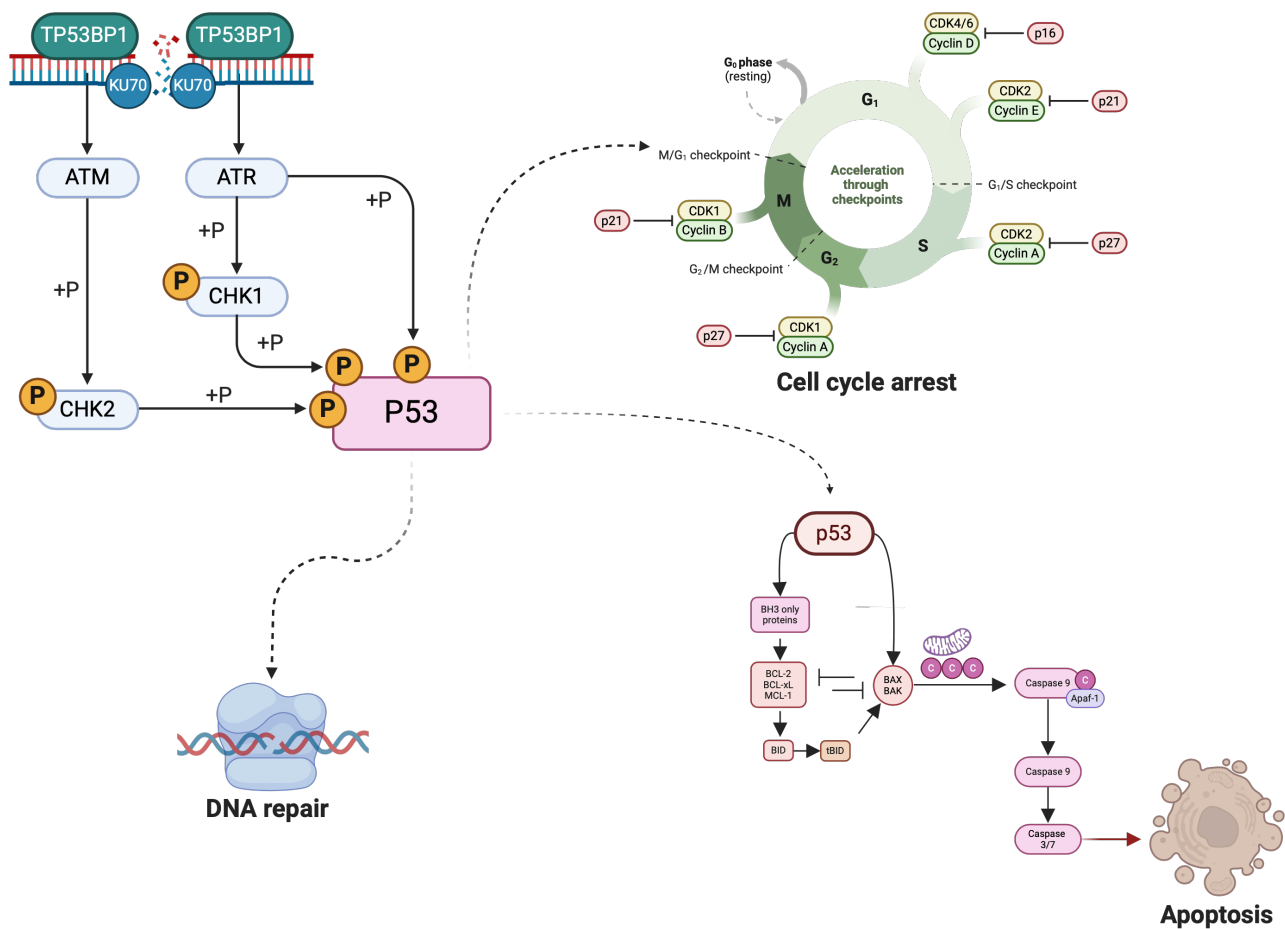


Figure 2.6 Schematic depiction of potential p53-mediated signalling pathways after CRISPR-induced DSB. p53 is activated by a DSB. DSBs lead to posttranslational modifications on p53, which increases the stability of p53, and therefore the intracellular level of p53 [71]. High levels of p53 enables p53's downstream functions including the activation of DNA-repair, the regulation of the cell cycle via p21 and the induction of apoptosis via BAX/BAK and Caspase 9 [221] [28] [66] [163].

- If the DNA-repair fails, p53 is also able to induce apoptosis through upregulation of pro-apoptotic genes, such as BAX, PUMA and NOXA. This results in permeabilization of the mitochondrial outer membrane, which then triggers Caspase 9, 3 and 7 and leads to apoptosis of the affected cells [33] [49].

The pivotal role of p53 is underscored by the fact that alterations of the p53-pathway are a hallmark of cancer development, with over 50% of cancers showing a mutation in the *TP53* gene [19] [78]. These mutations lead to a loss of tumor suppressive functions and increase genomic instability [25] [124].

Since CRISPR/Cas9 is used more and more in laboratories and clinics all over the globe, it would be very important to understand what can cause these large deletions, if there is an involvement of p53 and if there is any way to prevent them from happening.

2.6.2 Specificity of CRISPR-engineering

Although CRISPR/Cas9 is specifically introducing a DSB 2 -3 bps upstream of the PAM sequence, which and mostly results in point mutations or small deletions and insertions, also large deletions have been described. Kosicki et al. could show, that in cell lines and in embryonic stem cells that up to 20% of cells showed deletions larger than 250bps. Some deletions were even as long as 2kbps [185]. At sites rich in microhomologies 23% of edited cells carried unwanted large deletion in at least on allele when using Cas9, or Cas10a [205]. Adikusuma et colleagues could show that 37.5% of CRISPR-edited murine cells beared a large deletion [177]. Another study analyzed 17 gene loci in the mouse genome after CRISPR/Cas9 editing and found a rate of 40% for deletions larger than 200bps after single sgRNA editing [173]. This could have some serious implications for the clinical application of CRISPR/Cas9 edited cells, since there is a small chance of the deletion of important sequences in the genome, e.g. tumor-suppressor-genes. There is also the possibility of chromosomal rearrangements, which comes with the generation of large deletions into the genome. These chromosomal translocations could also be observed by Stadtmauer et al [223], but they also noticed that the rate of cells with chromosomal translocations decreased over time *in vivo*, but were still detectable in all patients on day 170 after infusion. Recent publications found aneuploidy to be a frequent event after CRISPR/Cas9 editing. They reported to found a chromosome 14 loss in up to 9% of cells after targeting the *TRAC*, which is located on chromosome 14. They also reported, that 1,4% of these edited cells have a gain of chromosome 14. The same findings were made for simultaneously editing the *TRBC2*-locus, which lead to additional chromosome 7 loss in 9,9% of the edited cells. These rates decreased *in vitro*, but aneuploidy was still found on day 11 after editing [241].

3 Aim of the thesis

Since the advent of CRISPR/Cas9 in basic and translational research, gene editing cells have become more and more achievable. This led to a huge increase in gene editing for a lot of applications, especially for cell therapeutics in clinical settings. The advantages of CRISPR/Cas9 are manifold. However, with an increase in use, there is also an increasing safety risk for cell products treated with CRISPR/Cas9, namely the risk for off-target mutations or large on-target deletions.

The rate of these mutations is fairly low, and since most of the DNA is non-coding, almost none of them have any influence on the edited cell as a whole. Although the risk for such a mutation is low, the consequences are possibly severe. For example, if a tumor suppressor gene is affected by a large on-target deletion, it could render its anti-tumor functions useless and enable malignant transformation in the affected cell.

A lot has been done, to predict the gene-editing outcome regarding the behaviour of CRISPR/Cas9. There are a lot of tools to generate optimal gRNA sequences and predict possible off-targets, like [201] [252] [161] [236].

This increase the on-target efficacy and reduces possible off-targets. However, the generation of indels on the editing site does not only depend on the sequence of the gRNA, but also on the DNA-damage-response from the target cell. There are various factors, which can have an influence on the indel formation, and more important on the generation of large deletions, off-targets and chromosomal aberrations, like the cell's metabolism, the preferred DNA-repair pathway in each cell, the current level of p53 when the editing takes place, the proliferation speed and activation status of the cell.

It was the aim of this thesis to elucidate the connection between T cell activation status, their proliferation speed and the mean deletion size after gene editing via CRISPR/Cas9. For this purpose I established a experimental workflow for the CRISPR-editing of primary human T cells, incorporating flow-cytometry and next-generation-sequencing, which allowed me to analyze deletions up to 200 bp after CRISPR-editing. This workflow was used for the analysis of multiple clinically relevant gene editing targets. Furthermore during the course of this thesis, I noticed a new function of an already known small molecule named pifithrin- α . This molecule, contrary to its known function as a p53-inhibitor, reduces the mean deletion size, if applied during CRISPR-editing.

Another goal was the translation of my findings to a larger scale with the help of a cooperation with the Cathomen workgroup. This was achieved via the use of a method called Chromosomal Aberrations Analysis By Single Targeted Linker-Mediated PCR Sequencing, which allowed the detection of deletions significantly larger than 200 bps and also chromosomal translocations. This method confirmed my findings for the differences in mean deletion size in non-activated versus activated T cells and for the effect of pifithrin- α in activated cells.

4 Material and Methods

4.1 Materials

4.1.1 guideRNA

All guideRNAs were manufactured by Integrated DNA Technologies Inc., Coralville.

Table 4.1 list of gRNA

Name	Sequence
CD4	CAGGGCCATTGGCTGCACCG
PDCD1	CGACTGGCCAGGGCGCCTGT
AAVS1	GGGACCACCTTATATTCCCA
TP53	TCCTCAGCATCTTATCCGAG
CXCR4	GAAGCGTGATGACAAAGAGG
LAG3	CTGTGCATTGGTTCCGGAAC
TRAC	AGAGTCTCTCAGCTGGTACA
non-targeting ctrl. (NT)	GGTTCTTGACTACCGTAATT
tracrRNA	n/a

4.1.2 Nucleofection Supply

Table 4.2 list of nucleofection supply

Name	Product number	Manufacturer
Streptococcus pyogenes Cas9-NLS	n/a	in-house
P3 Primary Cell 96-well Nucleofector™ Kit	V4SP-3960	Lonza
P3 Primary Cell 4D-Nucleofector® X Kit L	V4XP-3024	Lonza
Enhancer	n/a	Sigma-Aldrich

4.1.3 Buffer and media

All buffers for cell culture use were made under sterile conditions.

Table 4.3 list of buffers and media

Name	Ingredients
cRPMI	RPMI1640 10% FCS 1% HEPES 1% L-Glut 1% P/S 1% Non-essential Amino Acids (NEAA) 1% Na-Pyruvat
EasySep-Buffer	2% FCS 1mMol/l EDTA
Freezing medium	FCS 10% DMSO
FACS-Buffer	PBS 0,5% BSA 2mMol/l EDTA
Nucleofection-Buffer	18,18% Supplement 81,82% P3

4.1.4 Chemicals and molecules

All items in table 4.4 were stored according to the manufacturers recommendations.

Table 4.4 list of chemicals

Name	Product Number	Manufacturer
Penicillin-Streptomycin-Glutamine (100X)	10378016	ThermoFisher
HEPES, 1M Buffer Solution	15630056	ThermoFisher
MEM Non-Essential Amino Acids Solution (100X)	11140050	ThermoFisher
Pifithrin- α (hydrobromide)	HY-15484-5mg	Hözel Diagnostika
Pifithrin- μ	506155-10MG	Sigma
DPBS, no calcium, no magnesium	14190094	ThermoFisher
Ethylenediamine tetraacetic acid disodium salt dihydrate	8043.1	Carl Roth
Dimethylsulfoxide (DMSO)	A994.1	Carl Roth
Ethanol	T868.1	Carl Roth
FCS; Charge 2364724	10270106	ThermoFisher
Sodium Pyruvate (100 mM)	11360070	ThermoFisher
Propidium Iodide Solution	421301	Biolegend
RPMI 1640 Medium, no glutamine	31870074	ThermoFisher
DPBS, no calcium, no magnesium	14190094	ThermoFisher
Trypan Blue solution	T8154	Sigma-Aldrich
Hydrochloric acid	4625.1	Carl Roth
TRIS Hydrochlorid	9090.6	Carl Roth
Bovine Serum Albumin (BSA) Fraction V, US Origin, lyophilized powder	P06-1391100	PAN

4.1.5 Antibodies

All Antibodies are directed against human antigens and were titrated before use.

Table 4.5 list of antibodies and fluorophores

Name	Fluorophore	Clone	Product number	Manufacturer
PE anti-human CD184 (CXCR4)	PE	12G5	306506	Biologend
BV421™ anti-human CD184 (CXCR4)	BV421	12G5	306518	Biologend
BV785™ anti-human CD8	BV785	SK1	344740	Biologend
PE/Dazzle™ 594 anti-human CD8	PE/Dazzle™ 594	SK1	344744	Biologend
FITC anti-human CD8a	FITC	RPA-T8	301050	Biologend
Zombie Aqua™ Fixable Viability Kit	n/a	n/a	423101	Biologend
Zombie NIR™ Fixable Viability Kit	n/a	n/a	423106	Biologend
CFSE Cell Division Tracker Kit	CFSE	n/a	423801	Biologend
PE anti-human CD4	PE	SK3	344606	Biologend
Pacific Blue™ anti-human CD4	PacificBlue	SK3	344620	Biologend
PerCP anti-human CD4	PerCP	SK3	344624	Biologend
BV785™ anti-human CD4	BV785	SK3	344642	Biologend
APC anti-human CD3	APC	SK7	344812	Biologend
PE anti-human CD3	PE	SK7	344805	Biologend
BV785™ anti-human CD3	BV785	SK7	344842	Biologend
p53 - APC	APC	REA1132	130-109-571	Miltenyi
p53 pS15 - PE	PE	REA825	130-112-620	Miltenyi
PE anti-p53	PE	DO-7	645805	Biologend
APC anti-human CD279 (PD-1)	APC	EH12.2H7	329908	Biologend
BV650™ anti-human CD279 (PD-1)	BV650	EH12.2H7	329950	Biologend
PE anti-human CD279 (PD-1)	PE	EH12.2H7	329906	Biologend
PE anti-human α/β T Cell Receptor	PE	IP26	306708	Biologend
APC anti-human TCR α/β	APC	IP26	306718	Biologend
BV510™ anti-human CD223 (LAG-3)	BV510	11C3C65	369318	Biologend
123count eBeads	n/a	n/a	01-1234-42	ThermoFisher

4.1.6 Cell culture

Every item listed in table 4.6 was handled under sterile conditions, when used in cell culture and stored at the adequate temperature.

Table 4.6 list of reagents used in the cell culture

Name	Product number	Manufacturer
Recombinant Human IL-2	200-02-1000	Peprotech
Recombinant Human IL-7	200-07	Peprotech
Recombinant Human IL-15	200-15	Peprotech
Dynabeads™ Human T-Activator CD3/CD28 for T Cell Expansion and Activation	11132D	ThermoFisher
Ultra-LEAF™ Purified anti-human CD3 UCHT1	300465	Biolegend
Ultra-LEAF™ Purified anti-human CD28 CD28.2	302943	Biolegend
ImmunoCult™ Human CD3/CD28/CD2 T Cell Activator	10990	Stem Cell
15 mL High Clarity PP Centrifuge Tube, Conical Bottom	352096	Falcon
50 mL High Clarity PP Centrifuge Tube, Conical Bottom	352070	Falcon
MojoSort™ Human CD4 T Cell Isolation Kit	480130	Biolegend
MojoSort™ Human CD8 T Cell Isolation Kit	480129	Biolegend
QuickExtract™ DNA Extraction Solution	QE0905T	Lucigen
DNeasy Blood & tissue Kit	69504	Qiagen
Pancoll human, Density: 1.077 g/ml	P04-601000	PAN
SepMate™-50 (IVD)	85460	Stem Cell
96-well Clear Flat Bottom TC-treated Microplate, Sterile	3628	Corning
96-well Clear V-Bottom Polystyrene Not Treated	3896	Corning
48-well Clear Flat Bottom TC-treated Cell Culture Plate	353078	Falcon

4.1.7 Amplicon Next Generation Sequencing (NGS)

Table 4.7 list of supplies for Amplicon-NGS

Name	Product number	Manufacturer
96-well PCR Plate, non skirted	4ti-0750	4titude
2x GoTaq Long PCR Master Mix	M4021	Promega
Agencourt® AMPure® XP beads	A63880	Beckman Coulter
Nextera XT Index Kit v2 Set A	FC-131-2001	Illumina
Nextera XT Index Kit v2 Set B	FC-131-2002	Illumina
Nextera XT Index Kit v2 Set C	FC-131-2003	Illumina
Nextera XT Index Kit v2 Set D	FC-131-2004	Illumina
SpectraMax Quant AccuBlue HighRange dsDNA Kit	R8358	Molecular Devices
MiSeq Reagent Nano Kit v2 (500-cycles)	MS-103-1003	Illumina

4.1.8 Primer

All primers manufactured by Sigma-Aldrich, St. Louis. They were tested on unedited genomic DNA before use.

Table 4.8 list of primers

NAME	TARGET	SEQUENCE
CD4_ADAPTER_FWD1	CD4	TCGTCGGCAGCGTCAGATGTGTATAAGAGACAGGCA CTCACACACACAGCCCAGG
PD1_2_ADAPTER_FWD1	PD-1	TCGTCGGCAGCGTCAGATGTGTATAAGAGACAG TCACTCTCGCCACGTGGATGT
AAVS1-1,2,4_MISEQ_FWD2	AAVS1	TCGTCGGCAGCGTCAGATGTGTATAAGAGACAGGGT TCTGGGAGAGGGTAGCGCA
P53_6.1_MISEQ_FWD	P53	TCGTCGGCAGCGTCAGATGTGTATAAGAGACAGGCG CCATGGCCATCTACAAGCA
CXCR4_ADAPTER_FWD1	CXCR4	TCGTCGGCAGCGTCAGATGTGTATAAGAGACAGCCG AGGAAATGGGCTCAGGGGA
LAG3_MISEQ_FWD2	LAG3	TCGTCGGCAGCGTCAGATGTGTATAAGAGACAGGGG TTCCAGGCCAGGAAAACGG

TRAC2_MISEQ_FWD	TRAC2	TCGTCGGCAGCGTCAGATGTGTATAAGAGACAGTCC CAGTCCATCACGAGCAGCT
CD4_ADAPTER_REV1	CD4	GTCTCGTGGGCTCGGAGATGTGTATAAGAGACAGAG GACTCAGGGGTTTGAGGGCC
PD1_2_ADAPTER_REV1	PD-1	GTCTCGTGGGCTCGGAGATGTGTATAAGAGACAGGC TCAGGGTAAGGGGCAGAGCT
AAVS1-1,2,4_MISEQ_REV2	AAVS1	GTCTCGTGGGCTCGGAGATGTGTATAAGAGACAGCC GGGCCCTATGTCCACTTCA
P53_6.1_MISEQ_REV	P53	GTCTCGTGGGCTCGGAGATGTGTATAAGAGACAGTA AGCAGCAGGAGAAAGCCCCC
CXCR4_ADAPTER_REV1	CXCR4	GTCTCGTGGGCTCGGAGATGTGTATAAGAGACAGGC CAGGTAGCGGTCCAGACTGA
LAG3_MISEQ_REV2	LAG3	GTCTCGTGGGCTCGGAGATGTGTATAAGAGACAGTA GGTGAGGATGCAGCCCCAGG
TRAC2_MISEQ_REV	TRAC2	GTCTCGTGGGCTCGGAGATGTGTATAAGAGACAGTG CTGTTGTTGAAGGCGTTTGCA
LINKER_POS_STRAND	CAST-SEQ LINKER	GTAATACGACTCACTATAGGGCTCCGCTTAAGGGACT
LINKER_NEG_STRAN	CAST-SEQ LINKER	P-GTCCCTTAAGCGGAGC
CD4_BAIT_3	CD4	ACCTGACACAGAAGAAGATG
CD4_DECOY_F3	CD4	ATTTCTCTCCCTTGACAGTTC
LINKER_PREY_I	CAST-SEQ LINKER	GTAATACGACTCACTATAGGGC
CD4_BAIT_NESTED	CD4	GACTGGAGTTCAGACGTGTGCTCTTCCGATCTGA TGCCTAGCCCAATGAAAAGCAG
CD4_PREY_NESTED	CD4	ACACTCTACACTCTTTCCTACACGACGCTCTTC CGATCTAGGGCTCCGCTTAAGGGAC
RABL6_MISEQ_FWD1	RABL6	TCGTCGGCAGCGTCAGATGTGTATAAGAGACAGCTG CAGAGGGAGACGCTGTTGC
SPON2_MISEQ_FWD	SPON2	TCGTCGGCAGCGTCAGATGTGTATAAGAGACAGAGG AGGCTCCAGACAGTACCTGA

RABL6_MISEQ_REV	RABL6	GTCTCGTGGGCTCGGAGATGTGTATAAGAGACAGC CCAGCAGCACTCCATGAGCAC
SPON2_MISEQ_REV	SPON2	GTCTCGTGGGCTCGGAGATGTGTATAAGAGACAG CCTGACCCACGACCCAGCAATG

4.1.9 Software

Table 4.9 list of software

Software	Version	Company
FlowJo	10.7.1	Becton Dickinson & Company
CytExpert	2.3	Beckman Coulter
FACS Diva	8.0	Becton Dickinson & Company
Summit	6.3	Beckman Coulter
Prism 10 for macOS	10.2.1	GraphPad Software
RStudio	2023.03.1+446	Posit Software
CRISPResso2	2.2.7	Pinellolab
Microsoft Office 2019	16.78.3	Microsoft
Affinity Designer	1.10.6	Serif

4.1.10 Equipment

Table 4.10 list of equipment

Equipment	Name	Company
Biological Safety Cabinet	HeraSafe	Heraeus
Centrifuges	Multifuge	Heraeus
Flow Cytometer	Cytoflex LX	Beckman Coulter
	Cytoflex S	Beckman Coulter
Flow Cytometry Sorter	FACS Aria III	Becton Dickinson & Company
	MoFlo Astrios EQ	Beckman Coulter
Neubauer Chamber	Neubauer Improved	Schubert
Pipettes	Research Plus	Eppendorf
pH-Meter	MultiCal pH 526	WTW
PCR-Cycler	T3-Thermoblock	Biometra
Nucleofector	4D Nucleofector Core-Unit	LONZA
	4D Nucleofector X-Unit	LONZA
	4D Nucleofector 96-well shuttle	LONZA
NG-Sequencer	MiSeq	Illumina
Microplate reader	SpectraMax i3x	Molecular Devices

4.2 Isolation and culture of primary human T cells

PBMCs were generated from Buffy coats, which were collected by the German Heart Center Munich, with the approval of the Ethics Committee TUM School of Medicine and informed consent of the patients or from the "Blutspendedienst des Bayerischen Roten Kreuzes". The cells were isolated via gradient density centrifugation at 1200g for 20min with Pancoll in SepMate 50 tubes. The PBMCs were washed with EasySep buffer before CD4- or CD8-Enrichment was done using either the MojoSort Human CD4 T cell Isolation Kit or the MojoSort Human CD8 T cell Isolation Kit. The cells were then cultured at 37°C for 24 to 48 hours at a concentration of $1 - 2 \times 10^6$ cells/ml in complete Roswell Park Memorial Institute (cRPMI) medium. If PBMCs were used, which had been frozen for long-term storage in freezing medium, an additional overnight rest was added after slowly thawing the cells before CD4-/CD8-enrichment.

4.3 Cas9 RNP assembly and nucleofection

crRNA:tracrRNA duplexes were generated by mixing 100 μ M crRNA and 100 μ M tracrRNA in an equimolar ratio and incubate them for 5 min at 96°C. An equal volume of 40 μ M Streptococcus pyogenes Cas9-NLS (Cas9 expression plasmid pMJ915 (Addgene)) was carefully added to the crRNA-tracrRNA duplex and incubated for 20 min at room temperature (RT). Depending on the amount of cells either of the following reaction vessel was used:

- 96-well electroporation plate: 1×10^6 cells were resuspended in 20 μ l nucleofection buffer, 4 μ l of RNPs were added, together with 1 μ l of 100 μ mol/l electroporation enhancer. After nucleofection 80 μ l cRPMI was added.
- Nucleovette vessel: 10×10^6 cells were resuspended in 100 μ l nucleofection buffer, 20 μ l of RNPs were added, together with 5 μ l of 100 μ mol/l electroporation enhancer. After nucleofection 400 μ l cRPMI was added.

Program code EH-115 on a Lonza 4D-Nucleofector was used for Nucleofection. After Nucleofection cRPMI was added as mentioned above and the cells were incubated at 37°C to rest for 30min.

The cells were then transferred to a 96 well plate and 100U/ml of IL-2 together with Dynabeads Human T-Activator CD3/CD28 in a cell:bead ratio of 10:1 were added for the activated condition or 0,5 ng/ml IL-7 and 0,5 ng/ml IL-15 for the non-activated T cells. For the activated condition a second dose of 100U/ml IL-2 was given at day 6. Either 0,5 μ mol/l PFT- μ or 30 μ mol/l cyclic PFT- α was added directly after nucleofection to the resting medium and after transfer to the 96 well plate to the culture medium for the inhibitor experiments. For activation comparison, T cells were either pre-activated with Dynabeads Human T-Activator CD3/CD28 in a cell:bead ratio of 10:1 and 100 U/ml IL-2 in cRPMI 48h prior to Nucleofection or postactivated as

described above. If needed, T cells restimulated 24-48 hours before flow-sorting with 5 μ l Immunocult per 1×10^6 cells.

Sequential gene editing required two activation steps, the first one 48 hours before the first nucleofection with a α CD3-coated 48 well plate (10 μ g/ml clone UCHT1 in 150ml overnight at 4 $^{\circ}$ C) with 5 μ g/ml α CD28 (clone CD28.2) and 100 U/ml IL-2 for 1×10^6 cells and the second one 5 days after the first editing with 1 μ l Immunocult per 1×10^6 cells 48 hours before the second editing. Nucleofection was done as described above, with nucleovette vessel for the first nucleofection and with a 96 well reaction plate for the second nucleofection. 10×10^6 cells were used for each nucleovette vessel and $1,8 \times 10^6$ cells for the 96 reaction plates.

The simultaneous CD4/PDCD1-double CRISPR editing for CAST-Seq analysis was performed in Nucleocuvettes as described before, except for the addition of 20 μ l CD4 Cas9 RNP together with 20 μ l PD-1 Cas9 RNP.

4.4 CFSE T cell proliferation assay

T cells were washed twice with PBS, before being resuspended at 10×10^6 cells/ml 1 μ mol/l CFSE in PBS and then incubated for 20 min in the dark at RT. The staining was quenched by adding cRPMI at five times the volume of the original staining solution and an additional incubation of 10 min in the dark at RT. The T cells washed again for two times in PBS and then resuspended in nucleofection buffer. Electroporation and post activation was done as described above. The optimal time point for observing a proliferation pattern for flow cytometry sorting was at day 4-7 after nucleofection.

4.5 Flow cytometry staining

For flow cytometry staining the cells were transferred to a 96well V-bottom plate. To determine the absolute knock-out cell numbers optionally 123count eBeads™ Counting Beads were added. They were washed twice with PBS prior to being resuspended in 30 μ l of staining master mix per well. All antibodies are listed in 4.5 and have been titrated before use. All of the antibodies were added together in PBS. Live/dead staining was applied with propidiumiodide or protein-based live/dead dyes. After the master mix was applied, the cells were incubated at 4 $^{\circ}$ C in the dark for 30min. After that, the cells were washed twice with FACS-buffer and resuspended in 100 to 150 μ l FACS-buffer, before being analyzed with either a Cytoflex S or a Cytoflex LX.

4.6 Flow cytometry cell sorting and DNA extraction

T cells were stained as described above and sorted based on the targeted gene and/or the CFSE dilution pattern on a FACSAria III or a MoFlo Astrios EQ cell sorter. To lyse the cells and extract the DNA, the sorted cells were resuspended in DNA Quick Extraction solution and incubated at 65 °C for 5 min, then 95 °C for 5 min. The obtained DNA was stored at - 20 °C.

4.7 CAST-Seq analysis

Cast-Seq was performed by Julia Klermund at the Cathomen lab in Freiburg. After Extraction of the genomic DNA from three independent donors using the DNeasy Blood & tissue Kit, DNA was sequenced on a NovaSeq 6000 using 2x150bp paired-end sequencing (GENEWIZ, Azenta Life Sciences) with the following modifications to the already existing Cast-Seq protocol [234]:

- Target length of enzymatic fragmentation was set to 500 - 800 bp.
- The bioinformatic pipeline was adjusted for the use of two gRNAs.
- Targets had to be significant in two replicates to qualify for further analysis.

A score and a p-value was assigned to each sequence based on the alignment to the putative target site in comparison to randomly generated sequences. If the cut-off of 0,005 was reached, the sequence was declared a OMT. CAST-Seq read coverage was displayed in 100 bp bins for the region +/- 5 kb window around the on-target site. All reads were plotted as log2 read counts per million (CPM).

For the quantifications of the CAST-Seq coverage plots, the following formulae were used:

$$\text{percentage of large aberrations} = \frac{\text{sum of all reads in bins} > 200 \text{ bp from the cleavage site}}{\text{sum of all reads in all bins}}$$

$$\text{Mean deletion length} = \frac{\text{sum of}(\text{count of deletion reads} * \text{distance from the cleavage site})}{\text{sum of all deletion reads}}$$

4.8 Single cell copy number analysis and clustering (scKaryo-seq)

As described above, cells from two independent donors were activated with α CD3/CD28-coated beads, but in a ratio of 1:1, before nucleofection with Cas9 RNPs to generate a TRAC KO. After cultivation for 5 days, KO-cells were single cell sorted with a FACSAria III cell sorter into 384 well plates with 5 μ l of mineral oil/well. Before the sorting the cells were stained for living cells, CD8+ cells and human TCR and only

TCR-/CD8+ living cells were sorted. After sorting the cells were frozen at -80 °C. The following steps were performed at the SingleCell core facility of the Oncode Institute, Utrecht, the Netherlands. Sequencing was done on a NextSeq2000 with 2x100bp paired-end sequencing. The libraries were processed for Copy number variation using Aneufinder. All autosomes were analysed and GC-correction was enabled. The method "editive" and 100 random permutations were used and the single cells were then clustered and split into a group of higher and lower quality cells. Only the higher quality cells were used for further analysis.

4.9 Polymerase chain reaction (PCR)

PCR was used for determine KO-efficiency and for the detection of large deletions on the MiSeq. All the primers were designed using Benchling. Each PCR was carried out in 200µl thin-walled PCR-reaction strips. 25µl of reaction mix was used per reaction vessel. The mix consisted of 12,5 µl 2x GoTaq Long PCR MasterMix, 0.5 µl of 10 µmol/l forward primer, 0.5 µl of 10 µmol/l reverse primer, 1.5 µl H₂O and 10 µl of genomic DNA. If the DNA was concentrated higher, the volume of DNA was reduced (down to 1 µl) and instead the amount of H₂O was increased to obtain a total of 25 µl. The thermocycler setting are listed in table 4.11.

step	temperature	duration	number of repetitions	additional info
Initial denaturation	95 °C	60s	1x	
Denaturation	98 °C	10s	18x	-0.5 °C every cycle
Annealing	65 °C	15s		
Elongation	72 °C	15s		
Denaturation	98 °C	10s	15x	
Annealing	58 °C	15s		
Elongation	72 °C	15s		
Final elongation	72 °C	300s	1x	

Table 4.11 PCR-program

4.10 Amplicon NGS

Detection of large deletions of CRISPR/Cas9-edited human T cells was done by amplicon sequencing followed by NGS. The first PCR was executed as described above. The PCR clean-up was done using AMPure beads according to the manufacturer's recommendations and eluted in 50 µl 10 mM Tris. Bar-

coding was done with 2 µl of the purified DNA, added to 10 µl of 2x GoTaq Long PCR Master Mix, 2 µl of Nextera XT index 1 (i7) primer, 2 µl of Nextera XT index 2 (i5) primer and 4 µl of H₂O. The PCR was done with the thermocycler settings listed in table 4.12.

step	temperature	duration	number of repetitions
Initial denaturation	95 °C	180s	1x
Denaturation	95 °C	30s	8x
Annealing	55 °C	30s	
Elongation	72 °C	30s	
Final elongation	72 °C	300s	1x

Table 4.12 PCR-program

A second clean-up step with AMPure beads was performed and the obtained DNA was eluted in 27.5 µl 10 mM Tris. Quantification of the cleaned up PCR-product was done via the SpectraMax Quant AccuBlue HighRange dsDNA Kit on the SpectraMax i3x instrument. DNA was pooled with an equal amount for each sample and sequenced on an Illumina MiSeq instrument with a MiSeq Reagent Nano Kit v2 (500-cycles) according to the manufacturer's recommendations.

NGS sequencing results were analyzed using CRISPResso2 with the following prompt:

```
CRISPRessoBatch--batch_settings [name.batch]
--amplicon_seq [sequence amplicon]
-g [sequence gRNA]
-n nhej
-gn [name gRNA]
-w 0
--skip_failed
-o [name of output folder]
```

To determine KO efficiencies the setting -w 30 was used. The resulting data was merged into an excel file with the following code in RStudio:

```
library(readr)
library(openxlsx)

# Set the path to the directory containing the folders
main_directory <- "CRISPRessoBatch_on_[foldername]"
```

```

# Get a list of all folders in the directory
folders <- list.dirs(main_directory, full.names = FALSE)

# Initialize an empty list to store the second columns
result_list <- list()

# Initialize a variable to store the maximum number of rows
max_rows <- 0

# Loop through each folder
for (folder in folders) {
  # Read the file path for each Deletion_histogram.txt
  file_path <- file.path(main_directory, folder, "Deletion_histogram.txt")

  # Check if the file exists
  if (file.exists(file_path)) {
    # Read the data from the file
    data <- tryCatch(
      {
        read.delim(file_path, header = TRUE, sep = "\t")
      },
      error = function(e) {
        warning(paste("Error reading file in folder", folder))
        return(NULL)
      }
    )

    # Check if data is not NULL and has rows
    if (!is.null(data) && nrow(data) > 0) {
      # Extract the second column and append it to the result list
      result_list[[sub("CRISPResso_on_", "", folder)]] <- data[, 2]

      # Update max_rows if needed
      max_rows <- max(max_rows, nrow(data))
    }
  }
}

```

```

    } else {
      warning(paste("Empty or invalid data in file for folder", folder))
    }
  } else {
    warning(paste("File not found in folder", folder), print(folder))
    cat("Folder:", folder, "\n")
  }
}

# Fill missing values and combine the list of vectors into one data frame
result_df <- data.frame(
  lapply(result_list, function(x) c(x, rep(NA, max_rows - length(x))))
)

# Write the result to an Excel file using openxlsx
write.xlsx(result_df, "result_[resultfile].xlsx", rowNames = TRUE)

```

The resulting distribution of deletions or insertions was visualized using Prism 10. For descriptive statistics, the data were transformed also using RStudio with the following code:

```

library(tidyverse)
library(conflicted)

# Set conflict resolution to error for dplyr functions
conflict_prefer("dplyr", winner = "dplyr")

# Specify the directory containing the folders
main_directory <- "[result_folder_name]"

# Get a list of folders in the main directory
folders <- list.dirs(main_directory, full.names = FALSE)

# Loop through each folder
for (folder in folders) {
  # Create the file path for the "deletion_histogram.txt" file in the current folder

```

```

file_path <- file.path(main_directory, folder, "[Insertion/Deletion]_histogram.txt")

cat("Processing folder:", folder, "\n")
cat("File path:", file_path, "\n")

# Check if the file exists
if (file.exists(file_path)) {
  cat("File exists. Reading data...\n")

  # Read the data from the file
  d <- readr::read_table(file_path)

  # Remove first two rows
  d <- dplyr::slice(d, -c(1))

  # Replicate values based on the second column
  allvalues <- unlist(Map(function(value, count) rep(value, count), d$ins_size, d$fo

  # Print the data frame and the vector
  print(d)
  print(allvalues)

  # Create the file path for the output file (e.g., descriptive_deletions.txt)
  output_file_path <- file.path(main_directory, folder, "descriptive_[insertions/dele

  # Write the vector to the output file
  write.table(allvalues, file = output_file_path, col.names = FALSE)

  cat("Results for", folder, "have been saved to", output_file_path, "\n\n")
} else {
  cat("Warning: File not found for", folder, "\n\n")
}
}

```


5 Results

Parts of the data used in this thesis have been included in a manuscript (Ursch & Müschen et al.) submitted for publication. This includes parts of the following paragraphs: 5.1, 5.2, 5.3, 5.4 and 5.5. CAST-Seq and the subsequent analysis as shown in section 5.5 was performed by Julia Klermund at the Cathomen lab, university of Freiburg.

5.1 The frequency of large deletions is tied to the T cell activation status

Since it used to be quite challenging to generate a sufficient knock-out in primary human T-cells via CRISPR/Cas9, most of the existing gene-editing protocols try to maximize the number of successfully edited T cells. High knock-out (KO) cell numbers were mainly achieved by strong activation of the TCR [160] [188]. Currently, one of the most effective ways to genetically engineer primary human T cells is via nucleofection with Cas9 ribonucleoproteins (Cas9 RNPs), which have also been applied in the here presented data [160]. However, it is unclear if and how the activation status of the T cells also affects indel patterns. We, therefore, tested how TCR stimulation of CD4⁺ T cells affects the distribution of indels at the safe harbor gene locus *AAVS1*, the constitutively active locus *CD4* and *PDCD1*, which is expressed in an activation-dependent manner. We first examined activated versus non-activated T cells. In figure 5.1 the basic setup of our experiments is depicted. After obtaining CD4⁺ or CD8⁺ T cells from buffy coats, the cells were cultured in cRPMI for 2 days. On day 3, the cells were nucleofected with Cas9 RNPs to create a KO. Depending on the condition, the cells were then activated with CD3/CD28 beads at a cell-to-bead ratio of 10:1 and treated with IL-2 or incubated with IL-7 and IL-15 to keep the cells in a resting cell state. The cells were then cultured for another 5 days followed by cell sorting to isolate the live KO cell population. *AAVS1* KO cells were only sorted based on the live cell staining (flow cytometry sorting strategies are depicted in Figure 5.2 C). Directly after sorting, the DNA was extracted and stored at -20°C. The DNA was later on analyzed by amplicon NGS sequencing on an Illumina MiSeq and analyzed with CRISPResso2 (Figure 5.1).

The flow cytometry stainings allows us to determine the number of CD4 or PD-1-negative cells as well as the absolute KO cell numbers on the protein levels. The frequency and the absolute number of CD4⁻ and PD-1⁻ negative cells were higher in activated T cells compared to non-activated T cells. The differences

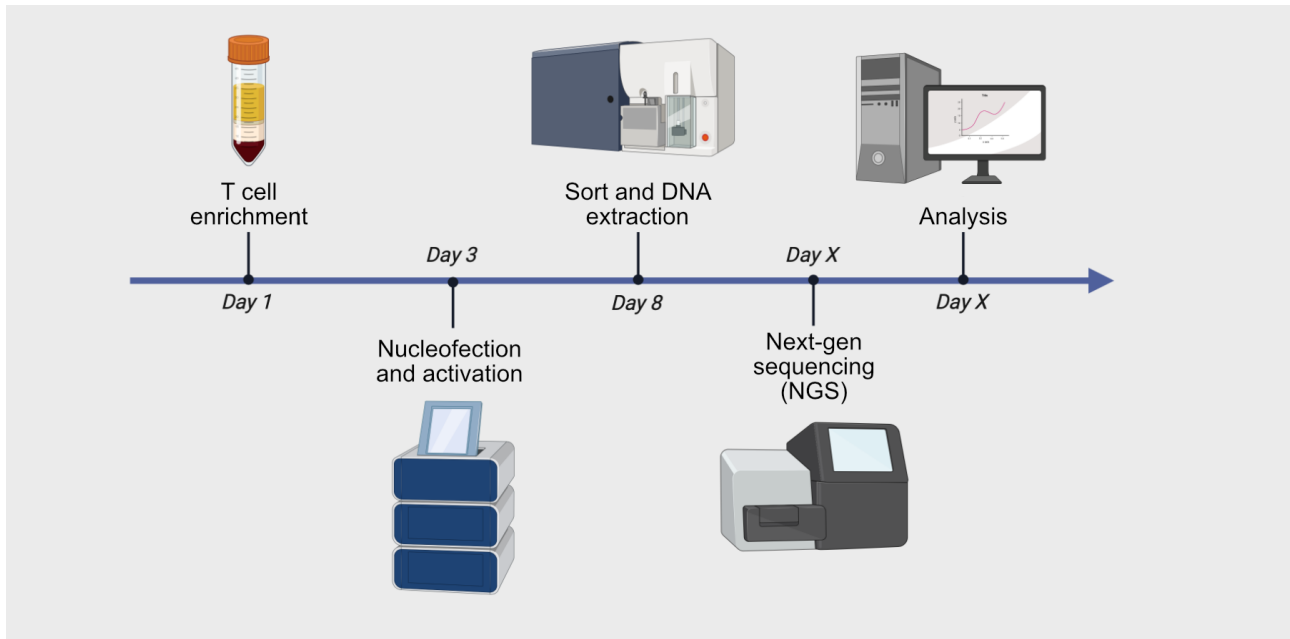


Figure 5.1 General workflow Depiction of the general workflow for KO generation, T cell activation, flow cytometry cell isolation and amplicon NGS sequencing. T cells were either activated using CD3/CD28 beads at a ratio of 10:1 (cell:beads) and 100U/ml of IL-2 or not activated and instead cultured with IL-7 and IL-15.

were more pronounced in the *CD4* KO conditions than in the *PDCD1* KO conditions. However, PD-1 is an activation-dependent marker and the flow cytometry enrichment of PD-1-negative, non-activated T cells, is therefore challenging, which could bias the results (Figure 5.3 A and B).

Since *AAVS1* is regarded as a safe harbor locus, which does not encode for a surface protein, it is not possible to stain for *AAVS1* with fluorescently-labeled antibodies [13]. Therefore, we instead compared the percentage of modified reads after NGS sequencing to quantify the KO rate in *AAVS1* samples (Figure 5.3). Singlet, live *AAVS1* KO cells were isolated by flow cytometry and the DNA was extracted for next-generation-sequencing (NGS) (Figure 5.2 C). PCR-amplicons with a length of 450 bp containing the *AAVS1* target site were generated and subjected to NGS. The resulting fastq-files were analyzed using CRISPResso2 [196]. CRISPResso2 aligns the fastq files to a given reference amplicon and is therefore able to recognize deletions, insertions and substitutions of various sizes up to a length of 200bp for each individual read. This allows us to determine the KO rates, but also how often a mutation of a specific size occurs. The CRISPResso results for the *AAVS1* locus showed a weak tendency towards higher KO frequencies in activated T cells compared to non-activated cells. However, in this case, no sort of enrichment of KO cells has been possible, which could have aggravated the analysis (Figure 5.2 C). The NGS analysis also allowed us to have a closer look at the distribution of deletions and insertions. In activated *AAVS1* KO T cells the mean deletion size was larger compared to the non-activated cells, as shown in Figure 5.4 B. We confirmed these results in *CD4* and *PDCD1* KO T cells using the same pipeline (Figure 5.1). Also at these two gene loci, TCR-stimulation increased the average deletion sizes. This effect was more

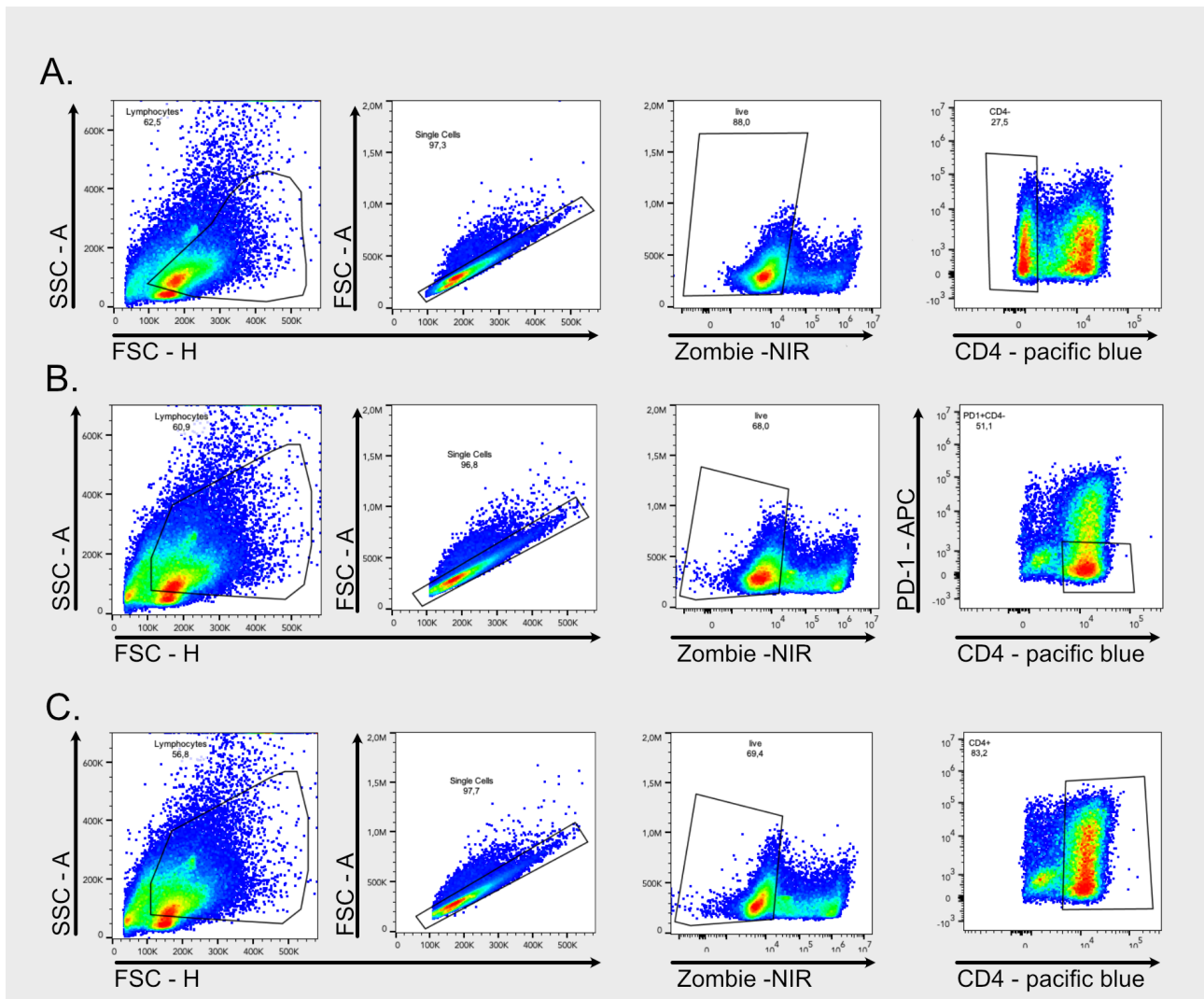


Figure 5.2 Flow cytometry gating Strategy for activated and non-activated T cells. A. CD4: Representative example for the gating strategy to isolate CD4-negative T cells. **B. PD-1:** Gating strategy to isolate single, living, CD4-positive and PD-1-negative T cells. **C. AAVS1:** Gating strategy for single, living, CD4-positive T cells. A, B, C: All gating strategies are exemplified in activated T cells. n = 3 biological replicates. (adapted from Ursch & Muschen et al.)

pronounced in the activation-dependent *PDCD1* locus. Overall, TCR-stimulation increases the frequency of larger deletions.

We observed similar tendencies for insertions at the *PDCD1* locus, an increase in the insertion sizes after activation of the T cells (Figure 5.5 C), but not for the other two gene loci tested (Figure 5.5 A and B). The overall frequencies for insertions were much lower compared to deletions. For this reason, we focused on differences in deletions sizes for all further experiments.

Many T cell CRISPR editing protocols apply stronger pre-activation before Cas9 RNP nucleofection [188] [189] [208]. In the next step, we compared the influence of two different activation protocols on editing outcomes. The main difference between both protocols was the time point at which activation

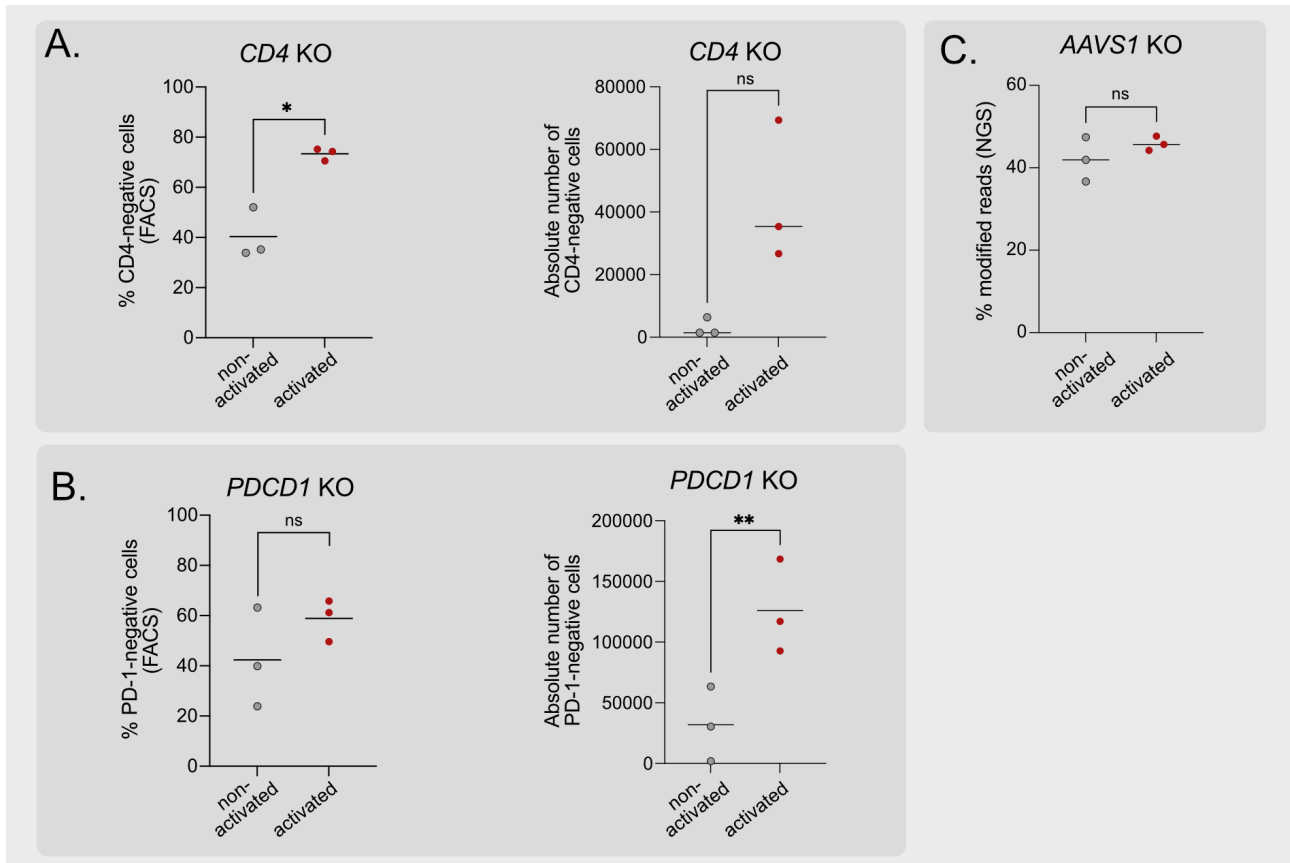


Figure 5.3 Characterization of KO efficiencies in activated and non-activated T cells. **A.** KO-efficiencies and absolute cell number in activated and non-activated *CD4* KO T cells. Data were generated using flow cytometry. Quantification of absolute cell numbers via counting beads. **B.** KO-efficiencies and absolute cell number in activated and non-activated *PDCD1* KO T cells. Data were generated using flow cytometry. Quantification of absolute cell numbers via counting beads. **C.** Frequencies of modified reads between activated and non-activated cells for *AAVS1* determined by NGS. $n = 3$ biological replicates. Paired t-test was used for all comparisons. ns = not significant, * $p < 0.05$, ** $p < 0.01$, (adapted from Ursch & Müschen et al.)

took place. T cells were either activated two days prior to nucleofection (“pre-activation”) or directly after nucleofection (“post-activation”) as in the previous experiments. In these experiments we targeted again *AAVS1* and *CD4* and additionally *LAG3* as another activation-dependent marker [30]. For both T cell activation protocol a bead:cell ratio of 1:10 was used. As depicted in Figure 5.6 the KO efficiencies were not significantly changed in *AAVS1* and *LAG3* KO cells. Only in *CD4* KO cells pre-activation results in significantly higher frequencies of CD4-negative T cells (Figure 5.6 B).

Next, we analyzed the deletion pattern at all three loci using the NGS pipeline. Pre-activation of T cells resulted in larger deletions compared to T cells activated after nucleofection (Figure 5.7).

These results together with the previous results indicate that the activation status of the cells impact CRISPR-induced deletion sizes.

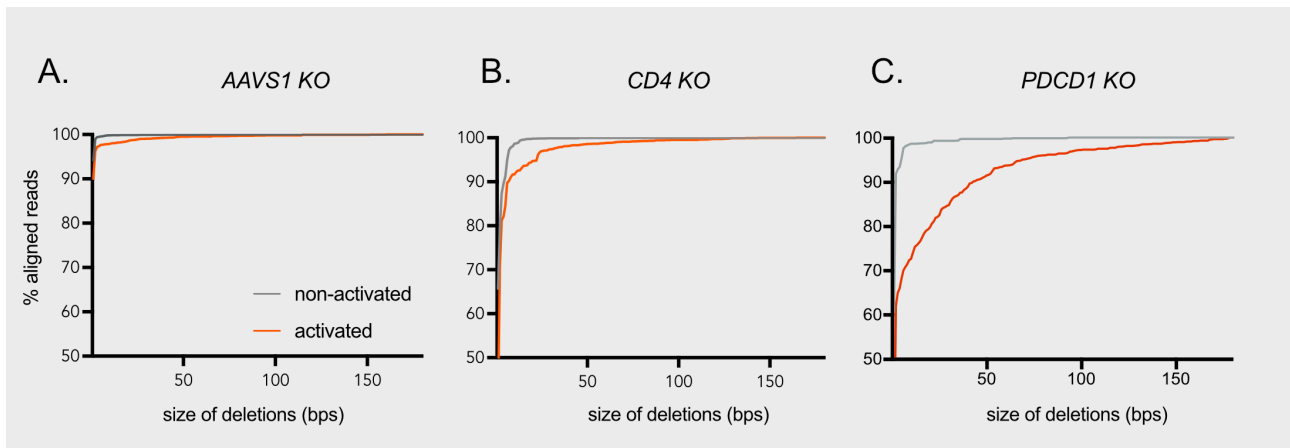


Figure 5.4 Deletion patterns in activated and non-activated T cells. Distribution of the deletions for *AAVS1* KO (A.), *CD4* KO (B.) and *PDCD1* KO (C.) T cells. The amount of each deletion size is given as a fraction of all aligned reads. (adapted from Ursch & Müschen et al.)

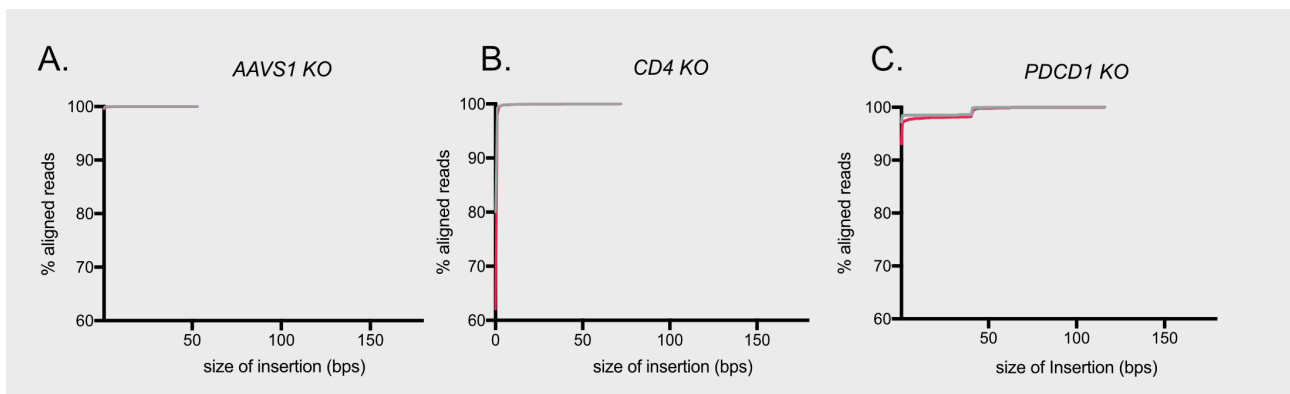


Figure 5.5 Insertion patterns in activated and non-activated T cells. A. Distribution of the insertions for *CD4* (A.), *AAVS1* (B.) and *PDCD1* KO (C.) T cells. The amount of each deletion size is given as a fraction of all aligned reads. (adapted from Ursch & Müschen et al.)

5.2 The impact of T cell proliferation speed on deletion patterns

Closely linked to the activation of T cells is their proliferative capacity. T cell proliferation is an intricate system of pro-proliferative and anti-proliferative components needed to provide a fine-tuned immune response in case of an infection. [10], [118]. Strongly activated T cells will proliferate faster [151]. Proliferating T cells have an intrinsic risk of accumulating DNA damage [168]. Thus, we hypothesized that the proliferation speed impacts the rate of large deletions in primary human T cells. Therefore we modified our existing experimental setup and stained our CD4 T cells with carboxyfluorescein succinimidyl ester (CFSE) on day 3 directly before the Cas9 RNP nucleofection, as shown in Figure 5.8.

CFSE is integrated into the cell membrane upon staining and gets diluted with every cell division, which allowed us to track the cell divisions via flow cytometry. We sorted the CFSE-labeled T cells based on the fluorescent intensity of the CFSE dye. The cells were pre-gated on lymphocytes, single cells, living

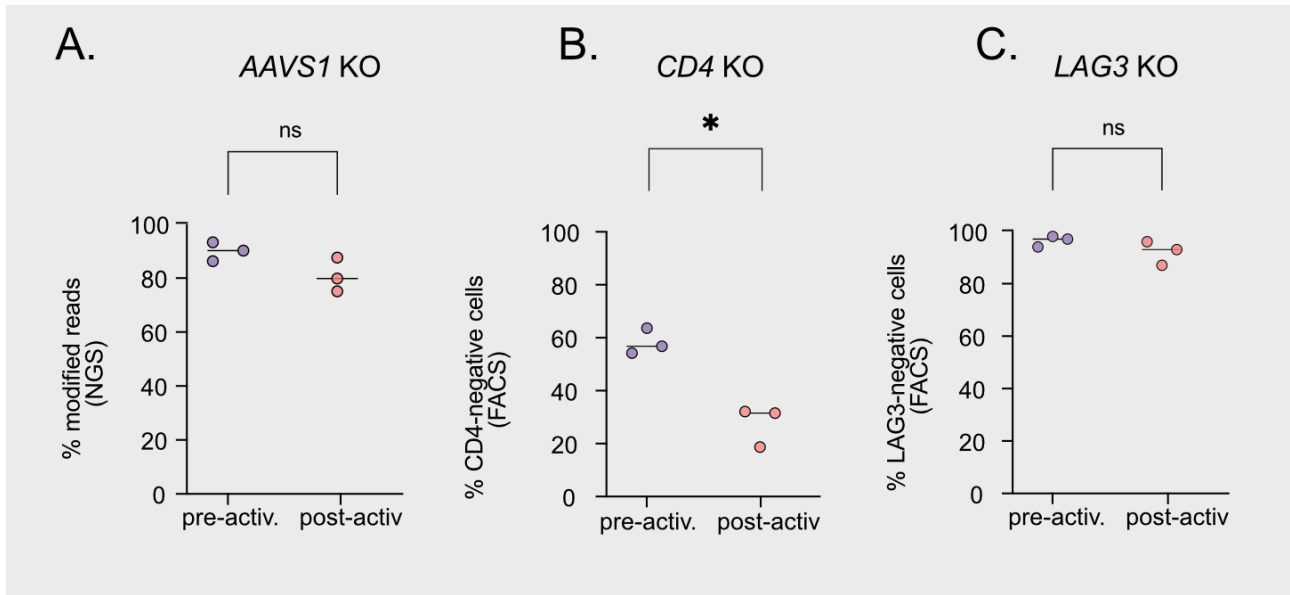


Figure 5.6 KO efficiencies in pre- and post-activation stimulation protocols. CRISPR editing frequencies are shown for *AAVS1* (A.), *CD4* (B.) and *LAG3* (C.). Data for *AAVS1* were generated via NGS. Data for *CD4* and *LAG3* was generated using flow cytometry. $n = 3$ biological replicates. Paired t-test was used for all comparisons. ns = not significant, * $p < 0.05$, (adapted from Ursch & Müschen et al.)

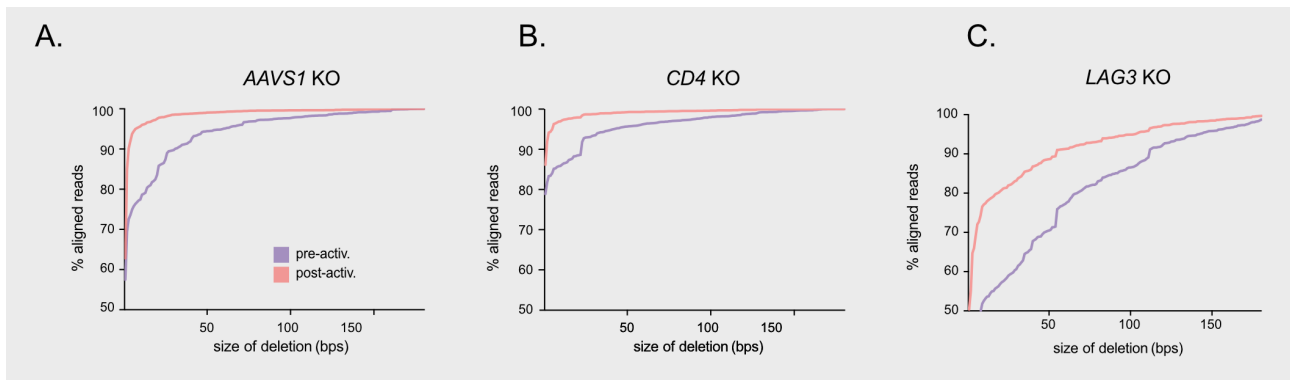


Figure 5.7 Deletion patterns in pre- and post-activated T cells. Distribution of deletions in *AAVS1*- (A.), *CD4*- (B.) and *LAG3*-KOs (C.) for T cells which were activated prior to the electroporation, versus cells activated after the electroporation.

cells, for CD4 and PD-1 on KO-cells, and then gated on either CFSE high or CFSE low cells as shown in Figure 5.10 A. Cells with lower CFSE intensity (shown in blue) underwent more cells divisions in the given timeframe and were therefore declared "fast proliferating" in comparison to the cells with higher CFSE intensity (shown in green), which were termed "slow proliferating". We excluded the first peak of the CFSE distribution pattern since these cells did not proliferate at all.

A comparison between the fast and slow proliferating cells in Figure 5.10 B shows that the frequency of PD-1- and CD4-negative cells are increased in fast-dividing cells. There is no clear effect of the cell proliferation speed on the *AAVS1* KO rate.

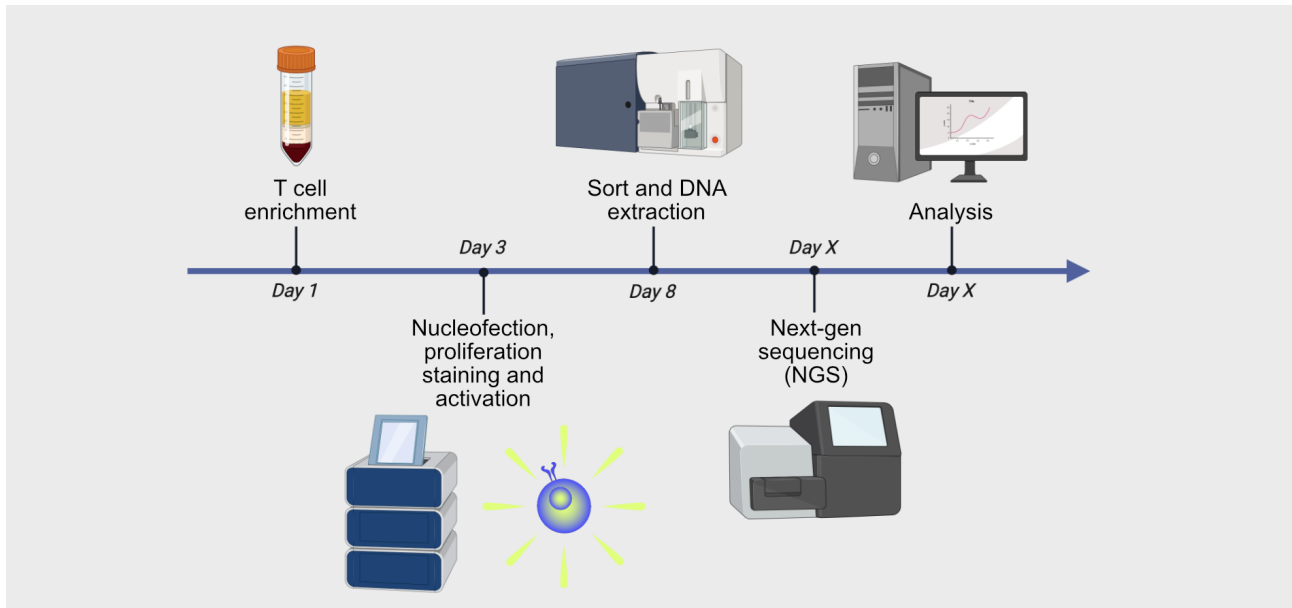


Figure 5.8 Depiction of the general workflow of T cell proliferation experiments. We modified our basic setup depicted in Figure 5.1 by adding the additional step of CFSE labelling on day 3, before nucleofection.

Next, we analyzed the distribution of deletions for the different KO conditions in slowly and fast-dividing cells. As further control the NGS sequencing results of edited, non-activated T cells were included into the Figure (Figure 5.10 C, D, E). Unsurprisingly, the non-activated cells always showed the lowest amount of large deletions. Most prominently in the *PDCD1* KO conditions, we could detect more large deletions in the fast proliferating cells compared to slowly dividing cells (Figure 5.10 E). Although less pronounced, the same patterns were detected in the *CD4* and *AAVS1* KO conditions (Figure 5.10 C, D). Taken together, these findings show that the proliferation speed of T cells after activation has, indeed, an impact on the editing outcome after CRISPR/Cas9 editing with a higher prevalence of larger deletions in fast dividing cells.

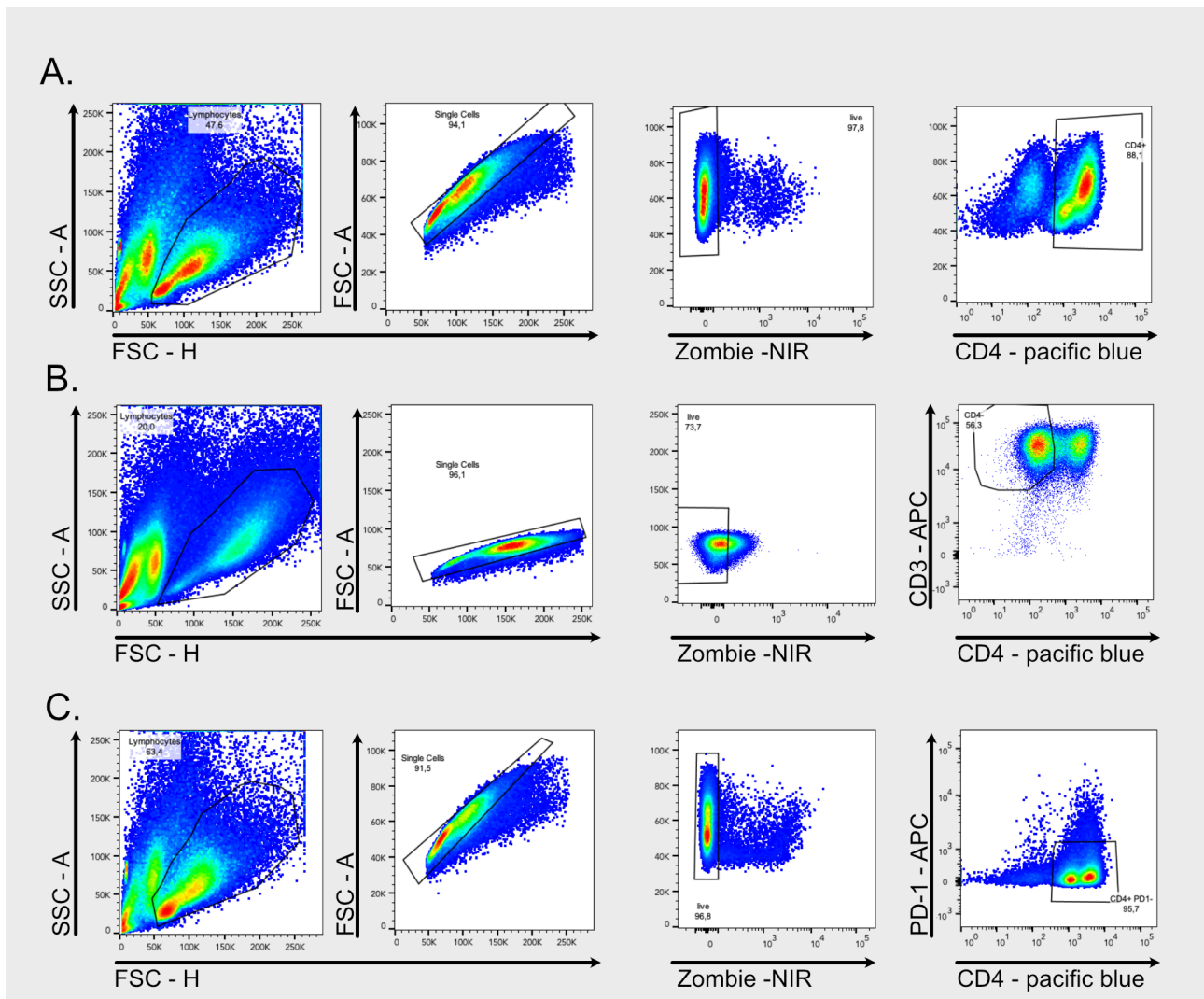


Figure 5.9 Gating strategy for T cell proliferation experiments. Gating strategy for CFSE-labeled T cells used in Figure 5.10 and Figure 5.12. **A.** *AAVS1* KO cells were sorted on single, live and CD4-positive T cells. **B.** *CD4* KO cells were sorted on single, live CD3-positive and CD4-negative cells. **(C.)** *PDCD1* KO T cells were sorted for single, live CD4-positive and PD-1-negative T cells. Representative CFSE-gating is depicted in Figure 5.10. For *AAVS1* KO and *CD4* KO T cells: n = 3 biological replicates, for *PDCD1* KO: n = 4 biological replicates. (adapted from Ursch & Müschen et al.)

5.3 Modulation of deletion patterns via small molecules

One major pathway, which links cell activation and DNA damage is the p53 pathway.

Based on the known functions of p53 we hypothesized that temporary inhibition of p53 would result in more large deletions. We first tested this hypothesis via the application of two inhibitors: Pifithrin- α (PFT- α) and Pifithrin- μ (PFT- μ). While PFT- α is more of a broad inhibitor of the downstream functions of p53, via inhibition of p53 transcriptional activation and apoptosis, PFT- μ is a specific inhibitor of p53 dependent apoptosis via inhibition of the interaction of p53 with Bcl-x and Bcl-xL [40] [79]. The inhibitors

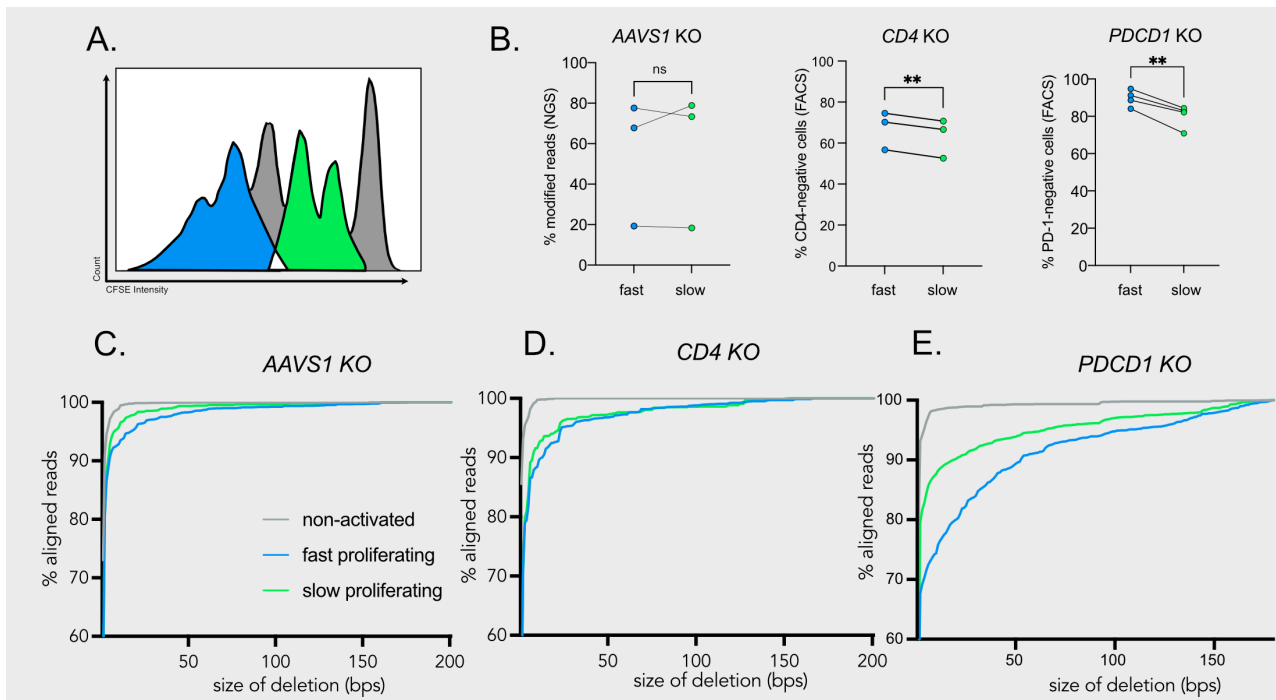


Figure 5.10 Deciphering the impact of T cell proliferation on the deletion pattern. **A.** Gating strategy for CFSE-labeled cells. The brightest peak was excluded, as this peak represents non-dividing cells, the second and third brightest peaks were sorted for the "slow proliferating" group, whereas the two peaks with the lowest CFSE signal represent the "fast proliferating" group. **B.** Comparison of KO-efficiencies between slow and fast proliferating cells for *AAVS1*, *CD4* and *PDCD1* KO-cells. Data for *AAVS1* KO were generated with NGS, whereas data for *CD4* and *PDCD1* KOs were generated using flow cytometry. Paired t-test was used for all comparisons. ns = not significant, * $p < 0.05$, ** $p < 0.01$. **C.** Distribution of deletions for *CD4*, *AAVS1* and *PDCD1* KO cells. For *AAVS1* KO and *CD4* KO conditions: $n = 3$ biological replicates, for *PDCD1* KO: $n = 4$ biological replicates. (adapted from Ursch & Müschen et al.)

were separately applied directly after Cas9 RNP nucleofection at a concentration of $30 \mu\text{mol/l}$ for PFT- α and $0.5 \mu\text{mol/l}$ for PFT- μ , as described before in the literature [40] [141]. Again, T cells were CFSE-labeled, nucleofected with Cas9 RNPs, activated, treated with the inhibitors, and flow cytometry sorted 4 days after activation (Figure 5.9). As a negative control, cells were treated with an equal volume of DMSO. Again, we also included non-activated T cells in these experiments. As shown in Figure 5.11, PFT- μ had no significant impact on the KO-efficiency for *AAVS1*, *PDCD1*, and *CD4* KO T cells. For PFT- α *PDCD1* KO T cells did not show a significant decrease in KO efficiency, whereas *AAVS1* and *CD4* KO conditions had significantly fewer KO cells after PFT- α treatment. Based on the CFSE dilution pattern (Figure 5.11 C), we were able to assess the influence of both inhibitors on the proliferative capacity of the T cells bearing a *AAVS1*, *PDCD1*, and *CD4* KO T cells. Both inhibitors did not affect the proliferation speed of *PDCD1* and *CD4* KO T cells, although the *AAVS1* KO condition showed a significant decrease in proliferating cells with PFT- α , not the with inhibitor PFT- μ (Figure 5.11 D).

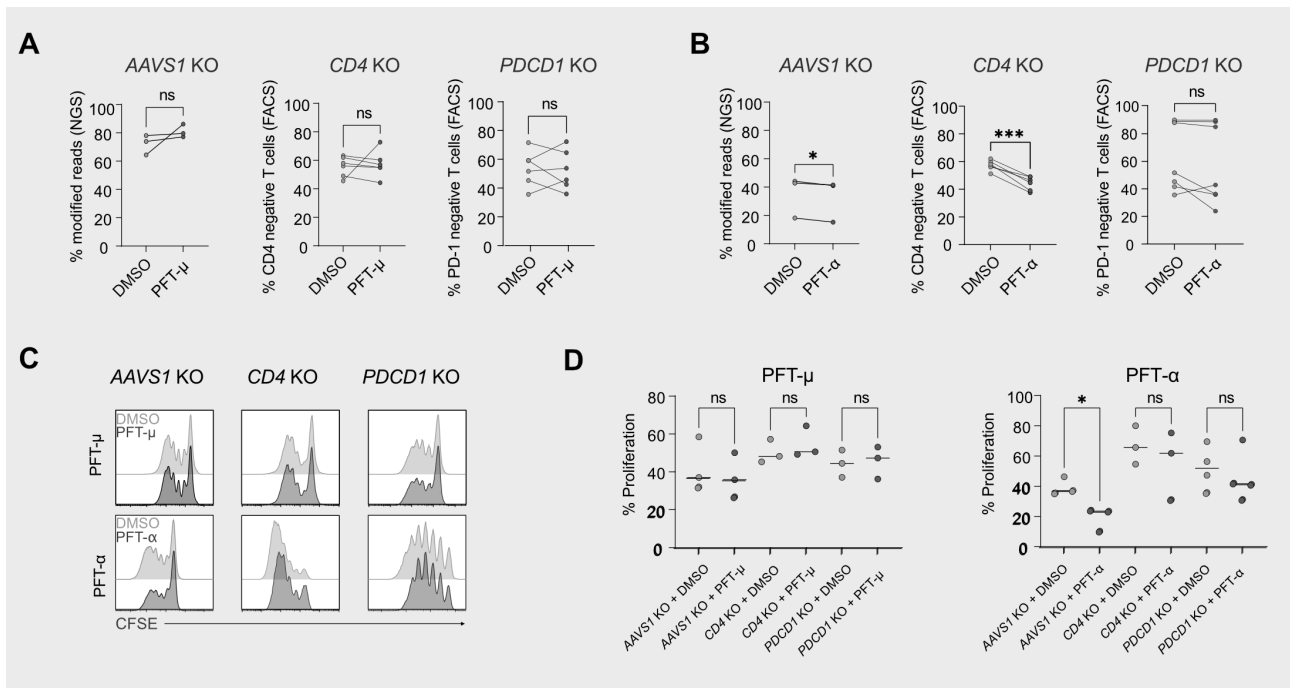


Figure 5.11 Analyzing the effect of p53 inhibitors on KO efficiencies and proliferation. A. KO-efficiencies for *AAVS1*, *PDCD1*, and *CD4* KO T cells with DMSO control or with the addition of PFT- μ . **B.** KO-efficiency for *AAVS1*, *PDCD1*, and *CD4* KO T cells with DMSO control or with the addition of PFT- α . **C.** Exemplary CFSE staining for *AAVS1*, *PDCD1*, and *CD4* KO T cells at day 4. **D.** Quantification of the cell proliferation. ns = not significant, * $p < 0.05$, ** $p < 0.01$, *** $p < 0.001$. $n = 3$ biological replicates. (adapted from Ursch & Muschen et al.)

Based on the known functions of p53 I expected the mean deletion size to increase with the application of these inhibitors. PFT- μ slightly increased the overall rate of deletion sizes in fast and slow-proliferating cells (Figure 5.12 A). However, PFT- α had the opposite effect and reduced the mean deletion size in all three loci tested in slowly and fast-dividing T cells (Figure 5.12 B). As observed before the effect was most pronounced in the *PDCD1* KO condition. Both inhibitors had only minor effects on non-activated T cells (Figure 5.12).

Puzzled by these results, I challenged pre- and post-activated T cells with PFT- α , to see if I can replicate these results. I tested PFT- α application in both activation strategies, pre- and post-activation, as described in Figure 5.7 for *AAVS1*, *CD4* and *LAG3* KOs. In all conditions, the rate of deletions was reduced after PFT- α application (Figure 5.13).

We tried to generalize our findings to more gene loci, *TIGIT* and *HAVCR2*, which encodes for TIM3. All of which showed a reduction of mean deletion size with PFT- α although none of them showed a strong dependence on the proliferation speed (Figure 5.15 A., B. and C.). A potential reason for this could be locus-specific effects of the targeted genes, which might interfere with T cell proliferation.

Another target we tested, was *CXCR4*. Although T cells, which were targeted with *CXCR4* Cas9 RNPs showed differences in the distribution of deletions between slow and fast proliferating, as well as between

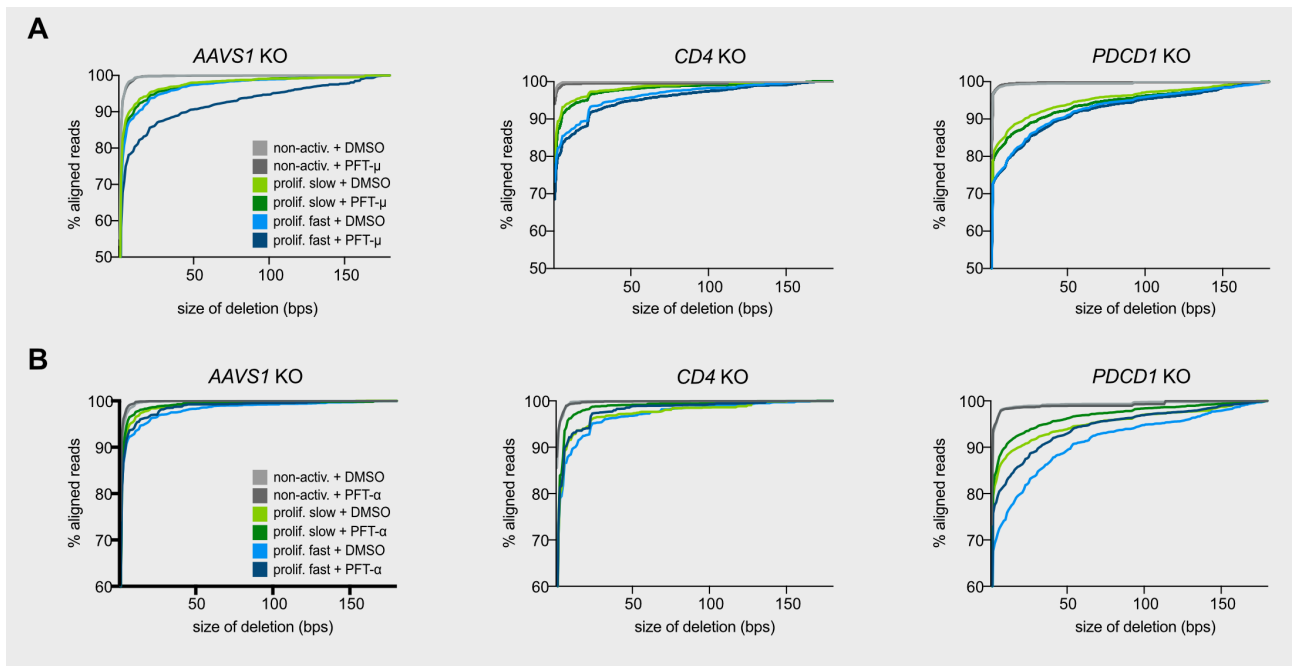


Figure 5.12 Analyzing the effect of p53 inhibitors on deletion sizes. **A.** Distribution of deletions for *AAVS1*, *PDCD1*, and *CD4 KO* T cells, sorted based on their proliferation speed indicated by CFSE dilution with DMSO control or with the addition of PFT- μ . **B.** Deletion sizes and distribution for *AAVS1*, *CD4* and *PDCD1 KO* T cells sorted based on their proliferation speed indicated by CFSE dilution with DMSO control or with the addition of PFT- α . The sort strategy is the same as in Figure 5.10. **A. B.** DMSO-treated samples are the same samples as displayed in Figure 5.10. $n = 3$ biological replicates. (adapted from Ursch & Műschen et al.)

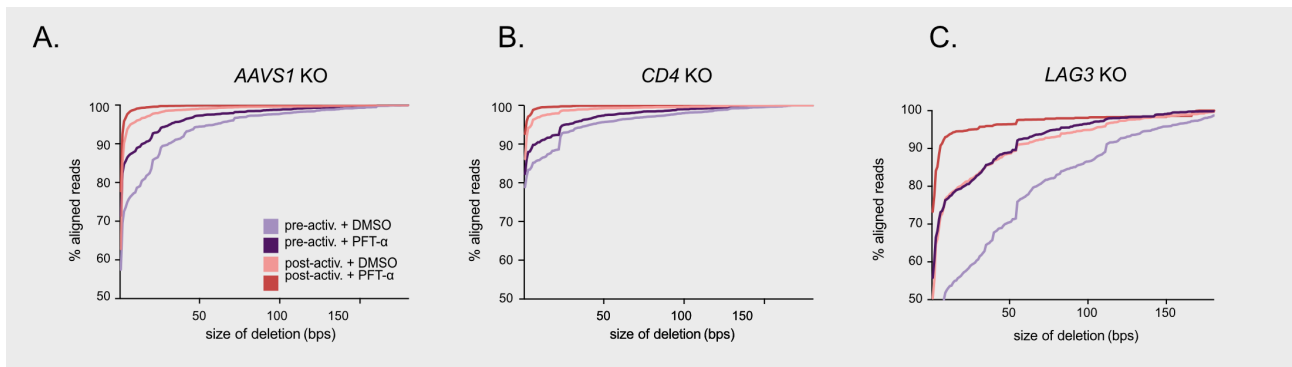


Figure 5.13 The impact of PFT- α on the deletion sizes in pre- and post-activated T cells. Distribution of deletions for *AAVS1* (**A.**), *CD4* (**B.**), and *LAG3 KO* (**C.**) T cells, which were either activated before or after nucleofection and treated with DMSO or with PFT- α . $n = 3$ biological replicates (adapted from Ursch & Műschen et al.)

T cells with DMSO or with PFT- α , the overall size of the effect was small, as shown in Figure 5.16. This could be due to a different repair pathway for DSB at this specific locus. We detected a prominent -2 deletion in high frequencies, which could be a hint towards MMEJ DNA repair at this site.

In summary, we observed opposite effects of PFT- α and PFT- μ . PFT- μ increased deletion sizes slightly whereas PFT- α decreased deletions in activated T cells.

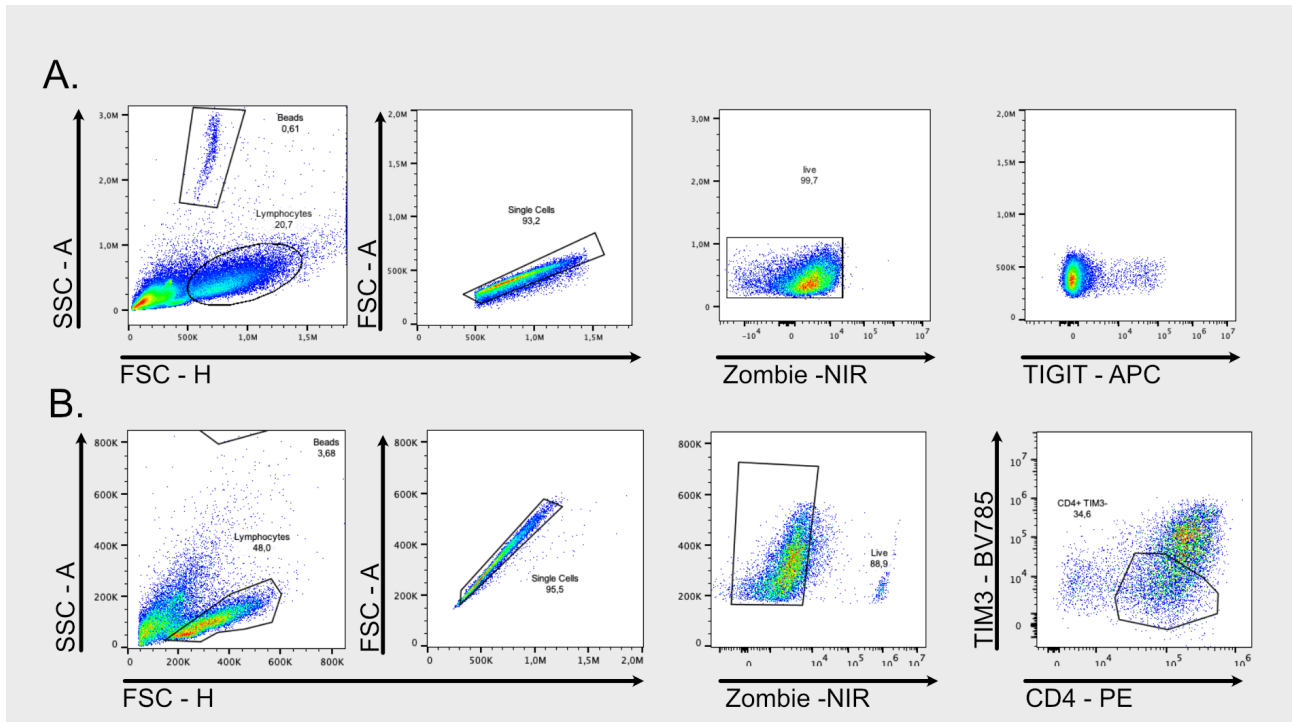


Figure 5.14 Gating strategy for *TIGIT* and *HAVCR2*. **A. *TIGIT*:** Representative example for the gating strategy to isolate single, living and *TIGIT*-negative T cells. **B. *TIM3*:** Gating strategy to isolate single, living, *CD4*-positive and *TIM3*-negative T cells.

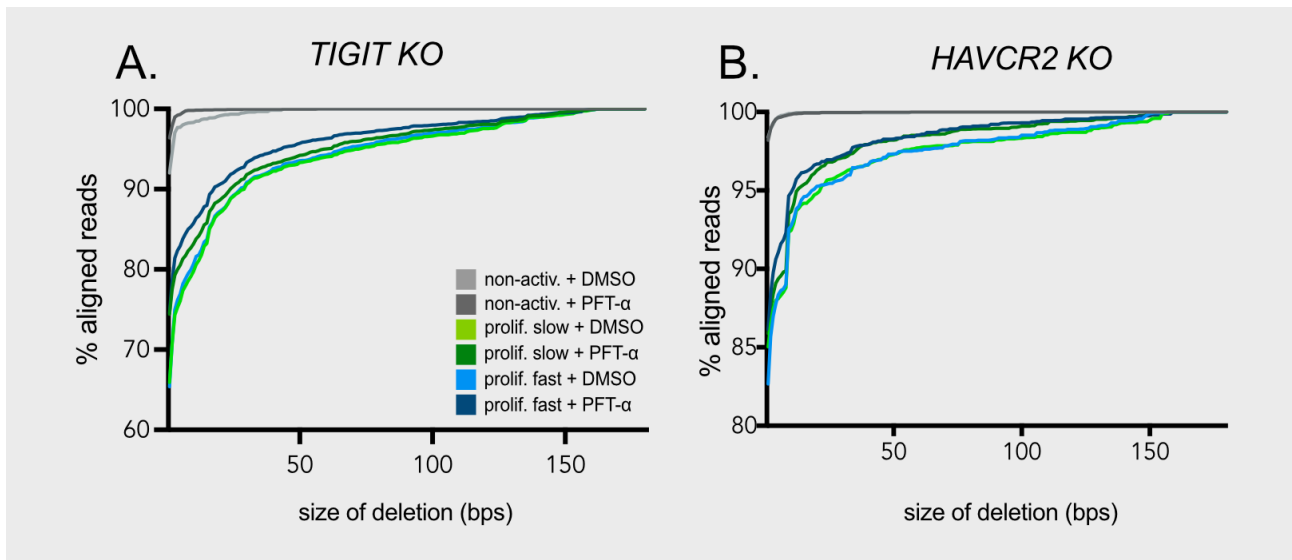


Figure 5.15 Distribution of deletions for *TIGIT* and *HAVCR2*. Effects of *PFT-α* on the distribution of deletions for *TIGIT* (A.) and *HAVCR2* (B.) KO T cells. $n = 3$ biological replicates.

5.4 Modulation of deletion patterns via *PFT-α* is independent of *p53*

The reduction of mean deletion sizes after *PFT-α* treatment contradicts the described mechanism of *PFT-α* as a *p53* inhibitor [40]. However, a few publications questioned the specificity of *PFT-α* and discussed

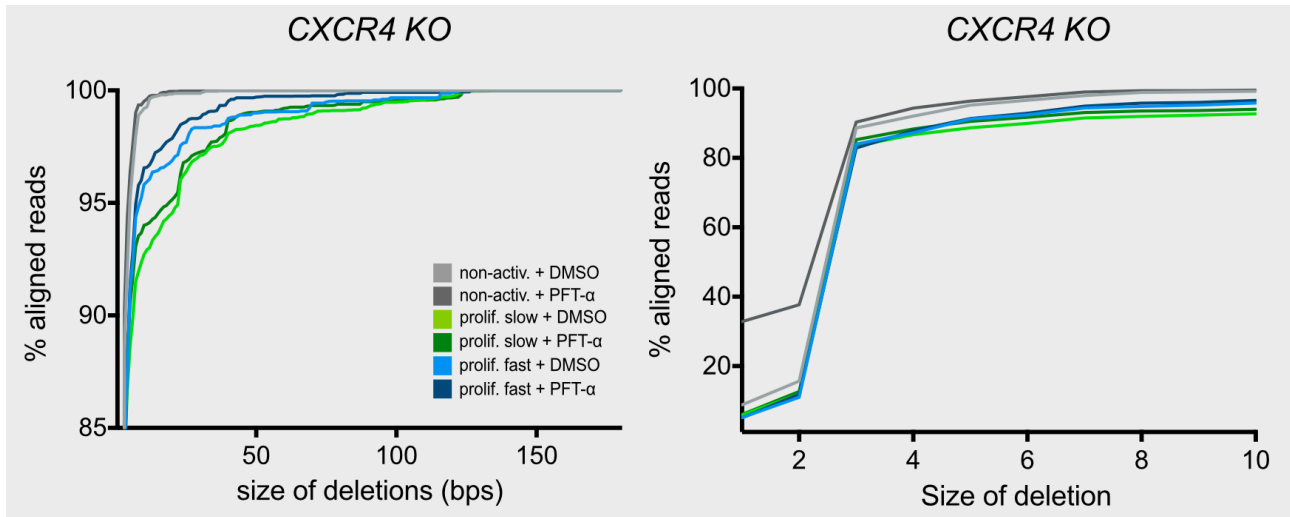


Figure 5.16 Distribution of deletions for *CXCR4* KO T cells On the left the y-axis depicts the range from 85% to 100% and the x-axis depicts a maximum size of deletion of 200 bps, whereas on the right side the y-axis shows the range from 0% to 100% and the x-axis shows a maximum deletion size of 10 bps. This illustrates the different repair pathways for this specific target site. n = 3 biological replicates. (adapted from Ursch & Mischen et al.)

alternative PFT- α targets such as aryl hydrocarbon receptor, caspase 3 and cyclin D1 [72] [100]. Therefore, we hypothesized that PFT- α acts in a p53-independent manner in the described experimental setups. To test this hypothesis, we modified the previously described workflow by generating first *TP53* KO or *AAVS1* KO control cells and subsequently challenged these cells one week later with a *CD4* or *PDCD1* KO with or without inhibitor application (Figure 5.17).

The KO rates of *AAVS1* and *TP53* were confirmed with amplicon NGS sequencings. The KO levels were, in both cases, comparable in all secondary KO and inhibitor conditions (Figure 5.18 A, B). In both secondary KOs, *CD4* and *PDCD1*, more large deletions could be observed in *TP53* KO cells compared to *AAVS1* KO. These results are in line with the published functions of p53 (Figure 5.18 C, D).

Next, we analyzed the impact of the inhibitor treatments on the CRISPR editing outcome. In the *AAVS1* KO conditions, both inhibitors showed the same effect as described before (Figure 5.18 C). PFT- α decreased the amount of large deletions for both, the *PDCD1* KO and the *CD4* T cells, whereas PFT- μ increased large deletions. In the *TP53* KO conditions, PFT- μ increased the deletion sizes in *TP53-PDCD1* double KO T cells. PFT- μ could not further increase the deletion sizes in *TP53-CD4* double KO T cells. Potentially the number of complete, homozygous *TP53* KO cells was higher in these conditions. Importantly, PFT- α reduced deletion sizes in *TP53-PDCD1* and *TP53-CD4* double KO T cells. These results suggest that PFT- α acts largely independent of p53.

Taken together, these findings show that we can use small molecules to modify the deletion pattern, whereas PFT- μ increases deletion sizes and PFT- α reduces the rate of large deletions. This holds true for cells with different proliferation speeds, various KOs, and different activation strategies. Furthermore, this

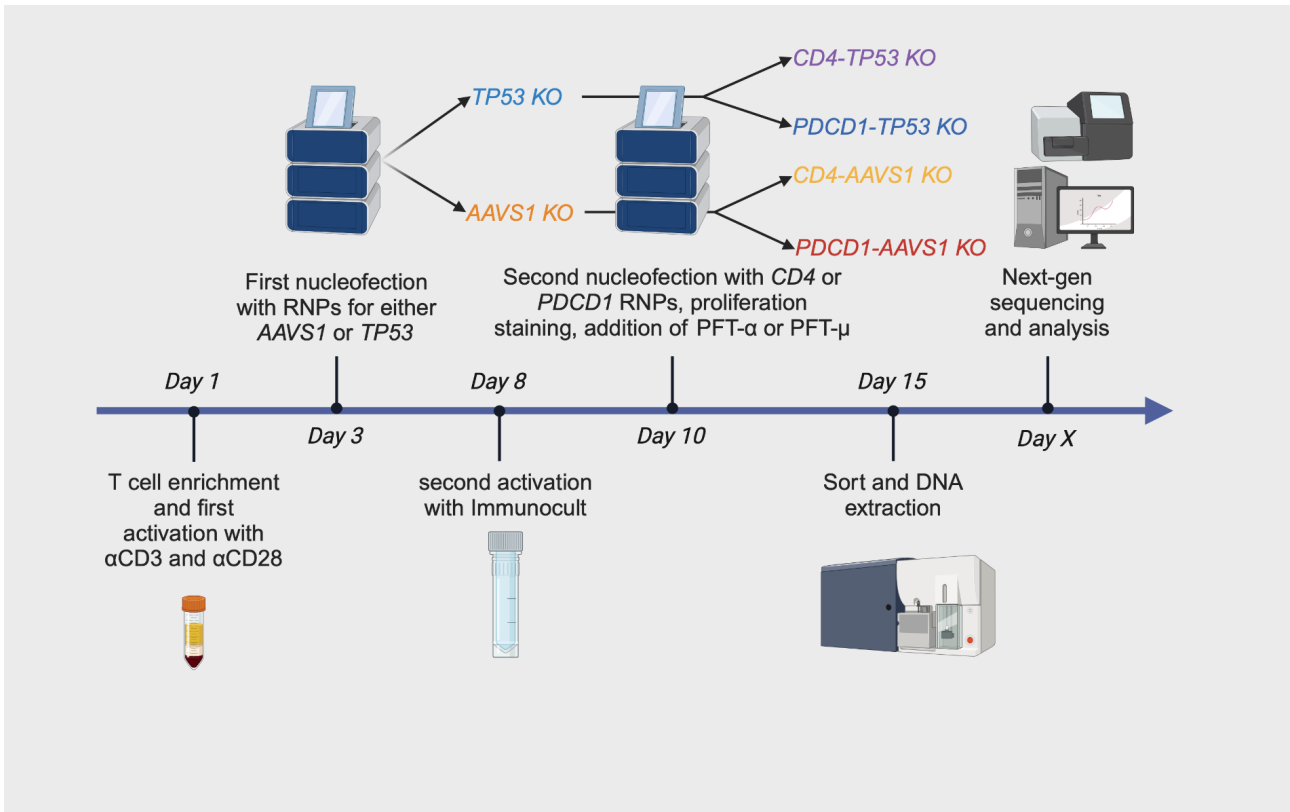


Figure 5.17 Workflow to generate *TP53* or *AAVS1* KO T cells and challenge with secondary KO and inhibitor treatment. A. Directly after T cell enrichment the T cells were activated on α CD3-coated 48 well plates in cRPMI with soluble α CD28 and IL-2. After 48 hours the cells were nucleofected with either *TP53*- or *AAVS1*-targeting Cas9 RNPs. After 5 days of cultivation, the cells were restimulated and 48 hours later nucleofected with either *CD4* or *PDCD1* Cas9 RNPs to generate the second KO, and treated with PFT- α or PFT- μ or DMSO. After 5 additional days, T cells were flow sorted and DNA isolated.

effect is preserved in cells bearing a p53-KO, which suggests a mechanism that is largely independent of the p53 pathway.

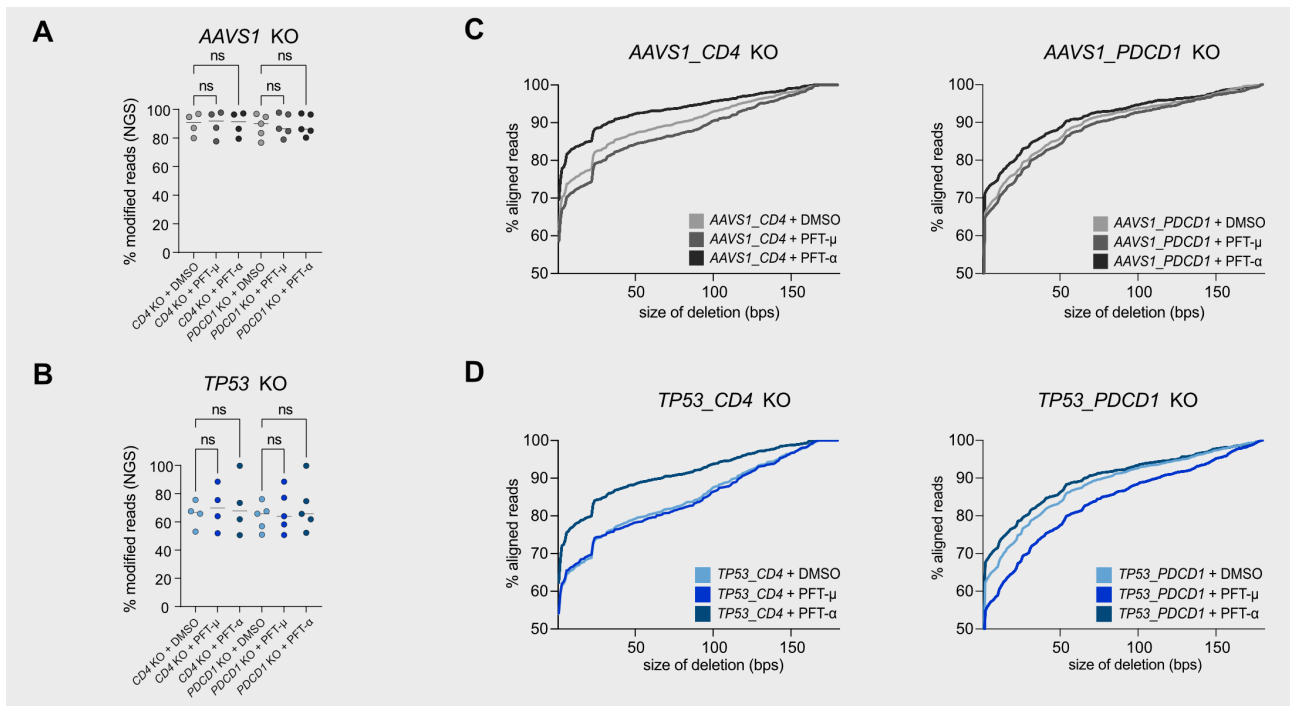


Figure 5.18 Testing the p53-dependence of PFT- α and PFT- μ . **A.** KO-efficiencies in the *AAVS1* KO conditions. **B.** KO-efficiencies in the *p53* KO conditions. **C.** Distribution of deletions at the *CD4* and *PDCD1* gene loci for *AAVS1-CD4* and *AAVS1-PDCD1* KO T cells. **D.** Distribution of deletions at the *CD4* and *PDCD1* gene loci for *TP53-CD4* and *TP53-PDCD1* KO T cells. $n = 4$, paired t-test was used for all comparisons. ns = not significant (adapted from Ursch & Müschen et al.)

5.5 Impact of the activation status and PFT- α treatment on deletions larger than 200 bps and chromosomal translocations

The described amplicon NGS pipeline for the detection of genetic aberrations enables us to find deletions up to 200 bp in size. This pipeline is suitable for a high-throughput workflow in our experimental setting. However, the detectable deletions sizes are limited. Therefore, we implemented a methodology, which can detect on- and off-target deletions, translocations and deletions larger than 200 bps. Chromosomal Aberrations Analysis By Single Targeted Linker-Mediated PCR Sequencing (CAST-Seq) is an amplicon sequencing-based approach for the detection of low-frequency chromosomal events like large deletions, translocation, inversions and off-targets through fragmentation, sequence-independent DNA-elongation, three nested PCRs and a combination of certain primers (Figure 5.19). By applying special primers for the target site, which block the amplification of unedited DNA and DNA fragments with point mutations, only amplicons with larger deletions are multiplied. This methodology pre-selects for larger deletions and enables the detection of editing events, with a low event rate. The CAST-seq library preparation consists of DNA fragmentation, linker ligation and three sequential PCRs. First, the the DNA is fragmented to a mean length of about 600 bp. The second step is the sequence-independent linker ligation of the DNA. This is

done by fusing a linker template to each of the DNA fragments in an sequence-independent way. The first PCR includes 4 primers: The bait , prey and two decoy primers:

- bait: This primer is designed to bind close to the expected cutting site.
- prey: This primer binds to the linker sequence, which is added to the DNA, after the fragmentation step.
- decoy: These primers (if possible, two) are located on the opposite side of the expected DSB in relation to the bait primer. The one, which is closer to the bait primer is located in a way that it can produce a PCR product together with the bait-primer. The one primer, which is further away has the same orientation as the bait-primer. It is important, that these two primers do not have any overlap.

Without the addition of decoy primer, the bait and prey primer can generate a PCR-product spanning from the editing site to the added linker site. This PCR product could then be sequenced.

To enrich for DNA fragments with chromosomal aberrations, two decoy primers are added to the first PCR reaction. In case of small scale CRISPR edits, both of these primers can bind and prevent a successful PCR product between bait and prey primers. Instead two shorter PCR-products are generated which cannot be multiplied in the second, nested PCR because of each of the generated fragments only allow for binding of one of the applied primers. This pre-selects for PCR products with chromosomal events. The sequence between the prey-primer and the cutting site can be used to locate and categorize the chromosomal event (Figure 5.19). A third PCR then adds the necessary barcodes for sequencing.

This method allows us to detect low frequency events, which are not detectable with our MiSeq approach because of their size.

The individual steps in case no chromosomal event has taken place are depicted in Figure 5.19 A., whereas the individual steps in case of a chromosomal event are depicted in Figure 5.19 B.

To induce translocation in T cells for CAST-Seq analysis we performed simultaneous double KOs (Figure 5.20). We again tested non-activated and activated T cells treated with DMSO control or PFT- α .

Displayed in Figure 5.21 A are the CAST-Seq results of *CD4-PDCD1* double edited cells as a Circos-plot. Circos plots are a schematic representation of the observed editing events and is not quantitative. The CAST-Seq library preparation was performed on the *CD4* locus. Shown in green is editing on the *CD4* locus, representing on target CRISPR edits larger than 200 bps and in blue the CRISPR-induced translocations from the *PDCD1* to the *CD4* locus. As expected we induced large-scale on target edits as well as translocations due to the double-editing in all conditions, independent of the activation status of the cells. Depicted in red is an off-target mediated translocation between the *CD4* and the *RABL6* locus. Since the off-target events are at the detection limit of CAST-Seq, we cannot rule out the possibility, that these off-target effects are maybe also present in the other conditions, but at a slightly lower rate.

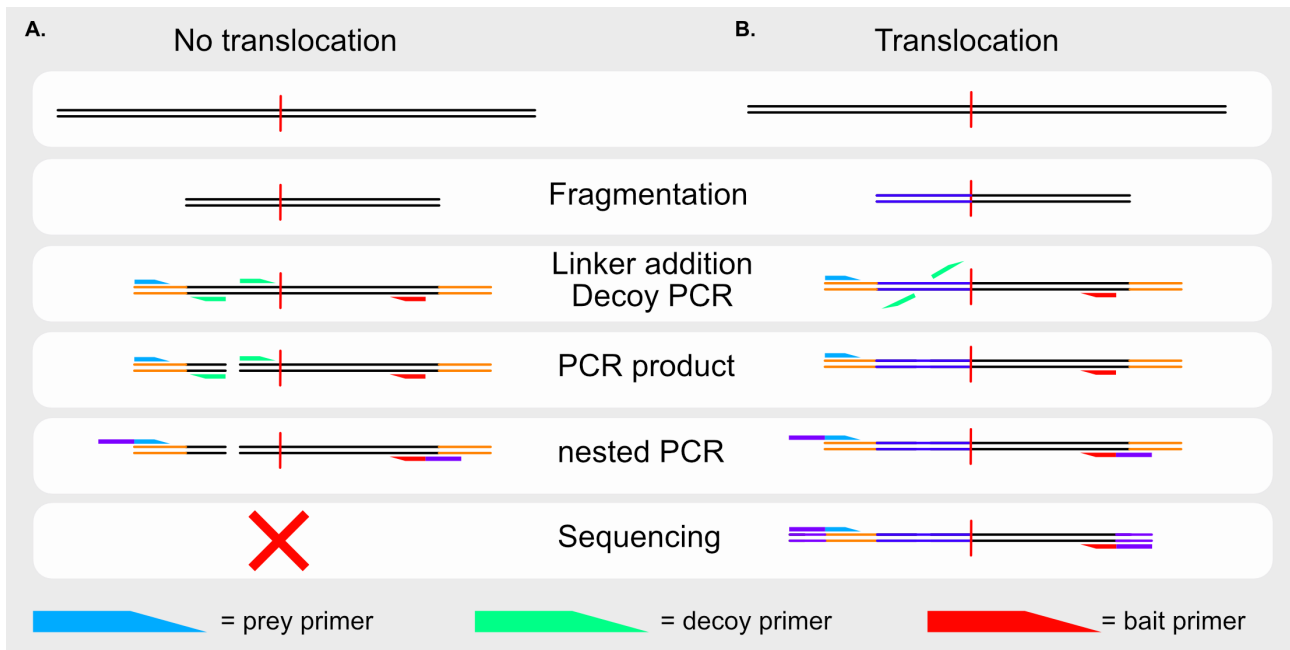


Figure 5.19 Schematic depiction of Cast-Seq. CAST-Seq relies on three distinct primers, which are shown in different colors (blue = prey primer, green = decoy primer, red = bait primer). After a first fragmentation step, linker DNA (orange) is added in a sequence-independent way to each of the generated fragments. Now, the bait primer (located on the fragment) and the prey primer (located on the linker) can potentially generate a PCR product. Which is amplified and barcoded later via the nested primers. **A.** Depiction of CAST-Seq for unedited DNA fragments. The binding of the decoy-primers (green) lead to the generation of two PCR-products, which cannot be amplified in the next step, since each of them only contains one primer binding site. **B.** Here, the translocation (violet), which is introduced via CRISPR-editing, prevents the decoy-primer from binding to the DNA, this leads to one long PCR-product, which then can be further multiplied and barcoded. (adapted from [234])

In order to look at on-target chromosomal aberrations, the normalized read coverage in a region +/- 5 kb around the *CD4* cut site was plotted for each condition (Figure 5.22 A). At the *CD4* locus, the non-activated conditions show a low frequency of deletions, as well as inversions, regardless of whether PFT- α was added or DMSO. Activated cells treated with DMSO show a high rate of deletions and inversions. The *AAVS1* control locus shows only a few background deletions. In line with our previous results, activated T cells treated with PFT- α showed a reduced number of deletions and inversions (Figure 5.22 A, B).

There is also a significant decrease in the mean deletion size for activated T cells treated with PFT- α compared to DMSO treated cells (Figure 5.22 C). Additionally, the rate of translocations between the *CD4* and *PDCD1* gene loci is also reduced in the PFT- α condition (Figure 5.22 D).

For the second on-target locus *PDCD1*, similar observations can be made. However, I want to point out that the *PDCD1* locus was not directly sequenced in these experiments and conclusions were made indirectly via detected translocations from the *PDCD1* locus to the *CD4* locus ("hits" Figure 5.24). While non-activated T cells already show very few hits, the rate of hits (successful translocations) for activated

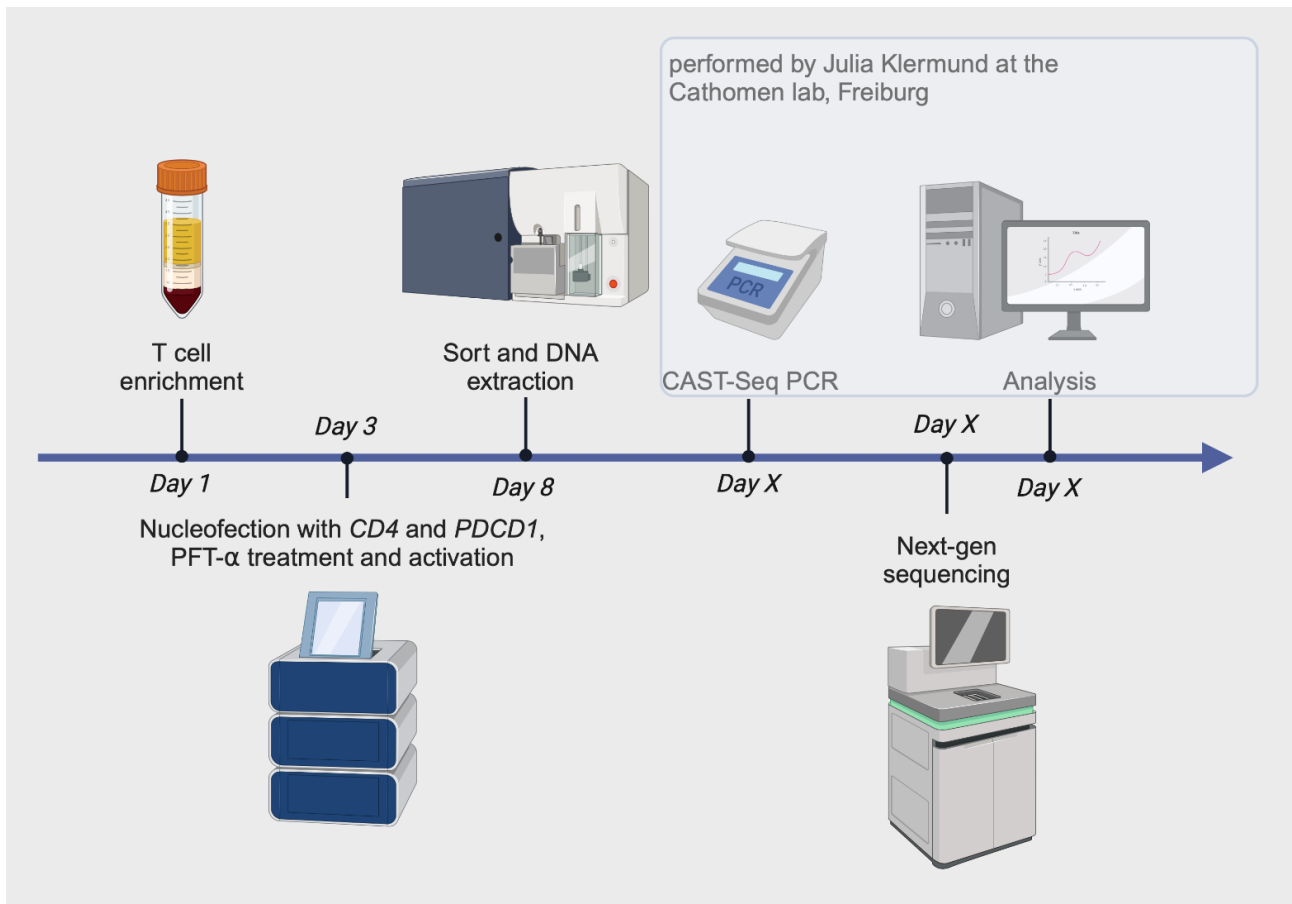


Figure 5.20 CAST-Seq analysis of DMSO- or PFT- α -treated double KO cells. A. T cells were isolated, nucleofected and activated as described before. One condition with a *AAVS1* KO served as a negative control for translocations and large deletions at the *CD4* locus. A simultaneous double KO for *CD4* and *PDCD1* was performed. After cell sorting, the DNA was isolated. CAST-Seq library preparation for the *CD4* gene locus, sequencing and analysis was performed by the Cathomen lab (University of Freiburg).

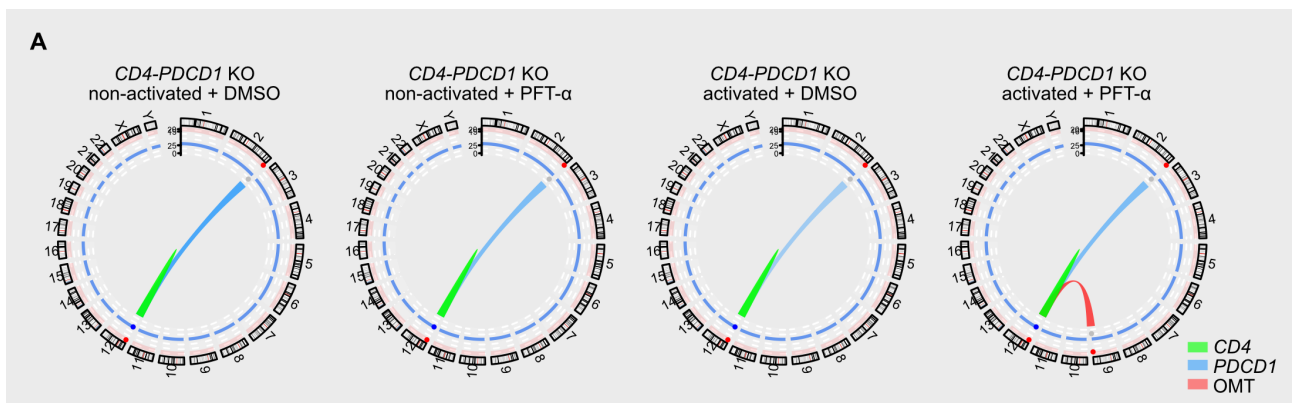


Figure 5.21 Circos-plots for double edited T cells with added DMSO or PFT- α . On-target-mediated events are shown in green (CD4) or blue (PD-1). Off-target-mediated events are shown in red (RABL6) n = 3 biological replicates (adapted from Ursch & Müschen et al.)

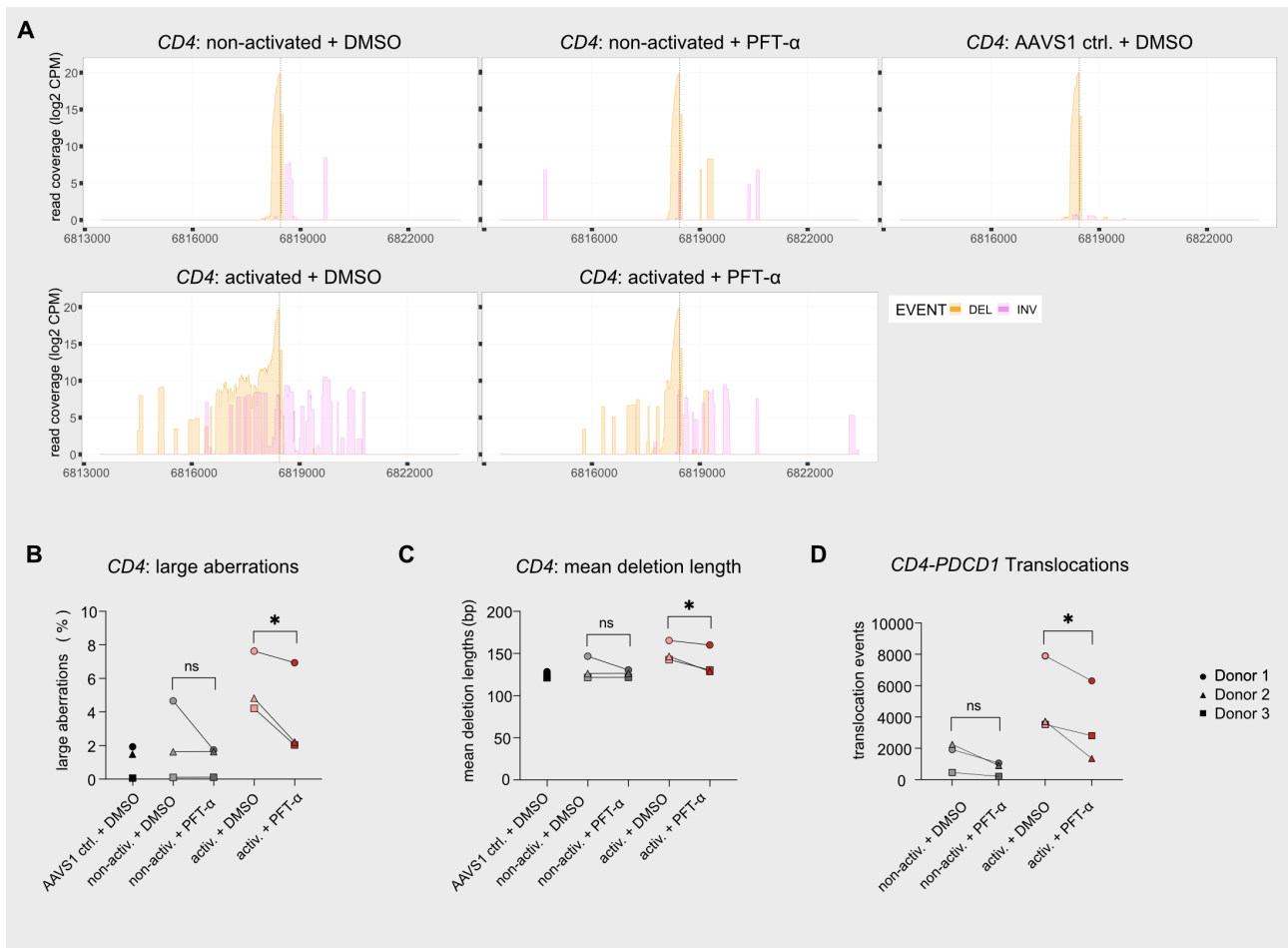


Figure 5.22 On-target results of CAST-Seq for T cells treated with DMSO or PFT- α . **A.** Editing events on the on target site, shown in yellow are the deletions, shown in pink are the inversions. Displayed on the y-axis is the read-coverage and on the x-axis the position of the editing site on the chromosome. The *CD4* on-target site is shown for all four conditions (activated vs non-activated, with versus without PFT- α) and *AAVS1* KO as a negative control. **B.** Percentage of large aberrations and the mean deletion length (**C.**) for the *CD4*-locus of the double-edited cells. **D.** Translocation events between *CD4* and *PDCD1* for the double edited cells. $n = 3$ biological replicates, Paired t-test was used for all comparisons. ns = not significant, * $p < 0.05$. (adapted from Ursch & M \ddot{u} schen et al.)

T cells were reduced in the PFT- α condition. Additionally, the quantification of the area under the curve indicating a reduction of the area around the *PDCD1* cut site, where the translocations stem from (Figure 5.24 B).

Finally, we analyzed the deletion pattern in KO cells by our regular amplicon NGS sequencing pipeline. Again PFT- α decreased the deletion sizes in activated cells. In non-activated T cells only minor changes were observed with PFT- α . Notably, the CAST-Seq experiment was performed with three donors, but due to an insufficient amount of residual DNA, MiSeq analysis was only performed with two of the three donors (Figure 5.23). We aimed to detect the off-target locus *RABL6* in our *CD4-PDCD1* KO T cells with our MiSeq based amplicon NGS approach. As shown in Figure 5.24, the rate of off-target deletions induced via

CD4-PDCD1 RNPs was in all conditions tested on the detection limit and we cannot draw clear conclusion based on this analysis.

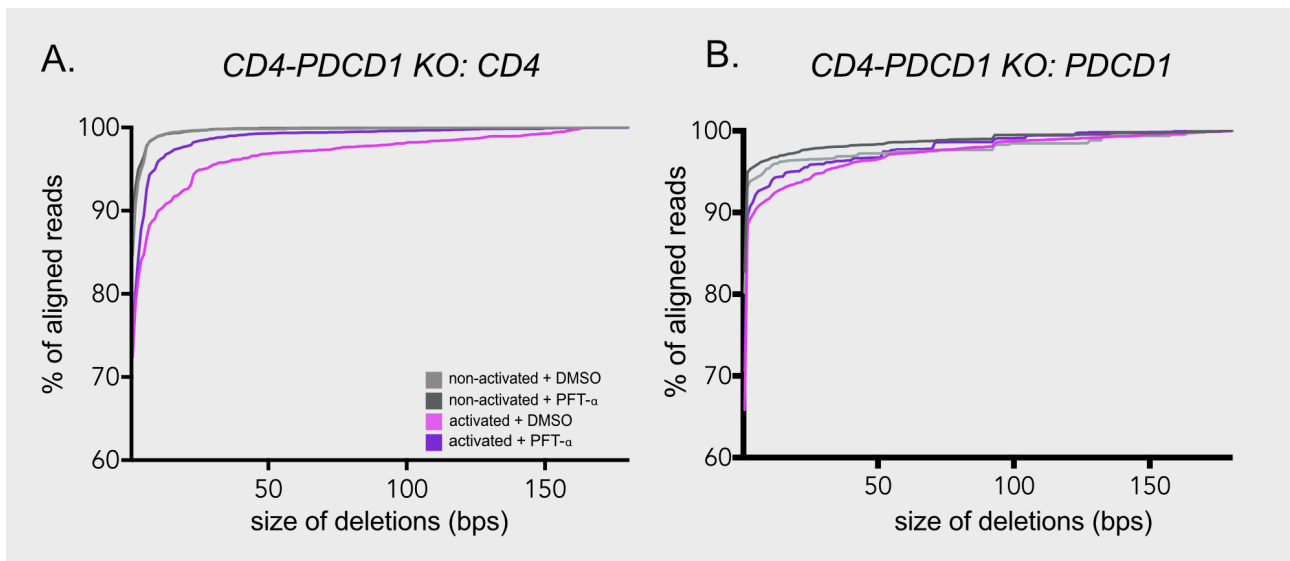


Figure 5.23 MiSeq analysis of DMSO- or PFT- α -treated double KO T cells. **A.** Distribution of deletions for the *CD4* locus in cells, which were CRISPR edited on the *CD4* and *PDCD1* locus simultaneously. The activated or non-activated cells were either treated with DMSO or 30 μ mol/l PFT- α . **B.** Distribution of deletions for the *PDCD1* locus in cells, which were edited on the *CD4* and *PDCD1* locus simultaneously. The activated or non-activated cells were either treated with DMSO or 30 μ mol/l PFT- α . n = 2 biological replicates for *CD4*, n = 3 biological replicates for *PDCD1*

In summary, the occurrence of large deletions is not only detected on a small scale with our MiSeq-based approach, but also detectable on a larger scale. The protective effect of PFT- α extends also to large scale aberrations, including chromosomal translocations. These results suggests, that PFT- α could be a useful addition to clinical CRISPR gene editing protocols to generate safer T cell products for patients.

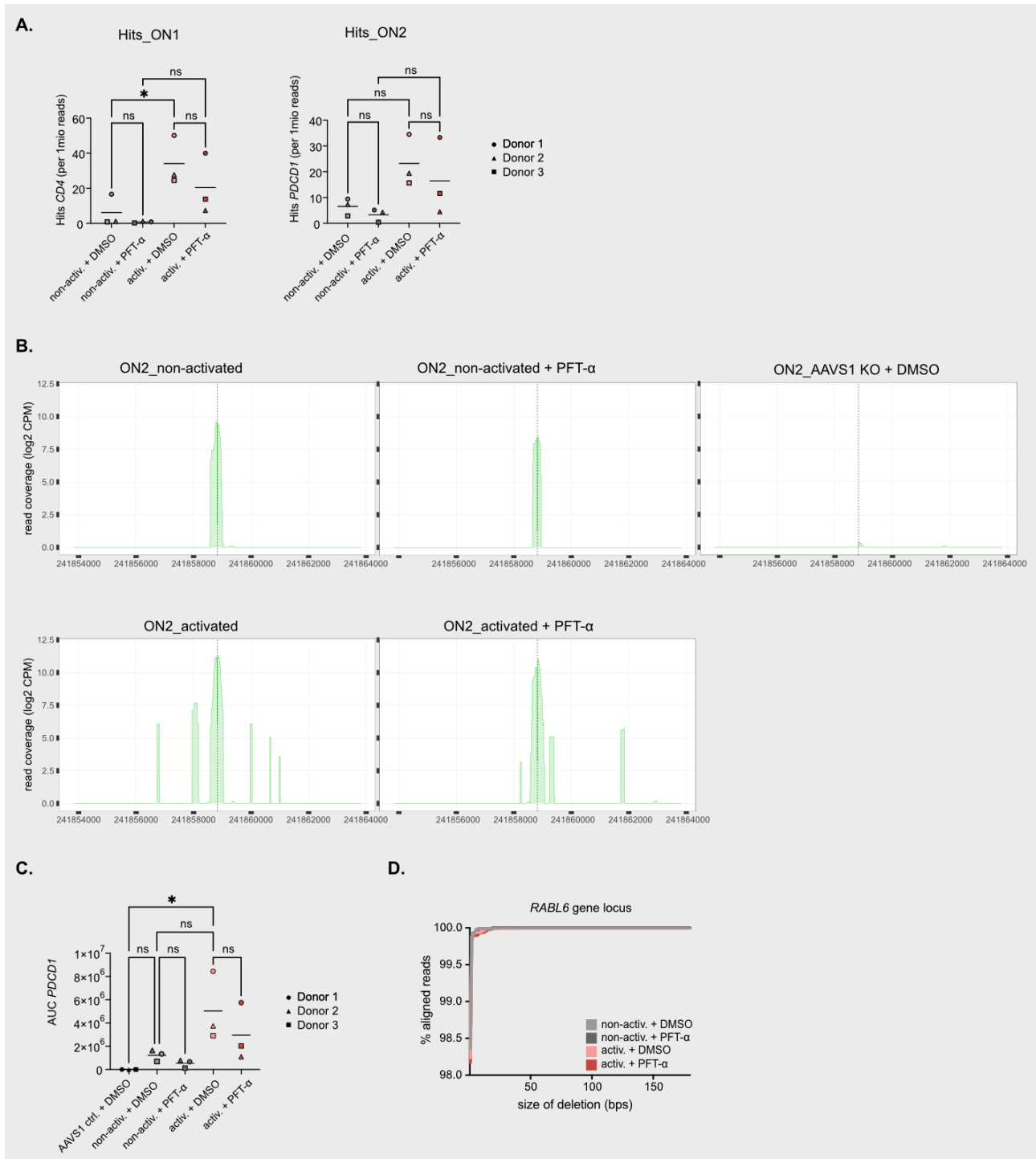


Figure 5.24 CAST-Seq results of chromosomal translocations to *PDCD1* target locus. A. On-target hits for *CD4* (Hits_ON1) and *PDCD1* KO (Hits_ON2) T cells. Number of NGS hits normalized to 10^6 reads at the *CD4* ON1 and from the *PDCD1* ON2 gene loci. **B.** CAST-Seq read coverage plots of +/- 5 kb around the *PDCD1* target site. x-axis indicates the chromosomal coordinates, the y-axis the log₂ read count per million (CPM), and the dotted line the cleavage site. **C.** Indicated the Area-under-the-curve (AUC) for the the *PDCD1* KO T cells. Higher AUC means larger on-target deletions. n = 3 biological replicates **D.** Distribution of deletions for the detected off-target *RABL6* in *CD4-PDCD1* KO T cells with DMSO or with PFT-α. n = 2 biological replicates, Paired t-test was used for all comparisons. ns = not significant, * p < 0.05. (adapted from Ursch & Müschen et al.)

6 Discussion

In my thesis, I systematically analyzed the impact of T cell-intrinsic parameters on the CRISPR editing outcome. The T cell activation status and proliferation speed can shape the deletion pattern. I also identified the small molecule PFT- α as an easily applicable reagent to control large deletions in primary human T cells. In the following sections, I will discuss in detail the technical and biological limitations.

6.1 Technical limitations

6.1.1 Experimental variables

Since I perform all my experiments in primary human T cells, I depend on blood products from human donors. These donors were completely anonymous, and no identifiers were accessible to us such as sex, age, pre-existing conditions, or current immune status. In general, a high variability of human T cells of different donors can be observed. The affected parameters can include cell survival, strength of T cell activation, and the proliferation rate. To address this, I always applied a minimum of 3 donors in my experiments.

A cell-dependent factor I did not control for, was the cell cycle phase during which the T cell editing took place. The cell cycle phase potentially has implications on the choice of DNA repair mechanism, which is applied by the cell to repair the DSB introduced by CRISPR/Cas9 [36] [84]. In these experiments I applied a pool of T cells, which were not pre-selected by any T cell activation or memory markers such as CD45RA and CD45RO, which should be tested in future experiments. Alternatively, cell cycle phases could be equalized by applying inhibitors such as aphidicolin, mimosine, hydroxyurea and thymidine for arrest at the entry of S-phase, nocodazole for arrest at the entry of M-phase and lovastatin for arrest at the entry of G1-phase for a clearer experimental readout [143].

Another factor that might influence the cellular response to PFT- α in the cells used, apart from the activation status, is the nucleofection procedure itself. Since nucleofection is known to alter CD4 T cell morphology, intracellular calcium levels, cell surface activation markers, and transcriptional activity, this could potentially affect the function of PFT- α [152]. To rule out nucleofection-dependent effects, alternative

methods to introduce Cas9 RNPs or Cas9 mRNA into the cells, such as peptide-mediated transfection, lipid nanoparticles or receptor-mediated endocytosis, could be applied [247] [226] [207].

Since both of my detection methods for large deletions, the MiSeq-based approach and CAST-Seq, are based on PCR amplification, I can not rule out the possibility of PCR biases. One concern is that during the PCR amplification, an overrepresentation of smaller amplicons occurs representing sequences with larger deletions [16]. Although this could affect my estimate for the overall occurrence of deletions after editing, these biases should affect all of the tested conditions to a similar degree and should not impact the conclusions drawn based on these results.

6.1.2 Potential impact on different T cell subsets or other cell types

The here described experiments were carried out in CD4⁺ T cells. The Schumann workgroup has an extensive experience in the genetic manipulation of CD4⁺ T cells. Therefore, all experiments were established in CD4⁺ T cells. In a next step, the here-described experimental procedures should be extended to other T cell subsets. Potentially the experimental procedures need to be adapted to the individual T cell subsets. Differences of CD4⁺ and CD8⁺ T cell activation and proliferation have been described for murine T cells. Rabestein et al. described, that the proliferation and expansion of CD4⁺ T cells depends on the continuous presence of antigen, while CD8⁺ T cells only need an antigen signal to start proliferation and do not depend on continuous antigen stimulation [146]. Foulds et al. described, that in mice upon infection CD4⁺ T cells undergo a limited amount of cell divisions, whereas CD8⁺ T cells continue to divide during the whole duration of infection [58].

In general, different DDR pathways are present in all cells, but some cells have preferences for specific pathways. For example mouse embryonic stem cells preferably use homology-directed repair for DSB compared to fibroblasts [113]. Since T cells need the NHEJ pathway in their development for VDJ recombination [18], these cells might have a stronger preference for this pathway compared to other cell types. Future studies will show if the results presented here are transferable to other cell types.

6.1.3 Dependency on gene locus

I tested various genetic loci to confirm my initial assumptions, that proliferation speed correlates with increased deletion sizes and PFT- α reduces the mean deletion size after gene editing with CRISPR/Cas9. I also tested whether PFT- α has any effect on T cell proliferation.

PFT- α 's effect of reducing the mean deletion size could be observed for the *AAVS1*, *CD4*, *CXCR4*, *HAVCR2*, *LAG3* and *TIGIT* gene locus, although the strength of its effect varied depending on the locus. Proliferation speed failed to show an effect for the *HAVCR2* and the *TIGIT* locus. Potentially these proteins are regulating the cell cycle progression in human T cells [128].

The *CXCR4* gene locus showed fewer large deletions compared to the other loci tested (Figure 5.16). Over 80% of the edited cells displayed a deletion of 2bp. Potentially the DNA at this target site is probably repaired using mostly microhomology-mediated end joining, which produces very defined deletions almost all of the time [195]. The remaining 10% of the deletions, which presumably are repaired by conventional-NHEJ show the expected deletion pattern based on proliferation speed and a comparable reduction in deletion sizes with PFT- α (Figure 5.16).

So even if I tested multiple genetic loci, and the PFT- α effect on the mean deletion size was observable in all of them and the dependence of the deletion size on the proliferation speed was observable in most of them. However, I still cannot rule out that some loci will react different to the PFT- α treatment or show a different deletion pattern based on their proliferation speed. This might be the case in gene loci regulating cell cycle progression or DNA repair.

Although described as a p53 inhibitor, conditions treated with PFT- α did not show an increase in absolute KO cell numbers, indicative of increased cell survival after gene editing (Figure 5.11). Instead, depending on the donor and the experimental setup PFT- α treatment even results in a decrease in proliferation, although only for *AAVS1* KO T cells. This further supports the conclusion that PFT- α is not targeting p53 in these experimental setups. These effects could rather be mediated through one of the proposed targets of PFT- α , the checkpoint inhibitor cyclin D1. This is discussed in more detail in section 6.3 in this thesis.

Arrest of the cell cycle would extend the time for DNA repair, which might also explain why PFT- α show a slight decrease in KO-efficiency for some targets (Figure 5.11 B). This would be in line with my observation, that faster proliferating cells generally show a higher KO-efficiency than slower proliferating cells (Figure 5.10 B). But both of these reductions in KO-efficiency are nearly as strong as the decrease in KO-efficiency for non-activated cells compared to activated cells.

6.1.4 Size limitations of amplicon MiSeq NGS data

There are different strategies to sequence amplicons on the MiSeq platform. The most important distinction is single-end versus paired-end reads. Single-end reads only sequences the DNA from one direction. This limits the possible overall length of the amplicon to 251 bp, but increases the sequencing depth. I chose to sacrifice sequencing depth by using paired-end reads to enable the sequencing of larger amplicons. In theory this allows for amplicons with a maximum size of 501 bp, but since the MiSeq sequencing reads were aligned using CRISPResso2, the usable amplicon size is around 450 bp, as the alignment tool needs an overlap of about 25bp to generate a single sequence out of the two reads, which result from the paired-end setup used for sequencing. After alignment of the paired-end reads, CRISPResso2 aligns in a second step the whole sequence to a reference amplicon, which has to be provided by the user. To successfully

execute this alignment, CRISPResso needs a match of around 100 bp at each end. This results in a detection limit of around 180-200 bp for large deletions using this pipeline. The majority of deletions after gene editing are in this size range [192], but there is still a proportion of larger deletions, which cannot be detected using this approach. I hypothesized that deletions larger than 200 bp behave the same way as smaller deletions. However, I could not fully exclude the possibility, that some effects differ. To attribute for that, CAST-Seq was applied in cooperation with the Cathomen workgroup in Freiburg, which enables the detection of considerably larger deletions as well as translocations, with a threshold for detection as low as 1 chromosomal aberration per 10^4 cells [234]. The results of CAST-Seq confirmed my findings generated using the MiSeq platform regarding the use of PFT- α and the impact of TCR-stimulation on large deletions. This suggests, that the mechanisms causing larger deletions > 200 bp are similar to the ones causing deletions < 200 bp.

6.1.5 Effects of PFT- μ

I also tested the effects of PFT- μ on the mean deletion size after gene editing. PFT- μ inhibits p53-dependent apoptosis by preventing p53 binding to Bcl-xL and Bcl-2 at the mitochondrial surface [79]. This is in line with my observations for PFT- μ , which increases the mean deletion size for *AAVS1*, *CD4* and *PDCD1*, but only in slow proliferating cells for *PDCD1* (Figure 5.11 A). The use of PFT- μ did not influence the cell proliferation (Figure 5.11 D). This effects seems to be p53-mediated, as it is partly abrogated in cells with a KO for *TP53* (Figure 5.18 D). The increase of deletion sizes with PFT- μ were rather modest and additional higher concentrations and different experimental settings should be tested in the future.

6.1.6 Unclear mode of action of PFT- α

Although PFT- α was first described over 20 years ago [40], the exact mechanisms, which mediate its function are not fully clear. PFT- α has been described as an inhibitor of the p53 pathway, specifically of the transcriptional activity of p53, which should result in the inhibition of apoptosis upon DNA damage [253] [100]. PFT- α does not alter the level of intracellular p53, but has been described to inhibit DNA binding activity of p53 [40]. PFT- α has also been described to increase efficacy of the anti-cancer drug topotecan in a p53-dependent manner in several cell lines indicating cell-specific effects [198]. A more recent study aimed to dissect the exact mechanism by which the effects of PFT- α are mediated and found that PFT- α modulates post-translational modifications of p53 to achieve its effects. The authors hypothesize, that PFT- α only modulates the kinases that modify p53, like DYRK2, CHK1, CHK2, CK2, HIPK2, JNK, LRRK2, p38, PKC δ , and PLK3. Based on this hypothesis, the effect of PFT- α is only measurable, if the specific kinase is already active and exerts some effects on p53 [228]. There is also evidence, that PFT- α inhibits apoptosis in a p53-independent way via modulation of cyclin D1 [100] or the activation of macro-

autophagy [158]. PFT- α has also been described to be neuroprotective in mice after traumatic brain injury via the regulation of oxidative stress, neuroinflammation, autophagy, and mitophagy in a p53-dependent as well as p53-independent manners [227]. Another target described for PFT- α is the Aryl hydrocarbon Receptor (AhR). PFT- α induces the dimerization of AhR with its DNA-binding partner Aryl hydrocarbon receptor nuclear translocator, this enables the formation of a DNA-binding complex. PFT- α also activates reporter activity, and upregulates CYP1A1. These effects might mediate p53-independent effects of PFT- α [72]. My results clearly showed an p53-independent mode of action. Genetical ablation of p53 did not affect the PFT- α dependent reduction of large deletions. One further explanation of the p53-independent effects could be PFT- α degradation. It has been described by Walton et al. that PFT- α is only stable for a limited amount of time, with a half-life of 59 min in cell culture conditions, before it condensates to PFT- β [76]. The degradation of PFT- α does not seem to negatively affect its functionality [227] [158] [117]. However, I must take into account, that the condensation to PFT- β might impact the results of the experiments. Fernandez-Cruz et al. describe, that the effects of PFT- α on the aryl hydrocarbon receptor might be mostly executed by its condensation-product PFT- β [117]. The possible influence of condensation products to our results cannot be ruled out by my experimental setup. To test the potential impact of PFT- β on my experimental setup, PFT- β should be tested alongside PFT- α and a known activator of the aryl hydrocarbon receptor called 2,3,7,8-tetrachlorodibenzo-p-dioxin [77]. Walton et al. also observed a lack of p53-dependent effects described for PFT- α in human cell lines. This is also in contrast to the subsequent studies mentioned above, which used PFT- α [100] [72] [117][40][228]. The authors of Walton et al. reasoned, that the protective effects of PFT- α observed in other studies originate from its capability to disrupt p53-dependent pro-apoptotic pathways in a tissue-context-dependent manner. Therefore it might be the case, that observations for one cell type are not transferable to other cell types [76].

6.2 Biological and gene engineering implications

6.2.1 Involvement of p53 in CRISPR-editing

The p53-pathway monitors DNA-damage, therefore it is not surprising, that p53 is also activated during gene editing, which introduces DSB. Taipale and colleagues described, that in immortalized human retinal pigment epithelial cells, gene editing leads to a response of the p53-pathway, which arrests the cell cycle for DNA-damage repair. The authors observed, that in a CRISPR screen with KO of various genes, KO cells with a depleted p53-pathway were enriched. These results suggest, that cells with a functional p53 pathway have a selective disadvantage, due to the cell cycle stop induced by p53 upon sensing of DNA-damage [182]. This was also confirmed by a publication by Kaykas et al., who showed, that the p53-pathway hinders efficient editing in human pluripotent stem cells, especially homology-directed repair [184]. Since then, many publications have tried to further investigate the intricacies between p53 and gene editing. Several publications confirmed the hypothesis by Taipale et al., that CRISPR-editing selects for p53-deficient cells. Ben-David et al. were able to show, that for 165 human cancer cell lines, the introduction of Cas9 leads to an initial upregulation of the p53-pathway, which then leads to a selection process for cells with defective p53 pathway [217]. In mouse cell lines, *TP53*-negative cells have a proliferation advantage over WT cells in a competitive assay, but only in the presence of CRISPR/Cas9 editing. The authors propose transient inhibition of p53 to omit the selective advantage of p53-deficient cells. They were able to show protective effects for inhibition of with siRNA targeting p53, but not for PFT- α [239]. [239]. The hypothesis, that p53 has a negative impact on gene editing and p53-deficient cells have a proliferative advantage over WT-cells, is also strengthened by a screen in a human MOLM13 cell line, in which various CRISPR-mediated KOs in p53 deficient and p53 wildtype cells, as well as a shRNA-based screen for the same targets were performed. The authors compared, which targets lead to a decrease in viability specifically in p53-WT cell lines compared to p53-mutant cell lines. These targets were deemed to be p53-dependent. They then tested, which of these p53-dependent targets decreased viability when performing a CRISPR KO screen, but not in the shRNA-based screens. Therefore, the identified targets decrease viability only for KOs generated with CRISPR in a p53-dependent way. They termed these targets "CRISPR-specific differentially essential positive" (CDE+) and observed, that they were often located next to chromosomal bands containing common fragile sites, which could act as potential breaking points for the chromosome. They also observed, that editing cells on these CDE+ targets positively selects for p53-deficient cells [233].

Transient inhibition of p53 has been proposed by a number of other publications, which focused on the selection of p53-deficient cells through p53-mediated apoptosis in CRISPR-editing, initially stated by Kaykas et al. [184]. Harty and colleagues describe, that p53 complicates the editing of CD8+ memory

T cells in mice and that CRISPR editing efficiencies can be increased by the transient inhibition of p53 via siRNAs [220]. An alternative approach is temporarily overexpressing anti-apoptotic BCL-XL in human pluripotent stem cell lines, which increases overall cell survival, as well as CRISPR editing efficiency [187]. A more in-depth characterization of p53 was performed by Alvarez and colleagues. By analyzing isogenic cell lines jointly with previous screening data from 900 cell lines, they found that the downstream functions of p53 are always activated to a similar extent during CRISPR editing, but the induction of apoptosis, which selects for p53-deficient cells, depends on the chromatin context and the presence of certain DNA motives next to the cutting site. Target regions within the euchromatin resulted in higher cell toxicity. Interestingly downstream activation of the NHEJ pathway resulted in much higher cell toxicity compared to HDR and MMEJ [237].

Seemingly, transient p53-inhibition solves both of the problems stated above – cell survival and editing efficiencies. However, there is a huge caveat to that, because CRISPR/Cas9 induces cell-cycle arrest for DNA-repair in a p53-dependent manner, which is crucial for maintaining genomic integrity [218]. Bedel et al described, that in CD34+ cells inhibition of p53 via siRNA during CRISPR editing results in a huge increase in "loss of heterozygosity" (LOH), which in this context can be understood as aneuploidy [245]. The authors also proved, that the rate of cells with LOH is connected to the proliferation speed in a way that fast proliferating cells have a higher frequency of LOH. The authors reasoned that this is due to cells with a faster proliferation speed having less time for DNA-repair [245]. A persisting DSB during replication, for example, could trigger a replication fork collapse, which may cause aneuploidy [186]. Over time the frequency of cells affected by LOH decreased in the overall cell population, but could still be detected after 16 days of culture [245].

In the here described experiments, I inhibited p53 transiently via PFT- μ and ablated *TP53* genetically via knockout. Both strategies resulted in more large deletions, with no change to the proliferation speed, which is in line with the described functions of p53 and the results presented by Bedel and colleagues [245].

6.2.2 Large deletions in CRISPR-engineered cell lines

Initially large deletions and chromosomal aberrations after CRISPR editing have been described in human cell lines or primary mouse cells [205] [185] [206]. It was first shown, that for mouse embryonic stem cells and immortalized human female retinal pigment epithelial cell lines, the use of CRISPR/Cas9 can result in up to 20% of cells with a deletion larger than 250 bps or 36% of cells with a deletion larger than 100 bps, respectively [185]. In cancer cell lines like COLO320, HCC2998 and SW1463, large deletions upon CRISPR-editing are also detectable with karyotyping and fluorescence in situ hybridization [206]. Hematopoietic stem and progenitor cells show deletions up to several kbps, when different genes, like

HBB (11.7 to 35.4%), *HBG* (14.3%), and *BCL11A* (13.2%) are targeted with CRISPR/Cas9. These frequencies were measured with different methods including clonal genotyping, droplet digital polymerase chain reaction, single-molecule real-time sequencing and long-amplicon sequencing assay [242].

A potential explanation for the generation of large deletions could possibly be the involvement of MMEJ in DNA-repair, since it has been shown, that deficiencies in MMEJ related genes (*Nbn* and *Polq*) decrease the frequency of large deletions in mouse stem cell lines [240]

6.2.3 Large deletions and aneuploidy in CRISPR-engineered T cells

Large deletions are not only described for cell lines, but also for primary human T cells. Large deletions are observable in 15.2% of cells edited at the *PDCD1* locus [242]. Primary human T cells edited on *EEF2*, *AAVS1*, and two separate locations on *BCL11A* showed a rate of 12% of deletions larger than 100bps [235].

Another related phenomenon is the occurrence of chromosomal loss/aneuploidy in primary T cells after CRISPR editing, which has been well described for primary human T cells [223] [241] [250].

KI of CAR constructs into the TRAC-locus as performed in a clinical trial resulted in higher and more reliable expression levels of the introduced CAR [223]. However, in another study targeting the TRAC locus with a Cas9 RNP resulted in up to 9% of chr14 loss on day 4 after CRISPR editing. Also the risk for chromosomal events such as aneuploidy or truncations was increased after performing a simultaneous KOs with gRNAs targeting the *TRAC*, *TRBC2* and *PDCD1*. In this case, the rate of chromosomal events (aneuploidy or truncations) was 9% for the *TRAC*-locus and additional 9,9% for the *TRBC2*-locus. Aneuploid T cells had a survival or proliferation disadvantage in prolonged cell cultures, but were still detectable on day 11 after CRISPR editing. The authors suggest using ddPCR to screen for such events, especially in the context of clinical applications [241]. In CD34+ cells, so-called chromothripsis has been detected after CRISPR editing [232]. Chromothripsis describes the event of multiple genetic rearrangements occurring at the same time, leading to cancer development in a single step [122]. Although, so far not observed in T cells, the underlying mechanism might also apply to this cell type further increasing the risk of adverse events for CRISPR editing in clinical settings.

The described study by Barzel et al. identified the risk of CRISPR induced aneuploidy in human T cells, however the cell-intrinsic driving forces were unclear [241]. A study by the Doudna laboratory addressed this issue by firstly confirming CRISPR-induced aneuploidy in human T cells for various different loci (e.g. TRAC, TRBC, PDCD1, B2M, IL2RA, CXCR4, CIITA, BCL11A, HBB, TTR, HTT, SERPINA1). Besides that, they also observing p53-activation in these cells, and a decrease of cells bearing chromosomal loss in cell culture conditions similar to existing clinical protocols. Interestingly, the authors did not observe any connection between the employed DNA repair pathways (NHEJ, MMEJ, HDR) and the rate of chromosomal

loss, suggesting an event prior to DNA repair as a possible cause for chromosomal loss [250]. When the authors screened the edited cells of the patients from the clinical study performed by June et al., the rate of chromosomal loss was surprisingly low compared to their *in vitro* results [223] [250]. This was attributed to a change in the CRISPR editing part of the clinical protocol [250]. Most of the T cell editing protocols activate the T cell prior to nucleofection, since this increases the gene editing efficacy, whereas the protocol used by June et al. nucleofected the cells prior to activation [223]. This activation strategy was similar to the protocol I applied in most of my experiments. The observed results are also similar, since post-activation of the cells lead to a decrease in chromosomal loss in the publication by Doudna et al., while I observed a decrease in the mean deletion size for the post-activated cells compared to pre-activated cells. Doudna and colleagues attributed this decrease in large chromosomal events to the different levels of p53 depending on the used protocol [250].

In order to expand, T cells downregulate p53 upon TCR-stimulation [150]. This difference in p53 levels could cause a high rate of chromosomal loss in the pre-activated T cell populations. Based on these differences in mean deletion size I observed for pre- versus post-activated cells, I would suggest to modify experimental protocols accordingly, depending on the desired outcome. This means activating the cells after gene editing to reduce the mean deletion size. This strategy has also been suggested by Doudna and colleagues [250]. Although this might reduce the risk of chromosomal loss, it might also not be feasible for application given the reduced editing efficiency observed in cells, which are activated after the nucleofection.

Another conclusion that can be drawn from my results is that the mean size of large deletions is dependent on the proliferation speed of the edited cells (Figure 5.10). Since in my experiments cells with faster proliferation speed also showed a higher mean deletion size, the problem might arise, that these faster proliferating cells out-compete the slower proliferating cells with a smaller mean deletion size. A potential solution for this problem could be cell sorting based on proliferation staining.

6.2.4 The use of PFT- α in genetic engineering

PFT- α has been employed for the inhibition in the context of gene editing before [245] [239] [218]. But only in cell lines [239] [218] or in CD34+ cells [245] and for the purpose of transient inhibition of p53 [239] [218]. Since the PFT- α is not very specific for p53 nor very efficient for p53-inhibition, it is not surprising, that, it failed to show any of the desired effects especially if compared to siRNAs targeting of *TP53* [228] [76] [158] [245] [239]. In fibroblasts repetitive treatment of 30 $\mu\text{mol/l}$ PFT- α before and for 5 days after nucleofection with Cas9 RNPs resulted in a higher rate of LOH [245]. Although this is not directly contrary to my results, since I did not quantify the rate of haploid cells but rather the mean size of the deletion, it is important to note, that the effects of PFT- α could differ. A possible explanation for the different observations might

be the different cell types used or the different cumulative dose of PFT- α , six doses of 30 μ mol/l PFT- α before and after nucleofection versus the transient single-dose administration of 30 μ mol/l I used directly after Cas9 RNP nucleofection. Potentially the p53-targeting effects of PFT- α are cell type-, context- and dose-dependent. Future studies testing different PFT- α administration protocols in a variety of cell lines and primary cells are necessary to clearly test for the impact of PFT- α on large deletions. In parallel, p53 KO should be performed in the respective cell types to clearly separate potential p53-dependent and independent effects.

6.3 Evaluating potential targets for PFT- α

Several targets of PFT- α have been described in the literature besides p53 including the aryl hydrocarbon receptor, cyclin D1 or COX2. They are listed in table 5.2 with their source publication. The effects of PFT- α are not necessarily limited to one target and can potentially also simultaneously affect multiple proteins. It is also worth mentioning, that the effects of PFT- α can presumably be cell-type specific. Further validation studies targeting the potential target of PFT- α via CRISPR-KO, inhibitors or siRNA will give us important insights about PFT- α 's mode of action.

target	publication
p53 binding activity	Komarov et al. [40]
Aryl hydrocarbon receptor	Hoagland et al. [72]
cyclin D1	Sohn et al. [100]
53BP1 foci generation	Geisinger et al. [218]
COX2	Kim et al. [105]

Table 6.1 List of potential targets for PFT- α

PFT- α has been widely described as a p53 inhibitor. I tested two different inhibitors of p53 and their impact on the CRISPR editing outcome. PFT- μ prevents p53 binding to Bcl-xL and Bcl-2 and, therefore, prevents p53 mediated apoptosis [79]. PFT- α has been described to inhibit the transcriptional activity of p53 [40]. To my surprise the effects of PFT- α and PFT- μ were opposite to each other. PFT- μ increased the average deletion size in line with the known functions of p53, whereas PFT- α reduces large deletions (Figure 5.12). I hypothesize that the effects of PFT- α are not mediated via the inhibition of p53. To test this hypothesis I generated a KO for p53 before introducing a second KO with the addition of PFT- α or PFT- μ . As shown in Figure 5.18, the effect of PFT- α seems to persist even in the absence of p53, which suggests that p53 is not necessary for PFT- α to execute its effects. PFT- μ treatment resulted in either no changes in deletion sizes in *TP53* KO T cells or even further increased deletion sizes by potentially acting on *TP53* haploid cells. However, although the mean KO-rate was around 70% for all conditions (figure 5.18 B), I can not totally exclude the possibility, that a remaining population of p53 positive cells influenced the outcome. Taken together, it seems likely that the mechanisms through which PFT- α executes its functions do not rely on the p53-pathway in my experimental setting and the used concentrations.

The **Arylhydrocarbon receptor (AhR)** has been implicated as another target of PFT- α [72]. AhR mediates the generation of ROS [59] and activates cytochrome p450 [156]. AhR is also involved in the NF- κ B pathway via RelB [86]. AhR has a role in T-cell-mediated immune responses by affecting the differentiation of activated T cells and is rapidly expressed after T cell activation [145] [101]. Taken into consideration the

publications by Walton et al. and Fernandenz-Cruz et al. it seems more likely, that the effects of PFT- α treatment on AhR signalling are carried out by PFT- α 's condensation product PFT- β [117] [76].

One potential mechanism for PFT- α could be the induction of a cell cycle arrest via **cyclin D1** inhibition. Sohn et al. showed that PFT- α exerts anti-apoptotic effects, but only in the presence of cyclin D1, which is a cell cycle regulator of the G1 to S-phase transition [100]. A knock-down of cyclin D1 abrogated the anti-apoptotic effect mediated by PFT- α . Since the repair mechanisms for DSB are cell cycle dependent (NHEJ mainly happens during G0/G1, while HDR predominantly happens during S/G2-phase of the cell cycle), potentially an extended period for DSB repair could decrease the risk of errors reducing the risk of large deletions. This hypothesis could be tested via the blockade of the cell cycle checkpoints between G1- and S-phase. Blockage could be potentially induced by the use of certain inhibitors like Aphidicolin, hydroxyurea, lovastatin, mimosine, nocodazole and thymidine, to lock the cells either into M-, G1- or S-phase, as already performed in the context of CRISPR editing [143]. This could potentially pinpoint possible cell cycle dependent effects of PFT- α .

Geisinger et al. observed a reduction of **53BP1 foci** at the location of DSB after the use of PFT- α [218]. Since 53BP1 is necessary for the induction of NHEJ, the use of PFT- α could potentially shift DSB repair-mechanisms more away from NHEJ and more towards HDR, which has potentially a lower risk of large deletions, since it is less prone to introducing errors [209]. The hypothesis that PFT- α mediates its function via 53BP1 inhibition or interference with 53BP1 foci formation could be tested by adding i53BP1, a 53BP1 inhibitor, to CRISPR-edited T cells [251].

A surprising target by which PFT- α potentially could mediate its effects might be the **cyclooxygenase-2 (COX2)**. COX2 is involved in inflammation and T cell activation [39] and is upregulated in the presence of PFT- α [105]. However, it is unclear if this is a direct or indirect effect. To test whether PFT- α does rely on COX2 to execute its effects, inhibition of COX2 via one of the many clinically approved selective COX2 inhibitors (e.g. celecoxib) could be tested.

Most likely, PFT- α affects several proteins and their combined effects result in the observed phenotypes. Therefore, I will most likely need to perform double/triple/etc. KOs in primary human T cells to be able to recapitulate the PFT- α phenotype. Furthermore, it is unclear if PFT- α also targets additional, so far not identified proteins. In this case, an unbiased, global protein identification approach should be performed. For example, technologies such as thermal proteome profiling [155] [200], click chemistry approaches [231] or metabolic fingerprinting [175] [191] could give important insights into PFT- α 's targets. The results shown in this study indicate a connection between T cell activation and various DNA repair mechanisms.

Further research is needed to pinpoint the exact targets of PFT- α , which then in turn could be valuable findings for the further investigation of the mechanism, which take place in cells after gene editing with CRISPR/Cas9.

6.4 Addressing safety

CRISPR-engineered adoptive T cell therapies are already tested in the clinic [223][238]. The goal of my thesis was to generate more precise and thus safer protocols for CRISPR-engineered T cells. Therefore, I also need to consider the potential safety implications, that the use of PFT- α could have for patients. Given the short half-life under cell-culture conditions of 59min [76], long-term effects from PFT- α are highly unlikely, but off-target effects, like the modulation of the AhR in the treated T cells could pose an issue [40] [245] [72]. It would also be reasonable to measure the levels of PFT- α 's condensation product PFT- β in the cell-culture medium to assess the potential risks of this byproduct.

6.4.1 Phenotypic characterization and killing capacity

Potentially PFT- α could negatively affect or change the phenotype of the treated cells. Therefore an extensive phenotypic characterization of the cells should be performed. This is especially important since there is little data on its use in T cells, except for a publication by Eleftheriadis et al., who did not observe an influence of PFT- α on glucose consumption, lactate production and cell proliferation in PBMCs [141]. CD8 T cells are used for adoptive T cell therapies to kill cancer cells [199]. Since tumor cell neutralization is the most important aspect for T cell therapeutics, the killing function of T cells treated with PFT- α should be measured in CAR or TCR-transgenic T cells for example in *in vitro* killing assays. Other phenotypic properties like the release of effector cytokines or the expression of exhaustion markers should also be examined in cells treated with PFT- α . The next step would be to challenge PFT- α or control-treated CAR or TCR-transgenic T cells *in vivo* in tumor models in humanized mice.

6.4.2 Assessing the rate of aneuploidy

As already mentioned in section 6.2.3, a main adverse event in the gene editing of T cells is the occurrence of aneuploidy in the edited cells [245] [241] [250]. Since PFT- α is able to decrease the mean deletion size for edited cells, there is reason to assume, that PFT- α also might decrease the rate of aneuploidy in T cells. This could be tested via the use of single cell karyotype sequencing, which would allow for the detection of copy number variations, after gene editing and the use of PFT- α , or scRNA-seq as applied before [194][241][126] [211].

6.5 Possible applications

6.5.1 Increasing safety in gene edited T cell products

My findings might be of clinical relevance, since the recently discovered appearance of large deletions or even chromosomal aberrations underscore the need for T cell editing protocols, which minimize the risk for such events. These events can potentially result in the malignant transformation of single T cells within the engineered T cell therapeutics, which could lead to the development of lymphoma in these patients [90]. Besides adapting TCR-stimulation protocols, the addition of the small molecule PFT- α , which is easy to integrate into existing protocols and does not compromise editing efficiency and T cell expansion, can reduce the risk of chromosomal aberrations in primary human CRISPR-engineered T cells.

Bibliography

- [1] N. Hozumi and S. Tonegawa, "Evidence for somatic rearrangement of immunoglobulin genes coding for variable and constant regions.", *Proceedings of the National Academy of Sciences*, vol. 73, no. 10, pp. 3628–3632, Oct. 1976, ISSN: 1091-6490. DOI: 10.1073/pnas.73.10.3628.
- [2] S. Gillis, M. M. Ferm, W. Ou, and K. A. Smith, "T cell growth factor: Parameters of production and a quantitative microassay for activity.", *Journal of immunology (Baltimore, Md. : 1950)*, vol. 120, pp. 2027–2032, 6 Jun. 1978, ISSN: 0022-1767, ppublish.
- [3] J. R. Totter, "Spontaneous cancer and its possible relationship to oxygen metabolism.", *Proceedings of the National Academy of Sciences*, vol. 77, no. 4, pp. 1763–1767, Apr. 1980, ISSN: 1091-6490. DOI: 10.1073/pnas.77.4.1763.
- [4] D. E. Brash and W. A. Haseltine, "Uv-induced mutation hotspots occur at dna damage hotspots", *Nature*, vol. 298, pp. 189–192, 1982. [Online]. Available: <https://api.semanticscholar.org/CorpusID:4275546>.
- [5] K. Itoh, A. B. Tilden, and C. M. Balch, "Interleukin 2 activation of cytotoxic t-lymphocytes infiltrating into human metastatic melanomas.", *Cancer research*, vol. 46, pp. 3011–3017, 6 Jun. 1986, ISSN: 0008-5472, ppublish.
- [6] A. Townsend, "The epitopes of influenza nucleoprotein recognized by cytotoxic t lymphocytes can be defined with short synthetic peptides", *Cell*, vol. 44, no. 6, pp. 959–968, Mar. 1986, ISSN: 0092-8674. DOI: 10.1016/0092-8674(86)90019-x.
- [7] P. J. Bjorkman, M. A. Saper, B. Samraoui, W. S. Bennett, J. L. Strominger, and D. C. Wiley, "Structure of the human class i histocompatibility antigen, hla-a2", *Nature*, vol. 329, no. 6139, pp. 506–512, Oct. 1987, ISSN: 1476-4687. DOI: 10.1038/329506a0.
- [8] Y. Ishino, H. Shinagawa, K. Makino, M. Amemura, and A. Nakata, "Nucleotide sequence of the iap gene, responsible for alkaline phosphatase isozyme conversion in escherichia coli, and identification of the gene product", *Journal of Bacteriology*, vol. 169, no. 12, pp. 5429–5433, Dec. 1987, ISSN: 1098-5530. DOI: 10.1128/jb.169.12.5429-5433.1987.
- [9] A. Veillette, M. A. Bookman, E. M. Horak, and J. B. Bolen, "The cd4 and cd8 t cell surface antigens are associated with the internal membrane tyrosine-protein kinase p56lck", *Cell*, vol. 55, no. 2, pp. 301–308, Oct. 1988, ISSN: 0092-8674. DOI: 10.1016/0092-8674(88)90053-0.
- [10] T. F. Gajewskj, S. R. Schell, G. Nau, and F. W. Fitch, "Regulation of TCell Activation; Differences among TCell Subsets", *Immunological Reviews*, vol. 111, no. 1, pp. 79–110, Oct. 1989.
- [11] G. Gross, T. Waks, and Z. Eshhar, "Expression of immunoglobulin-t-cell receptor chimeric molecules as functional receptors with antibody-type specificity.", *Proceedings of the National Academy of Sciences of the United States of America*, vol. 86, pp. 10024–10028, 24 Dec. 1989, ISSN: 0027-8424. DOI: 10.1073/pnas.86.24.10024, ppublish.
- [12] R. J. Pisani, P. J. Leibson, and D. J. McKean, "In vitro activation of lymphocytes from nonsmall cell cancer patients by interleukin 2 and anti-cd3 antibody", *Clinical Immunology and Immunopathology*, vol. 50, no. 3, pp. 348–363, Mar. 1989, ISSN: 0090-1229. DOI: 10.1016/0090-1229(89)90142-6.

- [13] R. M. Kotin, M. Siniscalco, R. J. Samulski, *et al.*, "Site-specific integration by adeno-associated virus.", *Proceedings of the National Academy of Sciences*, vol. 87, no. 6, pp. 2211–2215, Mar. 1990, ISSN: 1091-6490. DOI: 10.1073/pnas.87.6.2211.
- [14] M. J. Lenardo, "Interleukin-2 programs mouse $\alpha\beta$ t lymphocytes for apoptosis", *Nature*, vol. 353, no. 6347, pp. 858–861, Oct. 1991, ISSN: 1476-4687. DOI: 10.1038/353858a0.
- [15] Y. Ishida, Y. Agata, K. Shibahara, and T. Honjo, "Induced expression of pd-1, a novel member of the immunoglobulin gene superfamily, upon programmed cell death.", *The EMBO Journal*, vol. 11, no. 11, pp. 3887–3895, Nov. 1992, ISSN: 0261-4189. DOI: 10.1002/j.1460-2075.1992.tb05481.x.
- [16] P. S. Walsh, H. A. Erlich, and R. Higuchi, "Preferential pcr amplification of alleles: Mechanisms and solutions.", *Genome Research*, vol. 1, no. 4, pp. 241–250, May 1992, ISSN: 1054-9803. DOI: 10.1101/gr.1.4.241.
- [17] Z. Eshhar, T. Waks, G. Gross, and D. G. Schindler, "Specific activation and targeting of cytotoxic lymphocytes through chimeric single chains consisting of antibody-binding domains and the gamma or zeta subunits of the immunoglobulin and t-cell receptors.", *Proceedings of the National Academy of Sciences*, vol. 90, no. 2, pp. 720–724, Jan. 1993, ISSN: 1091-6490. DOI: 10.1073/pnas.90.2.720.
- [18] G. E. Taccioli, G. Rathbun, E. Oltz, T. Stamato, P. A. Jeggo, and F. W. Alt, "Impairment of v(d)j recombination in double-strand break repair mutants", *Science*, vol. 260, no. 5105, pp. 207–210, Apr. 1993, ISSN: 1095-9203. DOI: 10.1126/science.8469973.
- [19] D. Carson and A. Lois, "Cancer progression and p53", *The Lancet*, vol. 346, no. 8981, pp. 1009–1011, Oct. 1995, ISSN: 0140-6736. DOI: 10.1016/s0140-6736(95)91693-8.
- [20] R. Ahmed and D. Gray, "Immunological memory and protective immunity: Understanding their relation", *Science*, vol. 272, no. 5258, pp. 54–60, Apr. 1996, ISSN: 1095-9203. DOI: 10.1126/science.272.5258.54.
- [21] A. L. Gartel, M. S. Serfas, and A. L. Tyner, "P21–negative regulator of the cell cycle", *Experimental Biology and Medicine*, vol. 213, no. 2, pp. 138–149, Nov. 1996, ISSN: 1535-3699. DOI: 10.3181/00379727-213-44046.
- [22] F. Liang, P. J. Romanienko, D. T. Weaver, P. A. Jeggo, and M. Jasin, "Chromosomal double-strand break repair in ku80-deficient cells.", *Proceedings of the National Academy of Sciences*, vol. 93, no. 17, pp. 8929–8933, Aug. 1996, ISSN: 1091-6490. DOI: 10.1073/pnas.93.17.8929.
- [23] P. H. Shaw, "The role of p53 in cell cycle regulation", *Pathology - Research and Practice*, vol. 192, no. 7, pp. 669–675, Jan. 1996, ISSN: 0344-0338. DOI: 10.1016/s0344-0338(96)80088-4.
- [24] S. L. Swain, M. Croft, C. Dubey, *et al.*, "From naive to memory t cells", *Immunological Reviews*, vol. 150, no. 1, pp. 143–167, Apr. 1996, ISSN: 1600-065X. DOI: 10.1111/j.1600-065x.1996.tb00700.x.
- [25] P. Bertrand, D. Rouillard, A. Boulet, C. Levalois, T. Soussi, and B. S. Lopez, "Increase of spontaneous intrachromosomal homologous recombination in mammalian cells expressing a mutant p53 protein", *Oncogene*, vol. 14, no. 9, pp. 1117–1122, Mar. 1997, ISSN: 1476-5594. DOI: 10.1038/sj.onc.1200931.
- [26] J. R. Gruen and S. M. Weissman, "Evolving views of the major histocompatibility complex", *Blood*, vol. 90, no. 11, pp. 4252–4265, Dec. 1997, ISSN: 0006-4971. DOI: 10.1182/blood.v90.11.4252.
- [27] C. Martínez-A, "Role of nf-kappab in the control of apoptotic and proliferative responses in il-2-responsive t cells", *Frontiers in Bioscience*, vol. 2, no. 4, pp. d49–60, 1997, ISSN: 1093-4715. DOI: 10.2741/a174.

- [28] K. Polyak, Y. Xia, J. L. Zweier, K. W. Kinzler, and B. Vogelstein, "A model for p53-induced apoptosis", *Nature*, vol. 389, no. 6648, pp. 300–305, Sep. 1997, ISSN: 1476-4687. DOI: 10.1038/38525.
- [29] M.-L. Alegre, H. Shiels, C. B. Thompson, and T. F. Gajewski, "Expression and function of ctla-4 in th1 and th2 cells", *The Journal of Immunology*, vol. 161, no. 7, pp. 3347–3356, Oct. 1998, ISSN: 1550-6606. DOI: 10.4049/jimmunol.161.7.3347.
- [30] D. Bruniquel, N. Borie, S. Hannier, and F. Triebel, "Regulation of expression of the human lymphocyte activation gene-3 (lag-3) molecule, a ligand for mhc class ii", *Immunogenetics*, vol. 48, no. 2, pp. 116–124, Jun. 1998, ISSN: 1432-1211. DOI: 10.1007/s002510050411.
- [31] W. S. El-Deiry, "Regulation of p53 downstream genes", *Seminars in Cancer Biology*, vol. 8, no. 5, pp. 345–357, 1998, ISSN: 1044-579X. DOI: 10.1006/scbi.1998.0097.
- [32] P. Groscurth and L. Filgueira, "Killing mechanisms of cytotoxic t lymphocytes", *Physiology*, vol. 13, no. 1, pp. 17–21, Feb. 1998, ISSN: 1548-9221. DOI: 10.1152/physiologyonline.1998.13.1.17.
- [33] K. Kuida, T. F. Haydar, C.-Y. Kuan, *et al.*, "Reduced apoptosis and cytochrome c-mediated caspase activation in mice lacking caspase 9", *Cell*, vol. 94, no. 3, pp. 325–337, Aug. 1998, ISSN: 0092-8674. DOI: 10.1016/s0092-8674(00)81476-2.
- [34] S. D. Scott, "Rituximab: A new therapeutic monoclonal antibody for non-hodgkin's lymphoma", *Cancer Practice*, vol. 6, no. 3, pp. 195–197, May 1998, ISSN: 1523-5394. DOI: 10.1046/j.1523-5394.1998.006003195.x.
- [35] S. Shresta, C. T. Pham, D. A. Thomas, T. A. Graubert, and T. J. Ley, "How do cytotoxic lymphocytes kill their targets?", *Current Opinion in Immunology*, vol. 10, no. 5, pp. 581–587, Oct. 1998, ISSN: 0952-7915. DOI: 10.1016/s0952-7915(98)80227-6.
- [36] M. Takata, M. S. Sasaki, E. Sonoda, *et al.*, "Homologous recombination and non-homologous end-joining pathways of dna double-strand break repair have overlapping roles in the maintenance of chromosomal integrity in vertebrate cells", *The EMBO Journal*, vol. 17, no. 18, pp. 5497–5508, Sep. 1998, ISSN: 1460-2075. DOI: 10.1093/emboj/17.18.5497.
- [37] N. Barboule, C. Lafon, P. Chadebecq, S. Vidal, and A. Valette, "Involvement of p21 in the pkc-induced regulation of the g2/m cell cycle transition", *FEBS Letters*, vol. 444, no. 1, pp. 32–37, Feb. 1999, ISSN: 1873-3468. DOI: 10.1016/s0014-5793(99)00022-8.
- [38] D. C. Guttridge, C. Albanese, J. Y. Reuther, R. G. Pestell, and A. S. Baldwin, "Nf-kb controls cell growth and differentiation through transcriptional regulation of cyclin d1", *Molecular and Cellular Biology*, vol. 19, no. 8, pp. 5785–5799, Aug. 1999, ISSN: 1098-5549. DOI: 10.1128/mcb.19.8.5785.
- [39] M. A. Iñiguez, C. Punzón, and M. Fresno, "Induction of cyclooxygenase-2 on activated t lymphocytes: Regulation of t cell activation by cyclooxygenase-2 inhibitors", *The Journal of Immunology*, vol. 163, no. 1, pp. 111–119, Jul. 1999, ISSN: 1550-6606. DOI: 10.4049/jimmunol.163.1.111.
- [40] P. G. Komarov, E. A. Komarova, R. V. Kondratov, *et al.*, "A chemical inhibitor of p53 that protects mice from the side effects of cancer therapy", *Science*, vol. 285, no. 5434, pp. 1733–7, 1999, ISSN: 0036-8075 (Print) 0036-8075. DOI: 10.1126/science.285.5434.1733.
- [41] W. Zhang, C. L. Sommers, D. N. Burshtyn, *et al.*, "Essential role of lat in t cell development", *Immunity*, vol. 10, no. 3, pp. 323–332, Mar. 1999, ISSN: 1074-7613. DOI: 10.1016/s1074-7613(00)80032-1.
- [42] T. Marks and R. Sharp, "Bacteriophages and biotechnology: A review", *Journal of Chemical Technology & Biotechnology*, vol. 75, no. 1, pp. 6–17, 2000. DOI: [https://doi.org/10.1002/\(SICI\)1097-4660\(200001\)75:1<6::AID-JCTB157>3.0.CO;2-A](https://doi.org/10.1002/(SICI)1097-4660(200001)75:1<6::AID-JCTB157>3.0.CO;2-A). [Online]. Available: <https://analyticalsciencejournals.onlinelibrary.wiley.com/doi/abs/10.1002/%28SICI%291097-4660%28200001%2975%3A1%3C6%3A%3AAID-JCTB157%3E3.0.CO%3B2-A>.

- [43] J. Marks-Konczalik, S. Dubois, J. M. Losi, *et al.*, “Il-2-induced activation-induced cell death is inhibited in il-15 transgenic mice”, *Proceedings of the National Academy of Sciences*, vol. 97, no. 21, pp. 11 445–11 450, Oct. 2000, ISSN: 1091-6490. DOI: 10.1073/pnas.200363097.
- [44] C. M. Roifman, “Human il-2 receptor α chain deficiency”, *Pediatric Research*, vol. 48, no. 1, pp. 6–11, Jul. 2000, ISSN: 1530-0447. DOI: 10.1203/00006450-200007000-00004.
- [45] K. M. Ryan, M. K. Ernst, N. R. Rice, and K. H. Vousden, “Role of nf- κ b in p53-mediated programmed cell death”, *Nature*, vol. 404, no. 6780, pp. 892–897, Apr. 2000, ISSN: 1476-4687. DOI: 10.1038/35009130.
- [46] E. J. Small, P. Fratesi, D. M. Reese, *et al.*, “Immunotherapy of hormone-refractory prostate cancer with antigen-loaded dendritic cells”, *Journal of Clinical Oncology*, vol. 18, no. 23, pp. 3894–3903, Dec. 2000, ISSN: 1527-7755. DOI: 10.1200/jco.2000.18.23.3894.
- [47] B. Almand, J. I. Clark, E. Nikitina, *et al.*, “Increased production of immature myeloid cells in cancer patients: A mechanism of immunosuppression in cancer”, *The Journal of Immunology*, vol. 166, no. 1, pp. 678–689, Jan. 2001, ISSN: 1550-6606. DOI: 10.4049/jimmunol.166.1.678.
- [48] S. K. Bromley, A. Iaboni, S. J. Davis, *et al.*, “The immunological synapse and cd28-cd80 interactions”, *Nature Immunology*, vol. 2, no. 12, pp. 1159–1166, Nov. 2001, ISSN: 1529-2916. DOI: 10.1038/ni737.
- [49] C. Feng Gao, S. Ren, L. Zhang, *et al.*, “Caspase-dependent cytosolic release of cytochrome c and membrane translocation of bax in p53-induced apoptosis”, *Experimental Cell Research*, vol. 265, no. 1, pp. 145–151, Apr. 2001, ISSN: 0014-4827. DOI: 10.1006/excr.2001.5171.
- [50] R. D. Johnson and M. Jasin, “Double-strand-break-induced homologous recombination in mammalian cells”, *Biochemical Society Transactions*, vol. 29, no. 2, pp. 196–201, May 2001, ISSN: 1470-8752. DOI: 10.1042/bst0290196.
- [51] Y. Latchman, C. R. Wood, T. Chernova, *et al.*, “Pd-l2 is a second ligand for pd-1 and inhibits t cell activation”, *Nature Immunology*, vol. 2, no. 3, pp. 261–268, Mar. 2001, ISSN: 1529-2916. DOI: 10.1038/85330.
- [52] J. A. Villadangos, “Presentation of antigens by mhc class ii molecules: Getting the most out of them”, *Molecular Immunology*, vol. 38, no. 5, pp. 329–346, Sep. 2001, ISSN: 0161-5890. DOI: 10.1016/s0161-5890(01)00069-4.
- [53] J. J. Wallin, L. Liang, A. Bakardjiev, and W. C. Sha, “Enhancement of cd8+ t cell responses by icos/b7h costimulation”, *The Journal of Immunology*, vol. 167, no. 1, pp. 132–139, Jul. 2001, ISSN: 1550-6606. DOI: 10.4049/jimmunol.167.1.132.
- [54] G. Xiao, E. W. Harhaj, and S.-C. Sun, “Nf- κ b-inducing kinase regulates the processing of nf- κ b2 p100”, *Molecular Cell*, vol. 7, no. 2, pp. 401–409, Feb. 2001, ISSN: 1097-2765. DOI: 10.1016/s1097-2765(01)00187-3.
- [55] S. Baksh, H. R. Widlund, A. A. Frazer-Abel, *et al.*, “Nfatc2-mediated repression of cyclin-dependent kinase 4 expression”, *Molecular Cell*, vol. 10, no. 5, pp. 1071–1081, Nov. 2002, ISSN: 1097-2765. DOI: 10.1016/s1097-2765(02)00701-3.
- [56] S. C. Bunnell, D. I. Hong, J. R. Kardon, *et al.*, “T cell receptor ligation induces the formation of dynamically regulated signaling assemblies”, *The Journal of Cell Biology*, vol. 158, no. 7, pp. 1263–1275, Sep. 2002, ISSN: 0021-9525. DOI: 10.1083/jcb.200203043.
- [57] A. V. Collins, D. W. Brodie, R. J. Gilbert, *et al.*, “The interaction properties of costimulatory molecules revisited”, *Immunity*, vol. 17, no. 2, pp. 201–210, Aug. 2002, ISSN: 1074-7613. DOI: 10.1016/s1074-7613(02)00362-x.

- [58] K. E. Foulds, L. A. Zenewicz, D. J. Shedlock, J. Jiang, A. E. Troy, and H. Shen, "Cutting edge: Cd4 and cd8 t cells are intrinsically different in their proliferative responses", *The Journal of Immunology*, vol. 168, no. 4, pp. 1528–1532, Feb. 2002, ISSN: 1550-6606. DOI: 10.4049/jimmunol.168.4.1528.
- [59] B. Hennig, B. D. Hammock, R. Slim, M. Toborek, V. Saraswathi, and L. W. Robertson, "Pcb-induced oxidative stress in endothelial cells: Modulation by nutrients", *International Journal of Hygiene and Environmental Health*, vol. 205, no. 1–2, pp. 95–102, 2002, ISSN: 1438-4639. DOI: 10.1078/1438-4639-00134.
- [60] Y. Ma, U. Pannicke, K. Schwarz, and M. R. Lieber, "Hairpin opening and overhang processing by an artemis/dna-dependent protein kinase complex in nonhomologous end joining and v(d)j recombination", *Cell*, vol. 108, no. 6, pp. 781–794, Mar. 2002, ISSN: 0092-8674. DOI: 10.1016/s0092-8674(02)00671-2.
- [61] N. J. Solan, H. Miyoshi, E. M. Carmona, G. D. Bren, and C. V. Paya, "Relb cellular regulation and transcriptional activity are regulated by p100", *Journal of Biological Chemistry*, vol. 277, no. 2, pp. 1405–1418, Jan. 2002, ISSN: 0021-9258. DOI: 10.1074/jbc.M109619200.
- [62] M. Croft, "Co-stimulatory members of the tnfr family: Keys to effective t-cell immunity?", *Nature Reviews Immunology*, vol. 3, no. 8, pp. 609–620, Aug. 2003, ISSN: 1474-1741. DOI: 10.1038/nri1148.
- [63] D. M. Harper, E. L. Franco, C. Wheeler, *et al.*, "Efficacy of a bivalent I1 virus-like particle vaccine in prevention of infection with human papillomavirus types 16 and 18 in young women: A randomised controlled trial", *The Lancet*, vol. 364, no. 9447, pp. 1757–1765, Nov. 2004, ISSN: 0140-6736. DOI: 10.1016/s0140-6736(04)17398-4.
- [64] D. W. Meek, "The p53 response to dna damage", *DNA Repair*, vol. 3, no. 8–9, pp. 1049–1056, Aug. 2004, ISSN: 1568-7864. DOI: 10.1016/j.dnarep.2004.03.027.
- [65] A. O'Garra and D. Robinson, "Development and function of t helper 1 cells", in *T Cell Subsets: Cellular Selection, Commitment and Identity*. Elsevier, 2004, pp. 133–162, ISBN: 9780120224838. DOI: 10.1016/s0065-2776(04)83004-9.
- [66] J.-L. Perfettini, R. T. Kroemer, and G. Kroemer, "Fatal liaisons of p53 with bax and bak", *Nature Cell Biology*, vol. 6, no. 5, pp. 386–388, May 2004, ISSN: 1476-4679. DOI: 10.1038/ncb0504-386.
- [67] W. Rastetter, A. Molina, and C. A. White, "Rituximab: Expanding role in therapy for lymphomas and autoimmune diseases", *Annual Review of Medicine*, vol. 55, no. 1, pp. 477–503, Feb. 2004, ISSN: 1545-326X. DOI: 10.1146/annurev.med.55.091902.104249.
- [68] G. Richter and S. Burdach, "Icos: A new costimulatory ligand/receptor pair and its role in t-cell activation", *Oncology Research and Treatment*, vol. 27, no. 1, pp. 91–95, 2004, ISSN: 2296-5262. DOI: 10.1159/000075612.
- [69] N. Saleh-Gohari, "Conservative homologous recombination preferentially repairs dna double-strand breaks in the s phase of the cell cycle in human cells", *Nucleic Acids Research*, vol. 32, no. 12, pp. 3683–3688, Jul. 2004, ISSN: 1362-4962. DOI: 10.1093/nar/gkh703.
- [70] M. Viguier, F. Lemaître, O. Verola, *et al.*, "Foxp3 expressing cd4+cd25high regulatory t cells are overrepresented in human metastatic melanoma lymph nodes and inhibit the function of infiltrating t cells", *The Journal of Immunology*, vol. 173, no. 2, pp. 1444–1453, Jul. 2004, ISSN: 1550-6606. DOI: 10.4049/jimmunol.173.2.1444.
- [71] L. Feng, T. Lin, H. Uranishi, W. Gu, and Y. Xu, "Functional analysis of the roles of posttranslational modifications at the p53 c terminus in regulating p53 stability and activity", *Molecular and Cellular Biology*, vol. 25, no. 13, pp. 5389–5395, Jul. 2005, ISSN: 1098-5549. DOI: 10.1128/mcb.25.13.5389-5395.2005.

- [72] M. S. Hoagland, E. M. Hoagland, and H. I. Swanson, "The p53 inhibitor pifithrin- α is a potent agonist of the aryl hydrocarbon receptor", *Journal of Pharmacology and Experimental Therapeutics*, vol. 314, no. 2, pp. 603–610, Apr. 2005, ISSN: 1521-0103. DOI: 10.1124/jpet.105.084186.
- [73] F. Macian, "Nfat proteins: Key regulators of t-cell development and function", *Nature Reviews Immunology*, vol. 5, no. 6, pp. 472–484, Jun. 2005, ISSN: 1474-1741. DOI: 10.1038/nri1632.
- [74] B. Malissen, E. Aguado, and M. Malissen, "Role of the lat adaptor in t-cell development and th2 differentiation", in *Advances in Immunology*. Elsevier, 2005, pp. 1–25. DOI: 10.1016/s0065-2776(05)87001-4.
- [75] Y.-H. Ou, P.-H. Chung, T.-P. Sun, and S.-Y. Shieh, "P53 c-terminal phosphorylation by chk1 and chk2 participates in the regulation of dna-damage-induced c-terminal acetylation", *Molecular Biology of the Cell*, vol. 16, no. 4, pp. 1684–1695, Apr. 2005, ISSN: 1939-4586. DOI: 10.1091/mbc.e04-08-0689.
- [76] M. I. Walton, S. C. Wilson, I. R. Hardcastle, A. R. Mirza, and P. Workman, "An evaluation of the ability of pifithrin- α and - β to inhibit p53 function in two wild-type p53 human tumor cell lines", *Molecular Cancer Therapeutics*, vol. 4, no. 9, pp. 1369–1377, Sep. 2005, ISSN: 1538-8514. DOI: 10.1158/1535-7163.mct-04-0341.
- [77] K. W. Bock and C. Köhle, "Ah receptor: Dioxin-mediated toxic responses as hints to deregulated physiologic functions", *Biochemical Pharmacology*, vol. 72, no. 4, pp. 393–404, Aug. 2006, ISSN: 0006-2952. DOI: 10.1016/j.bcp.2006.01.017.
- [78] T. Soussi, C. Ishioka, M. Claustres, and C. Bérout, "Locus-specific mutation databases: Pitfalls and good practice based on the p53 experience", *Nature Reviews Cancer*, vol. 6, no. 1, pp. 83–90, Jan. 2006, ISSN: 1474-1768. DOI: 10.1038/nrc1783.
- [79] E. Strom, S. Sathe, P. G. Komarov, *et al.*, "Small-molecule inhibitor of p53 binding to mitochondria protects mice from gamma radiation", *NATURE CHEMICAL BIOLOGY*, vol. 2, no. 9, pp. 474–479, Sep. 2006, ISSN: 1552-4450. DOI: 10.1038/nchembio809.
- [80] R. Barrangou, C. Fremaux, H. Deveau, *et al.*, "Crispr provides acquired resistance against viruses in prokaryotes", *Science*, vol. 315, no. 5819, pp. 1709–1712, Mar. 2007, ISSN: 1095-9203. DOI: 10.1126/science.1138140.
- [81] S. Deindl, T. A. Kadlecsek, T. Brdicka, X. Cao, A. Weiss, and J. Kuriyan, "Structural basis for the inhibition of tyrosine kinase activity of zap-70", *Cell*, vol. 129, no. 4, pp. 735–746, May 2007, ISSN: 0092-8674. DOI: 10.1016/j.cell.2007.03.039.
- [82] J. Gu, H. Lu, B. Tippin, N. Shimazaki, M. F. Goodman, and M. R. Lieber, "Xrcc4:dna ligase iv can ligate incompatible dna ends and can ligate across gaps", *The EMBO Journal*, vol. 26, no. 4, pp. 1010–1023, Feb. 2007, ISSN: 1460-2075. DOI: 10.1038/sj.emboj.7601559.
- [83] J. Gu, H. Lu, A. G. Tsai, K. Schwarz, and M. R. Lieber, "Single-stranded dna ligation and xlf-stimulated incompatible dna end ligation by the xrcc4-dna ligase iv complex: Influence of terminal dna sequence", *Nucleic Acids Research*, vol. 35, no. 17, pp. 5755–5762, Aug. 2007, ISSN: 0305-1048. DOI: 10.1093/nar/gkm579.
- [84] O. Limbo, C. Chahwan, Y. Yamada, R. A. de Bruin, C. Wittenberg, and P. Russell, "Ctp1 is a cell-cycle-regulated protein that functions with mre11 complex to control double-strand break repair by homologous recombination", *Molecular Cell*, vol. 28, no. 1, pp. 134–146, Oct. 2007, ISSN: 1097-2765. DOI: 10.1016/j.molcel.2007.09.009.
- [85] K.-X. Shu, B. Li, and L.-X. Wu, "The p53 network: P53 and its downstream genes", *Colloids and Surfaces B: Biointerfaces*, vol. 55, no. 1, pp. 10–18, Mar. 2007, ISSN: 0927-7765. DOI: 10.1016/j.colsurfb.2006.11.003.
- [86] C. F. A. Vogel, E. Sciallo, W. Li, P. Wong, G. Lazenec, and F. Matsumura, "Relb, a new partner of aryl hydrocarbon receptor-mediated transcription", *Molecular Endocrinology*, vol. 21, no. 12, pp. 2941–2955, Dec. 2007, ISSN: 1944-9917. DOI: 10.1210/me.2007-0211.

- [87] K.-i. Yano, K. Morotomi-Yano, S.-Y. Wang, *et al.*, “Ku recruits xlf to dna double-strand breaks”, *EMBO reports*, vol. 9, no. 1, pp. 91–96, Dec. 2007, ISSN: 1469-3178. DOI: 10.1038/sj.embor.7401137.
- [88] N. Askenasy, A. Kaminitz, and S. Yarkoni, “Mechanisms of t regulatory cell function”, *Autoimmunity Reviews*, vol. 7, no. 5, pp. 370–375, May 2008, ISSN: 1568-9972. DOI: 10.1016/j.autrev.2008.03.001.
- [89] S. J. J. Brouns, M. M. Jore, M. Lundgren, *et al.*, “Small crispr rnas guide antiviral defense in prokaryotes”, *Science*, vol. 321, no. 5891, pp. 960–964, Aug. 2008, ISSN: 1095-9203. DOI: 10.1126/science.1159689.
- [90] S. Hacein-Bey-Abina, A. Garrigue, G. P. Wang, *et al.*, “Insertional oncogenesis in 4 patients after retrovirus-mediated gene therapy of scid-x1”, *J Clin Invest*, vol. 118, no. 9, pp. 3132–42, 2008, ISSN: 0021-9738 (Print) 0021-9738. DOI: 10.1172/jci35700.
- [91] X. Li and W.-D. Heyer, “Homologous recombination in dna repair and dna damage tolerance”, *Cell Research*, vol. 18, no. 1, pp. 99–113, Jan. 2008, ISSN: 1748-7838. DOI: 10.1038/cr.2008.1.
- [92] Z. Mao, M. Bozzella, A. Seluanov, and V. Gorbunova, “Dna repair by nonhomologous end joining and homologous recombination during cell cycle in human cells”, *Cell Cycle*, vol. 7, no. 18, pp. 2902–2906, Sep. 2008, ISSN: 1551-4005. DOI: 10.4161/cc.7.18.6679.
- [93] M. McVey and S. E. Lee, “Mmej repair of double-strand breaks (director’s cut): Deleted sequences and alternative endings”, *Trends in Genetics*, vol. 24, no. 11, pp. 529–538, Nov. 2008, ISSN: 0168-9525. DOI: 10.1016/j.tig.2008.08.007.
- [94] J. K. Whitmire, B. Eam, and J. L. Whitton, “Tentative t cells: Memory cells are quick to respond, but slow to divide”, *PLoS Pathogens*, vol. 4, no. 4, R. A. Koup, Ed., e1000041, Apr. 2008, ISSN: 1553-7374. DOI: 10.1371/journal.ppat.1000041.
- [95] K. A. Boehme and C. Blattner, “Regulation of p53 - insights into a complex process”, *Critical Reviews in Biochemistry and Molecular Biology*, vol. 44, no. 6, pp. 367–392, Nov. 2009, ISSN: 1549-7798. DOI: 10.3109/10409230903401507.
- [96] A. J. Hartlerode and R. Scully, “Mechanisms of double-strand break repair in somatic mammalian cells”, *Biochemical Journal*, vol. 423, no. 2, pp. 157–168, Sep. 2009, ISSN: 1470-8728. DOI: 10.1042/bj20090942.
- [97] T. Lawrence, “The nuclear factor nf- κ pathway in inflammation”, *Cold Spring Harbor Perspectives in Biology*, vol. 1, no. 6, a001651–a001651, Oct. 2009, ISSN: 1943-0264. DOI: 10.1101/cshperspect.a001651.
- [98] J. Louten, K. Boniface, and R. de Waal Malefyt, “Development and function of th17 cells in health and disease”, *Journal of Allergy and Clinical Immunology*, vol. 123, no. 5, pp. 1004–1011, May 2009, ISSN: 0091-6749. DOI: 10.1016/j.jaci.2009.04.003.
- [99] S. Mumprecht, C. Schürch, J. Schwaller, M. Solenthaler, and A. F. Ochsenbein, “Programmed death 1 signaling on chronic myeloid leukemia-specific t cells results in t-cell exhaustion and disease progression”, *Blood*, vol. 114, no. 8, pp. 1528–1536, Aug. 2009, ISSN: 1528-0020. DOI: 10.1182/blood-2008-09-179697.
- [100] D. Sohn, V. Graupner, D. Neise, F. Essmann, K. Schulze-Osthoff, and R. U. Jänicke, “Pifithrin- α protects against dna damage-induced apoptosis downstream of mitochondria independent of p53”, *Cell Death & Differentiation*, vol. 16, no. 6, pp. 869–878, 2009, ISSN: 1476-5403. DOI: 10.1038/cdd.2009.17. [Online]. Available: <https://doi.org/10.1038/cdd.2009.17>.
- [101] R. Gandhi, D. Kumar, E. J. Burns, *et al.*, “Activation of the aryl hydrocarbon receptor induces human type 1 regulatory t cell-like and foxp3+ regulatory t cells”, *Nature Immunology*, vol. 11, no. 9, pp. 846–853, Aug. 2010, ISSN: 1529-2916. DOI: 10.1038/ni.1915.

- [102] J. E. Garneau, M.-È. Dupuis, M. Villion, *et al.*, “The crispr/cas bacterial immune system cleaves bacteriophage and plasmid dna”, *Nature*, vol. 468, no. 7320, pp. 67–71, Nov. 2010, ISSN: 1476-4687. DOI: 10.1038/nature09523.
- [103] N. Jain, H. Nguyen, C. Chambers, and J. Kang, “Dual function of ctla-4 in regulatory t cells and conventional t cells to prevent multiorgan autoimmunity”, *Proceedings of the National Academy of Sciences*, vol. 107, no. 4, pp. 1524–1528, Jan. 2010, ISSN: 1091-6490. DOI: 10.1073/pnas.09103411107.
- [104] V. C. Janbandhu, A. K. Singh, A. Mukherji, and V. Kumar, “P65 negatively regulates transcription of the cyclin e gene”, *Journal of Biological Chemistry*, vol. 285, no. 23, pp. 17453–17464, Jun. 2010, ISSN: 0021-9258. DOI: 10.1074/jbc.M109.058974.
- [105] S. Kim, J. Han, S. K. Lee, *et al.*, “Pifithrin- α , an inhibitor of p53 transactivation, up-regulates cox-2 expression through an mapk-dependent pathway”, *Pharmacology*, vol. 86, no. 5–6, pp. 313–319, 2010, ISSN: 1423-0313. DOI: 10.1159/000321327.
- [106] J. N. Kochenderfer, W. H. Wilson, J. E. Janik, *et al.*, “Eradication of b-lineage cells and regression of lymphoma in a patient treated with autologous t cells genetically engineered to recognize cd19”, *Blood*, vol. 116, no. 20, pp. 4099–4102, Nov. 2010, ISSN: 1528-0020. DOI: 10.1182/blood-2010-04-281931.
- [107] A. KUROSAWA and N. ADACHI, “Functions and regulation of artemis: A goddess in the maintenance of genome integrity”, *Journal of Radiation Research*, vol. 51, no. 5, pp. 503–509, 2010, ISSN: 1349-9157. DOI: 10.1269/jrr.10017.
- [108] M. R. Lieber, “The mechanism of double-strand dna break repair by the nonhomologous dna end-joining pathway”, *Annual Review of Biochemistry*, vol. 79, no. 1, pp. 181–211, Jun. 2010, ISSN: 1545-4509. DOI: 10.1146/annurev.biochem.052308.093131.
- [109] R. A. Morgan, J. C. Yang, M. Kitano, M. E. Dudley, C. M. Laurencot, and S. A. Rosenberg, “Case report of a serious adverse event following the administration of t cells transduced with a chimeric antigen receptor recognizing erbb2”, *Molecular Therapy*, vol. 18, no. 4, pp. 843–851, Apr. 2010, ISSN: 1525-0016. DOI: 10.1038/mt.2010.24.
- [110] G. Schneider, A. Henrich, G. Greiner, *et al.*, “Cross talk between stimulated nf- κ b and the tumor suppressor p53”, *Oncogene*, vol. 29, no. 19, pp. 2795–2806, Mar. 2010, ISSN: 1476-5594. DOI: 10.1038/onc.2010.46.
- [111] D. Selewski, G. Shah, R. Mody, P. Rajdev, and S. Mukherji, “Rituximab (rituxan)”, *American Journal of Neuroradiology*, vol. 31, no. 7, pp. 1178–1180, May 2010, ISSN: 1936-959X. DOI: 10.3174/ajnr.a2142.
- [112] S.-C. Sun, “Non-canonical nf- κ b signaling pathway”, *Cell Research*, vol. 21, no. 1, pp. 71–85, Dec. 2010, ISSN: 1748-7838. DOI: 10.1038/cr.2010.177.
- [113] E. D. Tichy, R. Pillai, L. Deng, *et al.*, “Mouse embryonic stem cells, but not somatic cells, predominantly use homologous recombination to repair double-strand dna breaks”, *Stem Cells and Development*, vol. 19, no. 11, pp. 1699–1711, Nov. 2010, ISSN: 1557-8534. DOI: 10.1089/scd.2010.0058.
- [114] A. Vilborg, M. T. Wilhelm, and K. G. Wiman, “Regulation of tumor suppressor p53 at the rna level”, *Journal of Molecular Medicine*, vol. 88, no. 7, pp. 645–652, Mar. 2010, ISSN: 1432-1440. DOI: 10.1007/s00109-010-0609-2.
- [115] X.-d. Zhang, Z.-h. Qin, and J. Wang, “The role of p53 in cell metabolism”, *Acta Pharmacologica Sinica*, vol. 31, no. 9, pp. 1208–1212, Aug. 2010, ISSN: 1745-7254. DOI: 10.1038/aps.2010.151.
- [116] M. A. Cheever and C. S. Higano, “Provenge (sipuleucel-t) in prostate cancer: The first fda-approved therapeutic cancer vaccine”, *Clinical Cancer Research*, vol. 17, no. 11, pp. 3520–3526, Jun. 2011, ISSN: 1557-3265. DOI: 10.1158/1078-0432.ccr-10-3126.

- [117] M. L. Fernández-Cruz, A. Valdehita, M. Alonso, E. Mann, B. Herradón, and J. M. Navas, “Biological and chemical studies on aryl hydrocarbon receptor induction by the p53 inhibitor pifithrin- α and its condensation product pifithrin- β ”, *Life Sciences*, vol. 88, no. 17–18, pp. 774–783, Apr. 2011, ISSN: 0024-3205. DOI: 10.1016/j.lfs.2011.02.019.
- [118] S. Lemoine, A. Morva, P. Youinou, and C. Jamin, “Human T cells induce their own regulation through activation of B cells”, *Journal of Autoimmunity*, vol. 36, no. 3-4, pp. 228–238, May 2011.
- [119] E. J. Lipson and C. G. Drake, “Ipilimumab: An anti-ctla-4 antibody for metastatic melanoma”, *Clinical Cancer Research*, vol. 17, no. 22, pp. 6958–6962, Nov. 2011, ISSN: 1557-3265. DOI: 10.1158/1078-0432.ccr-11-1595.
- [120] T. Ozaki and A. Nakagawara, “Role of p53 in cell death and human cancers”, *Cancers*, vol. 3, no. 1, pp. 994–1013, Mar. 2011, ISSN: 2072-6694. DOI: 10.3390/cancers3010994.
- [121] D. L. Porter, B. L. Levine, M. Kalos, A. Bagg, and C. H. June, “Chimeric antigen receptor–modified t cells in chronic lymphoid leukemia”, *New England Journal of Medicine*, vol. 365, no. 8, pp. 725–733, Aug. 2011, ISSN: 1533-4406. DOI: 10.1056/nejmoa1103849.
- [122] P. J. Stephens, C. D. Greenman, B. Fu, *et al.*, “Massive genomic rearrangement acquired in a single catastrophic event during cancer development”, *Cell*, vol. 144, no. 1, pp. 27–40, Jan. 2011, ISSN: 0092-8674. DOI: 10.1016/j.cell.2010.11.055.
- [123] G. Gasiunas, R. Barrangou, P. Horvath, and V. Siksnys, “Cas9–crRNA ribonucleoprotein complex mediates specific DNA cleavage for adaptive immunity in bacteria”, *Proceedings of the National Academy of Sciences*, vol. 109, no. 39, Sep. 2012, ISSN: 1091-6490. DOI: 10.1073/pnas.1208507109.
- [124] W. Hanel and U. M. Moll, “Links between mutant p53 and genomic instability”, *Journal of Cellular Biochemistry*, vol. 113, no. 2, pp. 433–439, Jan. 2012, ISSN: 1097-4644. DOI: 10.1002/jcb.23400.
- [125] D. Heckl, A. Schwarzer, R. Haemmerle, *et al.*, “Lentiviral vector induced insertional haploinsufficiency of ebf1 causes murine leukemia”, *Molecular Therapy*, vol. 20, no. 6, pp. 1187–1195, Jun. 2012, ISSN: 1525-0016. DOI: 10.1038/mt.2012.59.
- [126] M. Jinek, K. Chylinski, I. Fonfara, M. Hauer, J. A. Doudna, and E. Charpentier, “A programmable dual-RNA–guided DNA endonuclease in adaptive bacterial immunity”, *Science*, vol. 337, no. 6096, pp. 816–821, Aug. 2012, ISSN: 1095-9203. DOI: 10.1126/science.1225829.
- [127] K. Karanam, R. Kafri, A. Loewer, and G. Lahav, “Quantitative live cell imaging reveals a gradual shift between DNA repair mechanisms and a maximal use of HR in mid S phase”, *Molecular Cell*, vol. 47, no. 2, pp. 320–329, Jul. 2012, ISSN: 1097-2765. DOI: 10.1016/j.molcel.2012.05.052.
- [128] E. Lozano, M. Dominguez-Villar, V. Kuchroo, and D. A. Hafler, “The TIGIT/CD226 axis regulates human T cell function”, *The Journal of Immunology*, vol. 188, no. 8, pp. 3869–3875, Apr. 2012, ISSN: 1550-6606. DOI: 10.4049/jimmunol.1103627.
- [129] N. Patsoukis, J. Brown, V. Petkova, F. Liu, L. Li, and V. A. Boussiotis, “Selective effects of PD-1 on Akt and Ras pathways regulate molecular components of the cell cycle and inhibit T cell proliferation”, *Science Signaling*, vol. 5, no. 230, Jun. 2012, ISSN: 1937-9145. DOI: 10.1126/scisignal.2002796.
- [130] P.-Y. Perera, J. H. Lichy, T. A. Waldmann, and L. P. Perera, “The role of interleukin-15 in inflammation and immune responses to infection: Implications for its therapeutic use”, *Microbes and Infection*, vol. 14, no. 3, pp. 247–261, Mar. 2012, ISSN: 1286-4579. DOI: 10.1016/j.micinf.2011.10.006.
- [131] R. J. Brownlie and R. Zamoyka, “T cell receptor signalling networks: Branched, diversified and bounded”, *Nature Reviews Immunology*, vol. 13, no. 4, pp. 257–269, Mar. 2013, ISSN: 1474-1741. DOI: 10.1038/nri3403.

- [132] P. Mali, L. Yang, K. M. Esvelt, *et al.*, “Rna-guided human genome engineering via cas9”, *Science*, vol. 339, no. 6121, pp. 823–826, 2013, ISSN: 00368075, 10959203. [Online]. Available: www.jstor.org/stable/23365969 <https://www.ncbi.nlm.nih.gov/pmc/articles/PMC3712628/pdf/nihms471334.pdf>.
- [133] A. Marechal and L. Zou, “Dna damage sensing by the atm and atr kinases”, *Cold Spring Harbor Perspectives in Biology*, vol. 5, no. 9, a012716–a012716, Sep. 2013, ISSN: 1943-0264. DOI: 10.1101/cshperspect.a012716.
- [134] M. Poltorak, B. Arndt, B. S. Kowtharapu, *et al.*, “Tcr activation kinetics and feedback regulation in primary human t cells”, *Cell Communication and Signaling*, vol. 11, no. 1, Jan. 2013, ISSN: 1478-811X. DOI: 10.1186/1478-811x-11-4.
- [135] F. A. Ran, P. D. Hsu, J. Wright, V. Agarwala, D. A. Scott, and F. Zhang, “Genome engineering using the crispr-cas9 system”, *Nature Protocols*, vol. 8, no. 11, pp. 2281–2308, Oct. 2013, ISSN: 1750-2799. DOI: 10.1038/nprot.2013.143.
- [136] T. R. Sampson, S. D. Saroj, A. C. Llewellyn, Y.-L. Tzeng, and D. S. Weiss, “A crispr/cas system mediates bacterial innate immune evasion and virulence”, *Nature*, vol. 497, no. 7448, pp. 254–257, Apr. 2013, ISSN: 1476-4687. DOI: 10.1038/nature12048.
- [137] S. A. Shah, S. Erdmann, F. J. Mojica, and R. A. Garrett, “Protospacer recognition motifs: Mixed identities and functional diversity”, *RNA Biology*, vol. 10, no. 5, pp. 891–899, Feb. 2013, ISSN: 1555-8584. DOI: 10.4161/rna.23764.
- [138] D. Woods and J. J. Turchi, “Chemotherapy induced dna damage response: Convergence of drugs and pathways”, *Cancer Biology & Therapy*, vol. 14, no. 5, pp. 379–389, May 2013, ISSN: 1555-8576. DOI: 10.4161/cbt.23761.
- [139] Z. Zhang, D. Li, H. Xu, *et al.*, “A simple and efficient method for assembling tale protein based on plasmid library”, *PLoS ONE*, vol. 8, no. 6, B. P. Chadwick, Ed., e66459, Jun. 2013, ISSN: 1932-6203. DOI: 10.1371/journal.pone.0066459.
- [140] R. Buisson, J. Niraj, J. Pauty, *et al.*, “Breast cancer proteins palb2 and brca2 stimulate polymerase η in recombination-associated dna synthesis at blocked replication forks”, *Cell Reports*, vol. 6, no. 3, pp. 553–564, Feb. 2014, ISSN: 2211-1247. DOI: 10.1016/j.celrep.2014.01.009.
- [141] T. Eleftheriadis, G. Pissas, G. Antoniadis, A. Spanoulis, V. Liakopoulos, and I. Stefanidis, “Indoleamine 2,3-dioxygenase increases p53 levels in alloreactive human t cells, and both indoleamine 2,3-dioxygenase and p53 suppress glucose uptake, glycolysis and proliferation”, *Int Immunol*, vol. 26, no. 12, pp. 673–84, 2014, ISSN: 0953-8178. DOI: 10.1093/intimm/dxu077.
- [142] D. W. Lee, R. Gardner, D. L. Porter, *et al.*, “Current concepts in the diagnosis and management of cytokine release syndrome”, *Blood*, vol. 124, no. 2, pp. 188–195, Jul. 2014, ISSN: 1528-0020. DOI: 10.1182/blood-2014-05-552729.
- [143] S. Lin, B. T. Staahl, R. K. Alla, and J. A. Doudna, “Enhanced homology-directed human genome engineering by controlled timing of crispr/cas9 delivery”, *eLife*, vol. 3, Dec. 2014, ISSN: 2050-084X. DOI: 10.7554/elife.04766.
- [144] D. Marvin, M. Symmons, and S. Straus, “Structure and assembly of filamentous bacteriophages”, *Progress in Biophysics and Molecular Biology*, vol. 114, no. 2, pp. 80–122, Apr. 2014, ISSN: 0079-6107. DOI: 10.1016/j.pbiomolbio.2014.02.003.
- [145] L. Prigent, M. Robineau, S. Jouneau, *et al.*, “The aryl hydrocarbon receptor is functionally upregulated early in the course of human t-cell activation”, *European Journal of Immunology*, vol. 44, no. 5, pp. 1330–1340, Feb. 2014, ISSN: 1521-4141. DOI: 10.1002/eji.201343920.
- [146] H. Rabenstein, A. C. Behrendt, J. W. Ellwart, *et al.*, “Differential kinetics of antigen dependency of cd4+ and cd8+ t cells”, *The Journal of Immunology*, vol. 192, no. 8, pp. 3507–3517, Apr. 2014, ISSN: 1550-6606. DOI: 10.4049/jimmunol.1302725.

- [147] L. S. Symington, "End resection at double-strand breaks: Mechanism and regulation", *Cold Spring Harbor Perspectives in Biology*, vol. 6, no. 8, a016436–a016436, Aug. 2014, ISSN: 1943-0264. DOI: 10.1101/cshperspect.a016436.
- [148] V. Tullio, R. Spaccapelo, and M. Polimeni, "Lysozymes in the animal kingdom", in *Human and Mosquito Lysozymes*. Springer International Publishing, Sep. 2014, pp. 45–57, ISBN: 9783319094328. DOI: 10.1007/978-3-319-09432-8_3.
- [149] W. Wang, C. Ye, J. Liu, D. Zhang, J. T. Kimata, and P. Zhou, "Ccr5 gene disruption via lentiviral vectors expressing cas9 and single guided rna renders cells resistant to hiv-1 infection", *PLoS ONE*, vol. 9, no. 12, S. Jiang, Ed., e115987, Dec. 2014, ISSN: 1932-6203. DOI: 10.1371/journal.pone.0115987.
- [150] M. Watanabe, K. D. Moon, M. S. Vacchio, K. S. Hathcock, and R. J. Hodes, "Downmodulation of tumor suppressor p53 by t cell receptor signaling is critical for antigen-specific cd4+ t cell responses", *Immunity*, vol. 40, no. 5, pp. 681–691, May 2014, ISSN: 1074-7613. DOI: 10.1016/j.immuni.2014.04.006.
- [151] B. B. Au-Yeung, J. Zikherman, J. L. Mueller, *et al.*, "A sharp t-cell antigen receptor signaling threshold for t-cell proliferation", *PROCEEDINGS OF THE NATIONAL ACADEMY OF SCIENCES OF THE UNITED STATES OF AMERICA*, vol. 111, no. 35, E3679–E3688, Sep. 2014, ISSN: 0027-8424. DOI: 10.1073/pnas.1413726111.
- [152] M. Zhang, Z. Ma, N. Selliah, *et al.*, "The impact of nucleofection® on the activation state of primary human cd4 t cells", *Journal of Immunological Methods*, vol. 408, pp. 123–131, Jun. 2014, ISSN: 0022-1759. DOI: 10.1016/j.jim.2014.05.014.
- [153] M. Zimmermann and T. de Lange, "53bp1: Pro choice in dna repair", *Trends in Cell Biology*, vol. 24, no. 2, pp. 108–117, 2014, ISSN: 0962-8924. DOI: <https://doi.org/10.1016/j.tcb.2013.09.003>. [Online]. Available: <https://www.sciencedirect.com/science/article/pii/S0962892413001554>.
- [154] J. Bellec, M. Bacchetta, D. Losa, I. Anegon, M. Chanson, and T. Nguyen, "Inactivation by lentiviral vector-mediated rna interference and crispr-cas9 genome editing in human airway epithelial cells", *Current Gene Therapy*, vol. 15, no. 5, pp. 447–459, Aug. 2015, ISSN: 1566-5232. DOI: 10.2174/1566523215666150812115939.
- [155] H. Franken, T. Mathieson, D. Childs, *et al.*, "Thermal proteome profiling for unbiased identification of direct and indirect drug targets using multiplexed quantitative mass spectrometry", *Nature Protocols*, vol. 10, no. 10, pp. 1567–1593, Sep. 2015, ISSN: 1750-2799. DOI: 10.1038/nprot.2015.101.
- [156] R.-E. Go, K.-A. Hwang, and K.-C. Choi, "Cytochrome p450 1 family and cancers", *The Journal of Steroid Biochemistry and Molecular Biology*, vol. 147, pp. 24–30, Mar. 2015, ISSN: 0960-0760. DOI: 10.1016/j.jsbmb.2014.11.003.
- [157] A. Hendel, R. O. Bak, J. T. Clark, *et al.*, "Chemically modified guide rnas enhance crispr-cas genome editing in human primary cells", *Nature Biotechnology*, vol. 33, no. 9, pp. 985–989, Sep. 2015, ISSN: 1546-1696. DOI: 10.1038/nbt.3290.
- [158] S.-i. Kanno, K. Kurauchi, A. Tomizawa, S. Yomogida, and M. Ishikawa, "Pifithrin-alpha has a p53-independent cytoprotective effect on docosahexaenoic acid-induced cytotoxicity in human hepatocellular carcinoma hepg2 cells", *Toxicology Letters*, vol. 232, no. 2, pp. 393–402, Jan. 2015, ISSN: 0378-4274. DOI: 10.1016/j.toxlet.2014.11.016.
- [159] E. M. Kennedy, L. C. Bassit, H. Mueller, *et al.*, "Suppression of hepatitis b virus dna accumulation in chronically infected cells using a bacterial crispr/cas rna-guided dna endonuclease", *Virology*, vol. 476, pp. 196–205, Feb. 2015, ISSN: 0042-6822. DOI: 10.1016/j.virol.2014.12.001.

- [160] K. Schumann, S. Lin, E. Boyer, *et al.*, “Generation of knock-in primary human t cells using cas9 ribonucleoproteins”, *Proc Natl Acad Sci U S A*, vol. 112, no. 33, pp. 10437–42, 2015, ISSN: 1091-6490 (Electronic) 0027-8424 (Linking). DOI: 10.1073/pnas.1512503112. [Online]. Available: <https://www.ncbi.nlm.nih.gov/pubmed/26216948>.
- [161] J. G. Doench, N. Fusi, M. Sullender, *et al.*, “Optimized sgrna design to maximize activity and minimize off-target effects of crispr-cas9”, *Nature Biotechnology*, vol. 34, no. 2, pp. 184–191, Jan. 2016, ISSN: 1546-1696. DOI: 10.1038/nbt.3437.
- [162] F. Jiang, D. W. Taylor, J. S. Chen, *et al.*, “Structures of a crispr-cas9 r-loop complex primed for dna cleavage”, *Science*, vol. 351, no. 6275, pp. 867–871, Feb. 2016, ISSN: 1095-9203. DOI: 10.1126/science.aad8282.
- [163] J. Le Pen, M. Laurent, K. Sarosiek, *et al.*, “Constitutive p53 heightens mitochondrial apoptotic priming and favors cell death induction by bh3 mimetic inhibitors of bcl-xl”, *Cell Death & Disease*, vol. 7, no. 2, e2083–e2083, Feb. 2016, ISSN: 2041-4889. DOI: 10.1038/cddis.2015.400.
- [164] H. O. Alsaab, S. Sau, R. Alzhrani, *et al.*, “Pd-1 and pd-l1 checkpoint signaling inhibition for cancer immunotherapy: Mechanism, combinations, and clinical outcome”, *Frontiers in Pharmacology*, vol. 8, Aug. 2017, ISSN: 1663-9812. DOI: 10.3389/fphar.2017.00561.
- [165] A. M. Kaiser and L. D. Attardi, “Deconstructing networks of p53-mediated tumor suppression in vivo”, *Cell Death & Differentiation*, vol. 25, no. 1, pp. 93–103, Nov. 2017, ISSN: 1476-5403. DOI: 10.1038/cdd.2017.171.
- [166] F. Kroschinsky, F. Stölzel, S. von Bonin, *et al.*, “New drugs, new toxicities: Severe side effects of modern targeted and immunotherapy of cancer and their management”, *Critical Care*, vol. 21, no. 1, Apr. 2017, ISSN: 1364-8535. DOI: 10.1186/s13054-017-1678-1.
- [167] T. Liu, L. Zhang, D. Joo, and S.-C. Sun, “Nf- κ b signaling in inflammation”, *Signal Transduction and Targeted Therapy*, vol. 2, no. 1, Jul. 2017, ISSN: 2059-3635. DOI: 10.1038/sigtrans.2017.23.
- [168] J. P. McNally, S. H. Millen, V. Chaturvedi, *et al.*, “Manipulating dna damage-response signaling for the treatment of immune-mediated diseases”, *Proceedings of the National Academy of Sciences*, vol. 114, no. 24, May 2017, ISSN: 1091-6490. DOI: 10.1073/pnas.1703683114.
- [169] T. P. Monie, “A snapshot of the innate immune system”, in *The Innate Immune System*. Elsevier, 2017, pp. 1–40, ISBN: 9780128044643. DOI: 10.1016/b978-0-12-804464-3.00001-6.
- [170] K. Murugan, K. Babu, R. Sundaresan, R. Rajan, and D. G. Sashital, “The revolution continues: Newly discovered systems expand the crispr-cas toolkit”, *Molecular Cell*, vol. 68, no. 1, pp. 15–25, Oct. 2017, ISSN: 1097-2765. DOI: 10.1016/j.molcel.2017.09.007.
- [171] T. Nakayama, K. Hirahara, A. Onodera, *et al.*, “Th2 cells in health and disease”, *Annual Review of Immunology*, vol. 35, no. 1, pp. 53–84, Apr. 2017, ISSN: 1545-3278. DOI: 10.1146/annurev-immunol-051116-052350.
- [172] D. M. O’Rourke, M. P. Nasrallah, A. Desai, *et al.*, “A single dose of peripherally infused egrviii-directed car t cells mediates antigen loss and induces adaptive resistance in patients with recurrent glioblastoma”, *Science Translational Medicine*, vol. 9, no. 399, Jul. 2017, ISSN: 1946-6242. DOI: 10.1126/scitranslmed.aaa0984.
- [173] H. Y. Shin, C. C. Wang, H. K. Lee, *et al.*, “Crispr/cas9 targeting events cause complex deletions and insertions at 17 sites in the mouse genome”, *Nature Communications*, vol. 8, p. 10, 2017, ISSN: 2041-1723. DOI: 10.1038/ncomms15464. [Online]. Available: <https://www.ncbi.nlm.nih.gov/pmc/articles/PMC5402389/>.
- [174] H. Tan, K. Yang, Y. Li, *et al.*, “Integrative proteomics and phosphoproteomics profiling reveals dynamic signaling networks and bioenergetics pathways underlying t cell activation”, *Immunity*, vol. 46, no. 3, pp. 488–503, Mar. 2017, ISSN: 1074-7613. DOI: 10.1016/j.immuni.2017.02.010.

- [175] M. Zampieri, M. Zimmermann, M. Claassen, and U. Sauer, "Nontargeted metabolomics reveals the multilevel response to antibiotic perturbations", *Cell Reports*, vol. 19, no. 6, pp. 1214–1228, May 2017, ISSN: 2211-1247. DOI: 10.1016/j.celrep.2017.04.002.
- [176] X. Zhao, C. Wei, J. Li, *et al.*, "Cell cycle-dependent control of homologous recombination", *Acta Biochimica et Biophysica Sinica*, vol. 49, no. 8, pp. 655–668, Aug. 2017, ISSN: 1672-9145. DOI: 10.1093/abbs/gmx055.
- [177] F. Adikusuma, S. Piltz, M. A. Corbett, *et al.*, "Large deletions induced by cas9 cleavage", *Nature*, vol. 560, no. 7717, E8–E9, Aug. 2018, ISSN: 1476-4687. DOI: 10.1038/s41586-018-0380-z.
- [178] M. M. Arbulo-Echevarria, I. Narbona-Sánchez, C. M. Fernandez-Ponce, *et al.*, "A stretch of negatively charged amino acids of linker for activation of t-cell adaptor has a dual role in t-cell antigen receptor intracellular signaling", *Frontiers in Immunology*, vol. 9, Feb. 2018, ISSN: 1664-3224. DOI: 10.3389/fimmu.2018.00115.
- [179] X. Chen, L. Kozhaya, C. Tastan, *et al.*, "Functional interrogation of primary human t cells via crispr genetic editing", *The Journal of Immunology*, vol. 201, no. 5, pp. 1586–1598, Sep. 2018, ISSN: 1550-6606. DOI: 10.4049/jimmunol.1701616.
- [180] A. Conti and R. Di Micco, "P53 activation: A checkpoint for precision genome editing?", *Genome Medicine*, vol. 10, no. 1, Aug. 2018, ISSN: 1756-994X. DOI: 10.1186/s13073-018-0578-6.
- [181] M. Foronda and L. E. Dow, "Crispr: Stressed about p53?", *Trends in Molecular Medicine*, vol. 24, no. 9, pp. 731–733, Sep. 2018, ISSN: 1471-4914. DOI: 10.1016/j.molmed.2018.06.010.
- [182] E. Haapaniemi, S. Botla, J. Persson, B. Schmierer, and J. Taipale, "Crispr-cas9 genome editing induces a p53-mediated dna damage response", *Nature Medicine*, vol. 24, no. 7, pp. 927–+, 2018, ISSN: 1078-8956. DOI: 10.1038/s41591-018-0049-z. [Online]. Available: %3CGo%20to%20ISI%3E://WOS:000438187700019%20https://www.nature.com/articles/s41591-018-0049-z.
- [183] Q. Hu, Y. Xie, Y. Ge, X. Nie, J. Tao, and Y. Zhao, "Resting t cells are hypersensitive to dna damage due to defective dna repair pathway", *Cell Death & Disease*, vol. 9, no. 6, p. 662, 2018, ISSN: 2041-4889. DOI: 10.1038/s41419-018-0649-z. [Online]. Available: https://doi.org/10.1038/s41419-018-0649-z.
- [184] R. J. Ihry, K. A. Worringer, M. R. Salick, *et al.*, "P53 inhibits crispr-cas9 engineering in human pluripotent stem cells", *Nature Medicine*, vol. 24, no. 7, pp. 939–946, 2018, ISSN: 1546-170X. DOI: 10.1038/s41591-018-0050-6. [Online]. Available: https://doi.org/10.1038/s41591-018-0050-6%20https://www.nature.com/articles/s41591-018-0050-6.
- [185] M. Kosicki, K. Tomberg, and A. Bradley, "Repair of double-strand breaks induced by crispr-cas9 leads to large deletions and complex rearrangements", *Nature Biotechnology*, vol. 36, no. 8, pp. 765–+, 2018, ISSN: 1087-0156. DOI: 10.1038/nbt.4192. [Online]. Available: %3CGo%20to%20ISI%3E://WOS:000458690600007%20https://www.ncbi.nlm.nih.gov/pmc/articles/PMC6390938/pdf/emss-81714.pdf.
- [186] M. S. Levine and A. J. Holland, "The impact of mitotic errors on cell proliferation and tumorigenesis", *Genes & Development*, vol. 32, no. 9–10, pp. 620–638, May 2018, ISSN: 1549-5477. DOI: 10.1101/gad.314351.118.
- [187] X.-L. Li, G.-H. Li, J. Fu, *et al.*, "Highly efficient genome editing via crispr-cas9 in human pluripotent stem cells is achieved by transient bcl-xl overexpression", *Nucleic Acids Research*, vol. 46, no. 19, pp. 10195–10215, Sep. 2018, ISSN: 1362-4962. DOI: 10.1093/nar/gky804.
- [188] T. L. Roth, C. Puig-Saus, R. Yu, *et al.*, "Reprogramming human t cell function and specificity with non-viral genome targeting", *Nature*, vol. 559, no. 7714, pp. 405–+, 2018, ISSN: 0028-0836. DOI: 10.1038/s41586-018-0326-5. [Online]. Available: %3CGo%20to%20ISI%3E://WOS:000439059800057%20https://www.ncbi.nlm.nih.gov/pmc/articles/PMC6239417/pdf/nihms-972895.pdf.

- [189] E. Shifrut, J. Carnevale, V. Tobin, *et al.*, “Genome-wide crispr screens in primary human t cells reveal key regulators of immune function”, *Cell*, vol. 175, no. 7, pp. 1958–+, 2018, ISSN: 0092-8674. DOI: 10.1016/j.cell.2018.10.024. [Online]. Available: %3CGo%20to%20ISI%3E://WOS:000453242200022%20https://www.cell.com/cell/pdf/S0092-8674(18)31333-3.pdf.
- [190] A. Syed and J. A. Tainer, “The mre11–rad50–nbs1 complex conducts the orchestration of damage signaling and outcomes to stress in dna replication and repair”, *Annual Review of Biochemistry*, vol. 87, no. 1, pp. 263–294, Jun. 2018, ISSN: 1545-4509. DOI: 10.1146/annurev-biochem-062917-012415.
- [191] M. Zampieri, B. Szappanos, M. V. Buchieri, *et al.*, “High-throughput metabolomic analysis predicts mode of action of uncharacterized antimicrobial compounds”, *Science Translational Medicine*, vol. 10, no. 429, Feb. 2018, ISSN: 1946-6242. DOI: 10.1126/scitranslmed.aal3973.
- [192] F. Allen, L. Crepaldi, C. Alsinet, *et al.*, “Predicting the mutations generated by repair of cas9-induced double-strand breaks”, *Nature Biotechnology*, vol. 37, pp. 64–+, 2019, ISSN: 1087-0156. DOI: 10.1038/nbt.4317.
- [193] A. V. Anzalone, P. B. Randolph, J. R. Davis, *et al.*, “Search-and-replace genome editing without double-strand breaks or donor dna”, *Nature*, vol. 576, no. 7785, pp. 149–157, 2019, ISSN: 1476-4687. DOI: 10.1038/s41586-019-1711-4. [Online]. Available: https://doi.org/10.1038/s41586-019-1711-4%20https://www.ncbi.nlm.nih.gov/pmc/articles/PMC6907074/pdf/nihms-1541141.pdf.
- [194] A. C. F. Bolhaqueiro, B. Ponsioen, B. Bakker, *et al.*, “Ongoing chromosomal instability and karyotype evolution in human colorectal cancer organoids”, *Nature Genetics*, vol. 51, no. 5, pp. 824–834, Apr. 2019, ISSN: 1546-1718. DOI: 10.1038/s41588-019-0399-6.
- [195] W. Chen, A. McKenna, J. Schreiber, *et al.*, “Massively parallel profiling and predictive modeling of the outcomes of crispr/cas9-mediated double-strand break repair”, *Nucleic Acids Research*, vol. 47, no. 15, pp. 7989–8003, Jun. 2019, ISSN: 1362-4962. DOI: 10.1093/nar/gkz487.
- [196] K. Clement, H. Rees, M. C. Canver, *et al.*, “Crispresso2 provides accurate and rapid genome editing sequence analysis”, *Nature Biotechnology*, vol. 37, no. 3, pp. 224–226, Feb. 2019, ISSN: 1546-1696. DOI: 10.1038/s41587-019-0032-3.
- [197] D. Dong, L. Zheng, J. Lin, *et al.*, “Structural basis of assembly of the human t cell receptor–cd3 complex”, *Nature*, vol. 573, no. 7775, pp. 546–552, Aug. 2019, ISSN: 1476-4687. DOI: 10.1038/s41586-019-1537-0.
- [198] J. Guo, Q. Tang, Q. Wang, *et al.*, “Pifithrin- α enhancing anticancer effect of topotecan on p53-expressing cancer cells”, *European Journal of Pharmaceutical Sciences*, vol. 128, pp. 61–72, Feb. 2019, ISSN: 0928-0987. DOI: 10.1016/j.ejps.2018.11.024.
- [199] X. Jiang, J. Xu, M. Liu, *et al.*, “Adoptive cd8+ t cell therapy against cancer:challenges and opportunities”, *Cancer Letters*, vol. 462, pp. 23–32, Oct. 2019, ISSN: 0304-3835. DOI: 10.1016/j.canlet.2019.07.017.
- [200] V. C. Kirsch, C. Orgler, S. Braig, *et al.*, “The cytotoxic natural product vioprolide a targets nucleolar protein 14, which is essential for ribosome biogenesis”, *Angewandte Chemie International Edition*, vol. 59, no. 4, pp. 1595–1600, Dec. 2019, ISSN: 1521-3773. DOI: 10.1002/anie.201911158.
- [201] K. Labun, T. G. Montague, M. Krause, Y. N. Torres Cleuren, H. Tjeldnes, and E. Valen, “Chopchop v3: Expanding the crispr web toolbox beyond genome editing”, *Nucleic Acids Research*, vol. 47, no. W1, W171–W174, May 2019, ISSN: 1362-4962. DOI: 10.1093/nar/gkz365.
- [202] A. Le Rhun, A. Escalera-Maurer, M. Bratovič, and E. Charpentier, “Crispr-cas in streptococcus pyogenes”, *RNA Biology*, vol. 16, no. 4, pp. 380–389, Mar. 2019, ISSN: 1555-8584. DOI: 10.1080/15476286.2019.1582974.

- [203] V. Lemiale, A.-P. Meert, F. Vincent, *et al.*, “Severe toxicity from checkpoint protein inhibitors: What intensive care physicians need to know?”, *Annals of Intensive Care*, vol. 9, no. 1, Feb. 2019, ISSN: 2110-5820. DOI: 10.1186/s13613-019-0487-x.
- [204] B. Lu, P. Javidi-Parsijani, V. Makani, *et al.*, “Delivering sacas9 mrna by lentivirus-like bionanoparticles for transient expression and efficient genome editing”, *Nucleic Acids Research*, vol. 47, no. 8, e44–e44, Feb. 2019, ISSN: 1362-4962. DOI: 10.1093/nar/gkz093.
- [205] D. D. G. Owens, A. Caulder, V. Frontera, *et al.*, “Microhomologies are prevalent at cas9-induced larger deletions”, *Nucleic Acids Research*, vol. 47, no. 14, pp. 7402–7417, 2019, ISSN: 0305-1048. DOI: 10.1093/nar/gkz459. [Online]. Available: <https://doi.org/10.1093/nar/gkz459> <https://www.ncbi.nlm.nih.gov/pmc/articles/PMC6698657/pdf/gkz459.pdf>.
- [206] E. Rayner, M.-A. Durin, R. Thomas, *et al.*, “Crispr-cas9 causes chromosomal instability and rearrangements in cancer cell lines, detectable by cytogenetic methods”, *The CRISPR Journal*, vol. 2, no. 6, pp. 406–416, Dec. 2019, ISSN: 2573-1602. DOI: 10.1089/crispr.2019.0006.
- [207] R. Rouet and D. Christ, “Efficient intracellular delivery of crispr-cas ribonucleoproteins through receptor mediated endocytosis”, *ACS Chemical Biology*, vol. 14, no. 3, pp. 554–561, Feb. 2019, ISSN: 1554-8937. DOI: 10.1021/acscchembio.9b00116.
- [208] K. Schober, T. R. Müller, F. Gökmen, *et al.*, “Orthotopic replacement of t-cell receptor α - and β -chains with preservation of near-physiological t-cell function”, *Nat Biomed Eng*, vol. 3, no. 12, pp. 974–984, 2019, ISSN: 2157-846x. DOI: 10.1038/s41551-019-0409-0.
- [209] R. Scully, A. Panday, R. Elango, and N. A. Willis, “Dna double-strand break repair-pathway choice in somatic mammalian cells”, *Nature Reviews Molecular Cell Biology*, vol. 20, no. 11, pp. 698–714, Jul. 2019, ISSN: 1471-0080. DOI: 10.1038/s41580-019-0152-0.
- [210] W. Song and J. Craft, “T follicular helper cell heterogeneity: Time, space, and function”, *Immunological Reviews*, vol. 288, no. 1, pp. 85–96, Mar. 2019, ISSN: 1600-065X. DOI: 10.1111/imr.12740.
- [211] P. A. Szabo, H. M. Levitin, M. Miron, *et al.*, “Single-cell transcriptomics of human t cells reveals tissue and activation signatures in health and disease”, *Nature Communications*, vol. 10, no. 1, Oct. 2019, ISSN: 2041-1723. DOI: 10.1038/s41467-019-12464-3.
- [212] X.-D. Tang, F. Gao, M.-J. Liu, Q.-L. Fan, D.-K. Chen, and W.-T. Ma, “Methods for enhancing clustered regularly interspaced short palindromic repeats/cas9-mediated homology-directed repair efficiency”, *Frontiers in Genetics*, vol. 10, Jun. 2019, ISSN: 1664-8021. DOI: 10.3389/fgene.2019.00551.
- [213] N. Wu, “Co-signaling receptors regulate t-cell plasticity and immune tolerance”, *Frontiers in Bioscience*, vol. 24, no. 1, pp. 96–132, 2019, ISSN: 1093-4715. DOI: 10.2741/4710.
- [214] A. Yamagishi, D. Matsumoto, Y. Kato, *et al.*, “Direct delivery of cas9-sgrna ribonucleoproteins into cells using a nanoneedle array”, *Applied Sciences*, vol. 9, no. 5, p. 965, Mar. 2019, ISSN: 2076-3417. DOI: 10.3390/app9050965.
- [215] S. Bradde, A. Nourmohammad, S. Goyal, and V. Balasubramanian, “The size of the immune repertoire of bacteria”, *Proceedings of the National Academy of Sciences*, vol. 117, no. 10, pp. 5144–5151, Feb. 2020, ISSN: 1091-6490. DOI: 10.1073/pnas.1903666117.
- [216] G. Carrà, M. F. Lingua, B. Maffeo, R. Tauli, and A. Morotti, “P53 vs nf- κ b: The role of nuclear factor-kappa b in the regulation of p53 activity and vice versa”, *Cellular and Molecular Life Sciences*, vol. 77, no. 22, pp. 4449–4458, Apr. 2020, ISSN: 1420-9071. DOI: 10.1007/s00018-020-03524-9.
- [217] O. M. Enache, V. Rendo, M. Abdusamad, *et al.*, “Cas9 activates the p53 pathway and selects for p53-inactivating mutations”, *Nature Genetics*, vol. 52, no. 7, pp. 662–668, May 2020, ISSN: 1546-1718. DOI: 10.1038/s41588-020-0623-4.

- [218] J. M. Geisinger and T. Stearns, “Crispr/cas9 treatment causes extended tp53-dependent cell cycle arrest in human cells”, *Nucleic Acids Research*, vol. 48, no. 16, pp. 9067–9081, Jul. 2020, ISSN: 1362-4962. DOI: 10.1093/nar/gkaa603.
- [219] P. Kumar, S. Saini, and B. S. Prabhakar, “Cancer immunotherapy with check point inhibitor can cause autoimmune adverse events due to loss of treg homeostasis”, *Seminars in Cancer Biology*, vol. 64, pp. 29–35, Aug. 2020, ISSN: 1044-579X. DOI: 10.1016/j.semcancer.2019.01.006.
- [220] S. P. Kurup, S. J. Moioffer, L. L. Pewe, and J. T. Harty, “P53 hinders crispr/cas9-mediated targeted gene disruption in memory cd8 t cells in vivo”, *Journal of Immunology*, vol. 205, no. 8, pp. 2222–2230, 2020, ISSN: 0022-1767. DOI: 10.4049/jimmunol.2000654. [Online]. Available: %3CGo%20to%20ISI%3E://WOS:000578996300023.
- [221] A. H. Moxley and D. Reisman, “Context is key: Understanding the regulation, functional control, and activities of the p53 tumour suppressor”, *Cell Biochem Funct*, 2020, 1099-0844 Moxley, Anne H Reisman, David Orcid: 0000-0002-7028-8500 Journal Article Review England Cell Biochem Funct. 2020 Sep 30. doi: 10.1002/cbf.3590., ISSN: 0263-6484. DOI: 10.1002/cbf.3590.
- [222] E. M. Porto, A. C. Komor, I. M. Slaymaker, and G. W. Yeo, “Base editing: Advances and therapeutic opportunities”, *Nature Reviews Drug Discovery*, vol. 19, no. 12, pp. 839–859, Oct. 2020, ISSN: 1474-1784. DOI: 10.1038/s41573-020-0084-6.
- [223] E. A. Stadtmauer, J. A. Fraietta, M. M. Davis, *et al.*, “Crispr-engineered t cells in patients with refractory cancer”, *Science*, vol. 367, no. 6481, eaba7365, 2020. DOI: 10.1126/science.aba7365. [Online]. Available: <https://science.sciencemag.org/content/sci/367/6481/eaba7365.full.pdf> <https://science.sciencemag.org/content/367/6481/eaba7365.long>.
- [224] A. S. Tocheva, M. Peled, M. Strazza, *et al.*, “Quantitative phosphoproteomic analysis reveals involvement of pd-1 in multiple t cell functions”, *Journal of Biological Chemistry*, vol. 295, no. 52, pp. 18036–18050, Dec. 2020, ISSN: 0021-9258. DOI: 10.1074/jbc.ra120.014745.
- [225] J. Wagner, E. Wickman, C. DeRenzo, and S. Gottschalk, “Car t cell therapy for solid tumors: Bright future or dark reality?”, *Molecular Therapy*, vol. 28, no. 11, pp. 2320–2339, Nov. 2020, ISSN: 1525-0016. DOI: 10.1016/j.ymt.2020.09.015.
- [226] T. Wei, Q. Cheng, Y.-L. Min, E. N. Olson, and D. J. Siegwart, “Systemic nanoparticle delivery of crispr-cas9 ribonucleoproteins for effective tissue specific genome editing”, *Nature Communications*, vol. 11, no. 1, Jun. 2020, ISSN: 2041-1723. DOI: 10.1038/s41467-020-17029-3.
- [227] L.-Y. Yang, N. H. Greig, D. Tweedie, *et al.*, “The p53 inactivators pifithrin- μ and pifithrin- α mitigate tbi-induced neuronal damage through regulation of oxidative stress, neuroinflammation, autophagy and mitophagy”, *Experimental Neurology*, vol. 324, p. 113135, Feb. 2020, ISSN: 0014-4886. DOI: 10.1016/j.expneurol.2019.113135.
- [228] J. Zhu, M. Singh, G. Selivanova, and S. Peugot, “Pifithrin- α alters p53 post-translational modifications pattern and differentially inhibits p53 target genes”, *Scientific Reports*, vol. 10, no. 1, Jan. 2020, ISSN: 2045-2322. DOI: 10.1038/s41598-020-58051-1.
- [229] D. Chen, T.-X. Tang, H. Deng, X.-P. Yang, and Z.-H. Tang, “Interleukin-7 biology and its effects on immune cells: Mediator of generation, differentiation, survival, and homeostasis”, *Frontiers in Immunology*, vol. 12, Dec. 2021, ISSN: 1664-3224. DOI: 10.3389/fimmu.2021.747324.
- [230] Z. Cui, H. Liu, H. Zhang, *et al.*, “The comparison of zfn, talen, and spcas9 by guide-seq in hpv-targeted gene therapy”, *Molecular Therapy - Nucleic Acids*, vol. 26, pp. 1466–1478, Dec. 2021, ISSN: 2162-2531. DOI: 10.1016/j.omtn.2021.08.008.
- [231] J. Ha, H. Park, J. Park, and S. B. Park, “Recent advances in identifying protein targets in drug discovery”, *Cell Chemical Biology*, vol. 28, no. 3, pp. 394–423, Mar. 2021, ISSN: 2451-9456. DOI: 10.1016/j.chembiol.2020.12.001.

- [232] M. L. Leibowitz, S. Papathanasiou, P. A. Doerfler, *et al.*, “Chromothripsis as an on-target consequence of crispr–cas9 genome editing”, *Nature Genetics*, vol. 53, no. 6, pp. 895–905, Apr. 2021, ISSN: 1546-1718. DOI: 10.1038/s41588-021-00838-7.
- [233] S. Sinha, K. Barbosa, K. Cheng, *et al.*, “A systematic genome-wide mapping of oncogenic mutation selection during crispr-cas9 genome editing”, *Nature Communications*, vol. 12, no. 1, Nov. 2021, ISSN: 2041-1723. DOI: 10.1038/s41467-021-26788-6.
- [234] G. Turchiano, G. Andrieux, J. Klermund, *et al.*, “Quantitative evaluation of chromosomal rearrangements in gene-edited human stem cells by cast-seq”, *Cell Stem Cell*, vol. 28, no. 6, 1136–1147.e5, 2021, ISSN: 1875-9777. DOI: 10.1016/j.stem.2021.02.002.
- [235] W. Wen, Z.-J. Quan, S.-A. Li, *et al.*, “Effective control of large deletions after double-strand breaks by homology-directed repair and dsodn insertion”, *Genome Biology*, vol. 22, no. 1, Aug. 2021, ISSN: 1474-760X. DOI: 10.1186/s13059-021-02462-4.
- [236] X. Xiang, G. I. Corsi, C. Anthon, *et al.*, “Enhancing crispr-cas9 grna efficiency prediction by data integration and deep learning”, *Nature Communications*, vol. 12, no. 1, May 2021, ISSN: 2041-1723. DOI: 10.1038/s41467-021-23576-0.
- [237] M. M. Álvarez, J. Biayna, and F. Supek, “Tp53-dependent toxicity of crispr/cas9 cuts is differential across genomic loci and can confound genetic screening”, *Nature Communications*, vol. 13, no. 1, Aug. 2022, ISSN: 2041-1723. DOI: 10.1038/s41467-022-32285-1.
- [238] S. P. Foy, K. Jacoby, D. A. Bota, *et al.*, “Non-viral precision t cell receptor replacement for personalized cell therapy”, *Nature*, vol. 615, no. 7953, pp. 687–696, Nov. 2022, ISSN: 1476-4687. DOI: 10.1038/s41586-022-05531-1.
- [239] L. Jiang, K. Ingelshed, Y. Shen, *et al.*, “Crispr/cas9-induced dna damage enriches for mutations in a p53-linked interactome: Implications for crispr-based therapies”, *Cancer Research*, vol. 82, no. 1, pp. 36–45, 2022, ISSN: 0008-5472. DOI: 10.1158/0008-5472.CAN-21-1692. [Online]. Available: <https://doi.org/10.1158/0008-5472.CAN-21-1692>.
- [240] M. Kosicki, F. Allen, F. Steward, K. Tomberg, Y. Pan, and A. Bradley, “Cas9-induced large deletions and small indels are controlled in a convergent fashion”, *Nature Communications*, vol. 13, no. 1, Jun. 2022, ISSN: 2041-1723. DOI: 10.1038/s41467-022-30480-8.
- [241] A. D. Nahmad, E. Reuveni, E. Goldschmidt, *et al.*, “Frequent aneuploidy in primary human t cells after crispr–cas9 cleavage”, *Nature Biotechnology*, vol. 40, no. 12, pp. 1807–1813, Jun. 2022, ISSN: 1546-1696. DOI: 10.1038/s41587-022-01377-0.
- [242] S. H. Park, M. Cao, Y. Pan, *et al.*, “Comprehensive analysis and accurate quantification of unintended large gene modifications induced by crispr-cas9 gene editing”, *Science Advances*, vol. 8, no. 42, Oct. 2022, ISSN: 2375-2548. DOI: 10.1126/sciadv.abo7676.
- [243] G. Schett, S. Boeltz, F. Müller, *et al.*, “Op0279 car-t cell treatment of refractory systemic lupus erythematosus- safety and preliminary efficacy data from the first four patients”, *Annals of the Rheumatic Diseases*, vol. 81, no. Suppl 1, pp. 185.1–185, May 2022, ISSN: 1468-2060. DOI: 10.1136/annrheumdis-2022-eular.1120.
- [244] M. Amberger, E. Grueso, and Z. Ivics, “Crisiss: A novel, transcriptionally and post-translationally inducible crispr/cas9-based cellular suicide switch”, *International Journal of Molecular Sciences*, vol. 24, no. 12, p. 9799, Jun. 2023, ISSN: 1422-0067. DOI: 10.3390/ijms24129799.
- [245] G. Cullot, J. Boutin, S. Fayet, *et al.*, “Cell cycle arrest and p53 prevent on-target megabase-scale rearrangements induced by crispr-cas9”, *Nature Communications*, vol. 14, no. 1, Jul. 2023, ISSN: 2041-1723. DOI: 10.1038/s41467-023-39632-w.
- [246] J. Feng, Y. HU, A. H. Chang, and H. Huang, “Cd19/bcma car-t cell therapy for refractory systemic lupus erythematosus - safety and preliminary efficacy data from a phase i clinical study”, *Blood*, vol. 142, no. Supplement 1, pp. 4835–4835, Nov. 2023, ISSN: 1528-0020. DOI: 10.1182/blood-2023-186669.

- [247] D. V. Foss, J. J. Muldoon, D. N. Nguyen, *et al.*, “Peptide-mediated delivery of crispr enzymes for the efficient editing of primary human lymphocytes”, *Nature Biomedical Engineering*, vol. 7, no. 5, pp. 647–660, Apr. 2023, ISSN: 2157-846X. DOI: 10.1038/s41551-023-01032-2.
- [248] R. Geczy, B. Thommandru, M. Swaminathan, *et al.*, “Lipid nanoparticle-mediated gene editing of human primary t cells and off-target analysis of the crispr-cas9 indels”, *Blood*, vol. 142, no. Supplement 1, pp. 6833–6833, Nov. 2023, ISSN: 1528-0020. DOI: 10.1182/blood-2023-185068.
- [249] B. Ibis, K. Aliazis, C. Cao, S. Yenyuwadee, and V. A. Boussiotis, “Immune-related adverse effects of checkpoint immunotherapy and implications for the treatment of patients with cancer and autoimmune diseases”, *Frontiers in Immunology*, vol. 14, Jun. 2023, ISSN: 1664-3224. DOI: 10.3389/fimmu.2023.1197364.
- [250] C. A. Tsuchida, N. Brandes, R. Bueno, *et al.*, “Mitigation of chromosome loss in clinical crispr-cas9-engineered t cells”, *Cell*, vol. 186, no. 21, 4567–4582.e20, Oct. 2023, ISSN: 0092-8674. DOI: 10.1016/j.cell.2023.08.041.
- [251] R. Baik, M. K. Cromer, S. E. Glenn, *et al.*, “Transient inhibition of 53bp1 increases the frequency of targeted integration in human hematopoietic stem and progenitor cells”, *Nature Communications*, vol. 15, no. 1, Jan. 2024, ISSN: 2041-1723. DOI: 10.1038/s41467-023-43413-w.
- [252] [Online]. Available: <https://design.synthego.com/#/>.
- [253] [Online]. Available: https://www.medchemexpress.com/Pifithrin-_alpha_-hydrobromide.html.

Danksagung

An dieser Stelle möchte ich mich nun endlich bei den zahlreichen Personen bedanken, die mir dabei geholfen haben, das Projekt zu beenden, das mich bisher am meisten gefordert hat in meinem Leben (besonders der letzte Teil in dem man die Sachen zu Papier bringen muss, die sich so zugetragen haben in den letzten 4,5 Jahren). Man sagt ja immer Wissenschaft sei eine Team-Aufgabe und ich glaube, das war selten so wahr wie in meinem Fall.

Als erstes möchte ich mich bei Kathrin bedanken, die mir in jeder Hinsicht geholfen hat, unter anderem, indem sie mir überhaupt erst ermöglicht hat, mich mal an der "echten" Wissenschaft zu versuchen. Nicht so einfach als Mediziner. Es gibt zahlreiche Dinge für die ich mich bedanken muss, am meisten jedoch für die schier unendliche Geduld, die sie mir gegenüber in jeder Situation gehabt hat. Bedanken möchte ich mich auch bei Wichtl und der ganzen Sort-facility, die insgesamt wahrscheinlich mehrere tausend Liter FACS-Buffer für mich durch den Aria geschickt haben.

Größter Dank gilt auch Jule, die das PFT- α Projekt, das sich doch als umfangreicher als anfangs gedacht herausstellte, übernommen hat und sicherlich erfolgreich zu Ende bringen wird.

Ohne Laborerfahrung in eine Doktorarbeit starten ist immer eine Herausforderung würde ich sagen, ich hatte jedoch Glück, in Form meiner damals Arbeitskollegen, die besten Startbedingungen zu haben, die es nur geben kann. Deshalb möchte ich mich hier einmal bei Saskia bedanken, die mir zu Beginn gezeigt hat, wie man sich in so einem Labor zu verhalten hat und mir für immer ein Vorbild in guter Planung und Disziplin sein wird, das ich nie im Leben erreichen werde, schade eigentlich. Nicht weniger hats geholfen, gemeinsam zu schimpfen, wenn die Experimente mal wieder nicht geklappt haben. Bei Betti möchte ich mich dafür bedanken, dass sie so eine Gelassenheit ins Laborleben gebracht hat und mir gezeigt hat, dass es kein Weltuntergang ist, wenn die meisten Dinge nicht aufs erste Mal klappen und man mit Ruhe meistens am besten beraten ist, wenns mal wieder stressig ist. Wenn es eine Person gibt, die Schuld daran ist, dass es bei mir jetzt doch geklappt hat mit dieser Doktorarbeit, dann ist es Julia. Ich kann gar nicht in Worte fassen, wie dankbar ich für alles bin, was du die letzten Jahre für mich und mein Projekt geleistet hast. Egal mit was für einem Problem ich zu dir gekommen bin, ich hab noch nicht erlebt, dass du es nicht lösen konntest.

Danke auch an Corinna, Leonie, Susanne und Konsti, dass ihr einfach immer gute Laune verbreitet habt, wenn ich euch über den Weg gelaufen bin. Bei Monika möchte ich mich für all die denkwürdigen

Gespräch, die wir hatten und alle Sprüche, die sie auf Lager hatte bedanken. Sehr wichtig für mich wars auch, mich immer mit Lisa unterhalten zu können, die gut nachvollziehen kann, wie das alles immer so läuft und viel Verständnis hat für jedes mal wenn ich wieder gejamert habe.

Vielen Dank auch für das Verständnis, das alle meine Freunde und besonders Laura dafür hatten, dass ich leider noch schnell zu den Zellis muss oder unbedingt jetzt noch ne Auswertung machen muss. Das machen auch nicht alle mit, danke.

Zum Schluss möchte ich mich noch bei meinen Brüdern, bei meinen Eltern und bei meinem Opa für den emotionalen und nicht zuletzt auch finanziellen Rückhalt bedanken.